NASA Conference Publication 2318

Polar Stratospheric Clouds

Their Role in Atmospheric Processes

(NASA-CP-2318) PROCEEDINGS OF A WORKSHOP ON POLAR STRATOSPHERIC CLOUDS. THEIR ROLE IN ATMOSPHERIC PROCESSES (NASA) 80 p
HC A05/MF A01 CSCL 04A G3/46
N84-32952
Unclas
20524

Report of a workshop held in Virginia Beach, Virginia June 26-28, 1983

NASA

NASA Conference Publication 2318

Polar Stratospheric Clouds

Their Role in Atmospheric Processes

Edited by
Patrick Hamill
San José State University
San Jose, California

Leonard R. McMaster
NASA Headquarters
Washington, D.C.

Report of a workshop sponsored by the
NASA Office of Space Science and Applications
and held in Virginia Beach, Virginia
June 20–22, 1983

NASA
National Aeronautics
and Space Administration

Scientific and Technical
Information Branch

1984

PREFACE

The workshop on Polar Stratospheric Clouds: Their Role in Atmospheric Processes, sponsored by the NASA Earth Science and Applications Division, Office of Space Science and Applications, was held in Virginia Beach, Virginia, on 20-22 June 1983. The purpose of the workshop was to review the existing data on polar stratospheric cloud observations, assess their potential role in various atmospheric processes, and identify specific scientific studies which could be addressed by NASA to further our understanding of global atmospheric chemistry and dynamics.

Approximately 20 scientists from university and government laboratories were invited to participate in this assessment. Several overview or tutorial presentations were given on NASA satellite observations of polar stratospheric clouds, along with preliminary analyses of the microphysical processes involved in the formation of polar stratospheric clouds and their potential impact on climate and radiation balance. The participants were then divided into two panels, one to address the potential effects of polar stratospheric clouds on climate, radiation balance, and atmospheric dynamics, and the other to address the effects on stratospheric chemistry, water vapor budget, and cloud microphysics. This report presents the conclusions and recommendations of the workshop along with a synopsis of the material presented by the participants and certain complementary material to support those conclusions and recommendations.

Special thanks are extended to Dr. Robert A. Schiffer, manager of the NASA Climate Research Program, and Dr. Robert T. Watson, manager of the NASA Upper Atmospheric Research Program, for initiating and supporting this study; to Dr. Adarsh Deepak, president of the Institute for Atmospheric Optics and Remote Sensing (IFAORS), and his staff for providing the logistics support at Virginia Beach and preparing the initial draft of this report; and to Melissa Miller, Marco E. Giordano, and Nidia N. Batlle of San José State University for assistance in preparing the final report.

Patrick Hamill, Chairman

Leonard R. McMaster, Co-Chairman

PRECEDING PAGE BLANK NOT FILMED

CONTENTS

PREFACE iii

PARTICIPANTS vii

1. INTRODUCTION 1

2. OBJECTIVES AND ORGANIZATION 1

3. SUMMARY 2

4. REVIEW OF OBSERVATIONS 4

4.1 Visual Observations of Stratospheric Clouds 4

4.2 Polar Stratospheric Cloud Observations by SAM II 5

4.3 SAGE Observations of Polar Stratospheric Clouds 17

4.4 The Occurrence and Distribution of Polar Stratospheric Clouds as Determined From Nimbus 7 LIMS Data 18

5. ROLE OF POLAR STRATOSPHERIC CLOUDS IN ATMOSPHERIC PROCESSES 26

5.1 Effect of Polar Stratospheric Clouds on the Global Radiation Balance 26

5.2 A Three-Dimensional Model Sensitivity Study of the Impact of Polar Stratospheric Clouds on Radiation Balance and Climate Feedbacks 28

5.3 Polar Meteorology 31

5.4 Potential Surface Effects of Polar Stratospheric Clouds 39

5.5 The Potential Role of Polar Stratospheric Clouds in Atmospheric Dynamical Processes 45

5.6 Effect of Polar Stratospheric Clouds on Stratospheric Water Vapor Distribution and Budget 46

5.7 Possible Effects of Polar Stratospheric Clouds on Trace Gases in the Upper Stratosphere 48

5.8 The Importance of Accurate Water and Temperature Measurements 49

5.9 Measurements of Stratospheric Water Vapor 49

5.10 Stratospheric Condensation Nuclei 50

5.11 Growth of Water Droplets and Ice Particles Within Polar Stratospheric Clouds 53

PRECEDING PAGE BLANK NOT FILMED

PAGE iv INTENTIONALLY BLANK

5.12 Gaseous Constituents in the Polar Region 54

5.13 Microphysical Processes and the Formation of Polar Stratospheric Clouds 56

5.14 Properties of Polar Stratospheric Clouds 63

5.15 Possible Effects of Polar Stratospheric Clouds on Satellite Remote Sensors 63

6. PANEL RECOMMENDATIONS 65

7. SYMBOLS AND ACRONYMS 68

8. REFERENCES 70

PARTICIPANTS

Dr. Edwin Danielsen
NASA Ames Research Center
Mail Code 245-3
Moffett Field, CA 94035

Dr. John H. DeLuisi
NOAA/ERL
Aeronomy Laboratory
Mail Stop R329
Boulder, CO 80303

Dr. Benjamin Fogle
National Science Foundation
1800 G. Street NW
Room 620
Washington, DC 20550

Dr. William L. Grose
NASA Langley Research Center
Mail Stop 401B
Hampton, VA 23665

Dr. Patrick Hamill
Department of Physics
San José State University
San Jose, CA 95192

Dr. James Hansen
Goddard Institute for Space Studies
2880 Broadway
New York, NY 10025

Dr. Andrew Heymsfield
National Center for Atmospheric Research
P. O. Box 3000
Boulder, CO 80307

Dr. David J. Hofmann
Department of Physics and Astronomy
University of Wyoming
University Station, Box 3905
Laramie, WY 82070

Dr. Austin W. Hogan
ASRC - ES 324
State University of New York at Albany
Albany, NY 12222

Dr. C. S. Kiang
Department of Geophysical Science
Georgia Institute of Technology
Atlanta, GA 30332

Dr. Dieter Kley
NOAA/ERL
Aeronomy Laboratory
Mail Stop R448
Boulder, CO 80303

Dr. M. Patrick McCormick
NASA Langley Research Center
Mail Stop 475
Hampton, VA 23665

Mr. Leonard R. McMaster
NASA Headquarters
Code EE-8
Washington, DC 20546

Dr. James B. Pollack
NASA Ames Research Center
Mail Code 245-3
Moffett Field, CA 94035

Dr. Ellis E. Remsberg
NASA Langley Research Center
Mail Stop 401B
Hampton, VA 23665

Dr. Robert A. Schiffer
NASA Headquarters
Code EE-8
Washington, DC 20546

Dr. Thomas J. Swissler
Systems and Applied Sciences
Corporation
17 Research Drive
Hampton, VA 23666

Dr. David E. Thompson
NASA Headquarters
Code EE-8
Washington, DC 20546

Dr. Owen B. Toon
NASA Ames Research Center
Mail Code 245-3
Moffett Field, CA 94035

Dr. Richard P. Turco
R&D Associates
P.O. Box 9695
Marina Del Rey, CA 90291

1. INTRODUCTION

Since its launch in 1978, the NASA Stratospheric Aerosol Measurement (SAM II) Sun photometer, flown on the Nimbus 7 satellite, has observed significantly enhanced extinction in the Arctic and Antarctic polar stratosphere during each local winter. A preliminary investigation of these so-called polar stratospheric clouds and their possible formation mechanisms revealed a high correlation between their occurrence and temperature. The high values of extinction coefficient associated with the clouds suggested that their existence could have an impact on global water vapor and radiation budgets as well as on polar climatology (McCormick et al., 1982; Steele et al., 1983). Although there had been well-documented reports of visual sightings in the past (Stanford and Davis, 1974) and analyses of their potential impact on atmospheric processes (Stanford, 1973a), the SAM II observations indicated a far greater frequency of occurrence than had been expected and suggested that their role in global as well as polar climatology should be reconsidered.

A workshop entitled Polar Stratospheric Clouds: Their Role in Atmospheric Processes was thus held in Virginia Beach, Virginia, 20-22 June 1983. The workshop was sponsored jointly by the NASA Climate Research and Upper Atmospheric Research Programs, Office of Space Science and Applications. The workshop was chaired by Dr. Patrick Hamill of San José State University and co-chaired by Mr. Leonard R. McMaster of NASA Headquarters. The stated purpose of the workshop was to review the existing data on polar stratospheric clouds (PSC's), assess their potential role in various atmospheric processes, and identify specific scientific studies which could be addressed by NASA to further our understanding of global atmospheric chemistry and dynamics. A list of workshop participants appears on page vii of this document.

2. OBJECTIVES AND ORGANIZATION

The introductory session of the workshop consisted of a number of overview or tutorial presentations. Topics covered included satellite observations of polar stratospheric clouds (PCS's), polar meteorology, an analysis of the microphysical processes that could affect PSC formation, and the preliminary results of model calculations to evaluate the potential effects of PSC's on climate and radiation balance. At the second session, the workshop objectives were discussed and the general format of the final report was considered. The workshop participants were then broken up into two panels: a panel on Radiation Balance, Climate, and Dynamics, chaired by James Hansen, and a panel on Stratospheric Chemistry, Water Vapor, and Cloud Microphysics, chaired by M. P. McCormick. The members of each group and the tasks assigned to the two groups are presented subsequently.

These groups then met separately to identify the important scientific problems associated with PSC's and to draft their recommendations for further studies.

A concluding session was held in which all participants met to review both their assessments of the potential effect of PSC's on atmospheric processes and their draft recommendations. The participants felt that even though the net effect of polar stratospheric clouds on the global radiation budget may be slight, their study is justified in its own right as an interesting scientific problem that can be addressed using common, well-tested measurement techniques. The result of such a study would have a high probability of success because PSC's present a simple system with few of the complicating factors that plague tropospheric studies. The results

PANELS, PANEL MEMBERS, AND SUGGESTED TASKS

Panel	Members	Tasks
Radiation Balance, Climate, and Dynamics	J. Hansen (Chair)	Meteorological conditions for PSC formation
	A. W. Hogan	Polar meteorology
	E. Danielsen	Effects of polar vortex and stratospheric warmings on PSC formation
	B. Fogle	Infrared budget
	W. L. Grose	Radiation dynamics coupling
	D. E. Thompson	Role of subvisible clouds
	T. J. Swissler	Surface effects of PSC's
	J. H. DeLuisi	
	J. B. Pollack	
	R. A. Schiffer	
Stratospheric Chemistry, Water Vapor, and Cloud Microphysics	M. P. McCormick (Chair)	CN and CCN and PSC's
	P. Hamill	Particle nucleation, growth, and sedimentation
	A. Heymsfield	Properties of PSC particles
	O. B. Toon	Polar night chemistry
	D. J. Hofmann	Role of water vapor
	D. Kley	Tropospheric-stratospheric exchange
	R. P. Turco	Heterogeneous chemistry
	E. E. Remsberg	
	C. S. Kiang	

of such a study would deepen our knowledge of microphysical processes, heterogeneous interactions in the stratosphere, and the stratospheric water vapor budget. The results might help in understanding polar night chemistry and could perhaps serve as a test of some theories of the effect of polar clouds on the radiation balance and dynamics of the stratosphere. Finally, the results of such a study would have the practical benefit of allowing a determination of the effects of PSC's on remote sensors, whether on satellites, on aircraft, or on the ground.

The panel recommendations are detailed in the final section of this report, but it might be mentioned that the primary recommendations are (1) to continue analyzing the SAM II data for PSC events; (2) to analyze other satellite and nonsatellite data for information on PSC's; (3) to carry out modeling studies; (4) to determine the polar radiation and temperature fields and the water vapor distribution; and (5) to determine the physical properties of PSC's and PSC particles.

3. SUMMARY

In this section we include a brief overview of the presentations and discussions at the workshop. These will be described more fully in the following section.

At the first general meeting, overview or tutorial presentations were given by M. P. McCormick, E. E. Remsberg, P. Hamill, A. W. Hogan, J. B. Pollack, J. Hansen, and A. Heymsfield. The presentation by McCormick covered the observations of polar stratospheric clouds by the SAM II satellite system and statistical studies of these

observations, and pointed out in particular the strong correlation between PSC observations and low temperatures. A compilation of recent data was presented. These data had been analyzed by McCormick, T. J. Swissler, and U. Farrukh, and consisted of analyses of the altitudes, geographic locations, and longitudinal distributions of PSC's. Statistical correlations of PSC sightings with low temperatures indicated a high probability of cloud formation whenever temperatures fell below about 190 K. McCormick also presented plots of optical depth in the northern and southern polar regions as a function of time. These indicated an order-of-magnitude increase in optical depth during the PSC events as well as a secular increase in optical depth during the past several years. These increases are probably due to volcanic eruptions. A summary of McCormick's presentation, entitled "Polar Stratospheric Cloud Observations by SAM II," is given in the next section of the report.

Ellis E. Remsberg presented an overview of the observations of PSC's in the LIMS data. This work was prepared by Remsberg, J. M. Russell, and L. L. Gordley. The LIMS data can be used to determine the spatial distribution of PSC's and the frequency and duration of PSC events. Furthermore, the LIMS results give stratospheric temperature distributions at the locations of the PSC's as well as concurrent water vapor distributions at locations adjacent to PSC events. The PSC's are observed in the LIMS data as (unwanted) added emitters in the ozone, water vapor, and nitric acid channels. Using the correlated temperature and water vapor data (from nearby points), one finds that the PSC's occur in regions where there is just enough water vapor to get saturation with respect to ice. Remsberg concluded that: (1) LIMS and SAM II generally agree with respect to PSC locations and times, (2) PSC sightings occur near temperature minima, and (3) PSC's are less transient than might be inferred from the SAM II data. A summary of Remsberg's presentation, entitled "The Occurrence and Distribution of Polar Stratospheric Clouds as Determined From Nimbus 7 LIMS Data," appears in the next section of the report.

Patrick Hamill presented an analysis of some of the microphysical processes which would affect the formation of polar stratospheric clouds. This work, which was performed in collaboration with H. M. Steele, M. P. McCormick, and T. J. Swissler, showed that the most probable formation mechanism for PSC's is the dilution and freezing of stratospheric aerosol particles. Ice growth onto these nuclei would then account for the observed values of extinction. Plots of theoretically evaluated extinction versus extinction measured by the SAM II instrument show good agreement if the particles are assumed to have a log normal size distribution and a number density of about 10 cm^{-3}. This then implies stratospheric water vapor densities in the range of 6 to 8 ppmv. These results are described in the section entitled "Microphysical Processes and the Formation of Polar Stratospheric Clouds."

Austin W. Hogan presented information on the temperature structure of the air over the South Pole in winter. He showed that Antarctic tropospheric temperatures are lowest over the pole. A 16-year mean sounding for August at the pole shows very low temperatures and a strong inversion near the surface.

J. B. Pollack presented model results of a calculation intended to determine whether a stratospheric cloud will warm or cool its environment by absorbing thermal radiation from the lower atmosphere and radiating to higher and lower altitudes. Two cases were considered, a "grey" case and a "nongrey" case. For the grey case, the results were inconclusive in the sense that the cloud may either cool or warm the atmosphere slightly, depending on the choice of several parameters, such as the

difference between cloud temperature and surface temperature. For the nongrey case, a net cooling was obtained at long wavelengths and a net warming at short wavelengths. Water ice has a strong absorption at 45 μm, resulting in a cooling, and also at 12 μm, which results in a warming. These tended to cancel, and once again the results were inconclusive.

Pollack presented sample calculations using a temperature profile obtained from the SAM II data and nominal choices of aerosol parameters and water vapor mixing ratio. The results of these calculations indicated that the presence of polar stratospheric clouds would have essentially no effect on stratospheric temperatures and consequently would not affect dynamical processes. These model calculations and results are described further in section 5.1.

James Hansen gave a short presentation describing model calculations to evaluate the potential effects of polar stratospheric clouds on climate. Hansen used the GISS 9 layer model, assuming that the probability of cloud occurrence in the top two layers was that given by the SAM II data. In the model, PSC's were assigned the properties of cirrus clouds; therefore the optical thickness assumed was one order of magnitude larger than actually occurs in polar stratospheric clouds and the particle size was also larger than observed. Model results showed a significant change in the temperature of the layer in which the cloud appeared. This cooling caused more clouds to form; thus a positive-feedback mechanism seems to be in effect. Furthermore, the cooling tended to make the clouds grow bigger. The change in surface temperature, however, was minimal. The planetary radiation balance would not be significantly affected even though PSC's could cause an increased cooling of several W m^{-2}. Naturally, this would be very important if it were to occur all over the globe, but because PSC's are restricted to a small geographic area and have an optical depth quite a bit less than that used in the model, it is probably safe to say that PSC's have little impact on surface climate.

Finally, A. Heymsfield showed a series of photographs of ice crystals formed at about 17 km at a temperature of 194 K. The particles were columnar ice crystals, as would be expected for crystal growth at that temperature, although the smaller particles were trigonal plates. The mean size of the particles ranged from 2 to 3 μm up to 12 μm, and the water content was 10^{-4} g m^{-3}.

After the general meeting the working groups met separately and discussed a variety of topics, trying to identify the important scientific problems associated with PSC's. Short reports on various topics were presented and discussed at a general meeting, and at the final session the recommendations of the working groups were reviewed and approved.

4. REVIEW OF OBSERVATIONS

4.1 Visual Observations of Stratospheric Clouds

The water vapor mixing ratio in the stratosphere is a few ppmv and the temperature is about 220 K. This means that the relative humidity is less than a few percent. Consequently, one would certainly not expect to find clouds in the stratosphere. However, observations (mainly in Scandinavia) of nacreous (mother-of-pearl) clouds indicate that these clouds are formed at altitudes that clearly place them in the stratosphere (Stormer, 1929). Analysis of temperature soundings indicates that the air masses in which the clouds form are so cold that high relative humidities

are reached. Such cold temperatures are usually associated with orographically induced waves, which result in the lifting and adiabatic cooling of the air parcels. Stanford (1973b) showed that this mechanism could account for an 8°C cooling of the air masses. Hesstvedt (1969) proposed a model for the formation of nacreous clouds in which an orographic lee wave caused the lifting of air parcels to saturation. The particle growth would be such that in any particular region of the cloud, the particles would have a monodisperse size distribution, leading to the formation of colored bands having the approximate shape of the cloud.

Visual observations of mother-of-pearl clouds (MPC's) are quite infrequent. Stanford and Davis (1974) compiled a list of MPC observations recorded during a period of nearly 100 years and found about 150 sightings in the Northern Hemisphere, most over Scandinavia in the winter. The Southern Hemispheric sightings are much more scarce because there are no habitable regions at the latitudes at which stratospheric clouds would be expected to form. Nevertheless, the observations from Antarctica by a Norwegian-Swedish-British expedition in 1950 (Liljequist, 1956) indicated a persistent cirrostratus cloud bank at stratospheric altitudes. This led Stanford (1977) to suggest that Antarctic stratospheric clouds could be an important sink for stratospheric water vapor.

Satellite observations have ushered in a new era of stratospheric cloud observations. The SAM II experiment and the LIMS experiment (both mounted on the Nimbus 7 satellite) have reported sightings of stratospheric clouds, as has the SAGE experiment. These observations are described in the following sections. However, it might be pointed out that the stratospheric clouds seen in the satellite data may not be the mother-of-pearl clouds reported in visual observations. The reason is that the clouds observed by the satellites are not related to orographic features and appear to be larger and more persistent than mother-of-pearl clouds. Furthermore, it is still uncertain whether or not the objects observed by the satellite would be visible to a ground observer. For this reason, the term "polar stratospheric cloud" was coined.

4.2 Polar Stratospheric Cloud Observations by SAM II

The Stratospheric Aerosol Measurement (SAM II) experiment is mounted on the Nimbus 7 satellite, which was launched on 24 October 1978. It began taking data a few days later and has been in continuous operation up to the present time (McCormick et al., 1979).

The SAM II instrument consists of a 1-μm radiometer which uses solar occultation (i.e., measures solar radiance as a function of time during each spacecraft sunrise and sunset) to determine atmospheric transmission. (See fig. 1.) These transmission data are then inverted to yield profiles of atmospheric extinction as a function of altitude (Chu and McCormick, 1979).

The Nimbus 7 high-noon Sun-synchronous orbit limits solar occultation measurements to the polar regions such that sunrises are encountered in the Southern Hemisphere between 65°S and 81°S and sunsets are encountered in the Northern Hemisphere between 65°N and 81°N (depending on the season). The orbital period of Nimbus 7 is 104 minutes; therefore 15 sunrises and 15 sunsets (separated by 26° in longitude) are encountered each day.

ORIGINAL PAGE IS
OF POOR QUALITY

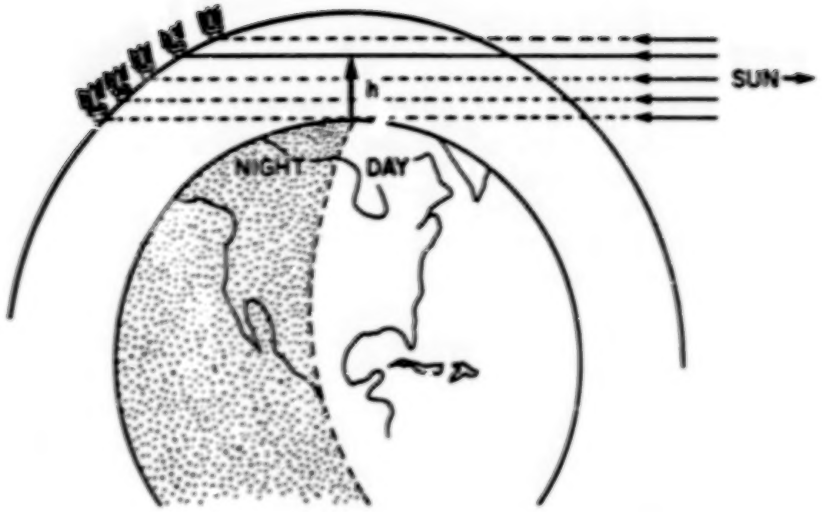

Figure 1.- Schematic representation of solar occultation technique employed by Nimbus 7 SAM II instrument. The attenuation of solar radiation through successive layers of the atmosphere at tangent height h is measured during spacecraft sunrise and sunset.

In figure 2 we present average extinction and temperature profiles calculated using all of the individual profiles obtained during a 1-month period. The temperature profiles are generated by the National Meteorological Center of NOAA at the time and place of the SAM II measurements from an interpolation of a gridded analysis. The temperature profiles are believed to be accurate to about 3°C.

The profiles obtained in one day of SAM II operation can be used to generate a global map of extinction (at a given latitude) by interpolating between the 15 individual extinction profiles to obtain extinction isopleths as a function of altitude and longitude. Figure 3 shows such a plot of extinction isopleths as well as the corresponding temperature fields.

The SAM II data for January 1979 revealed a number of extinction profiles in which the extinction was unusually large. (See, for example, McCormick et al., 1982.) Two examples of such profiles are given in figure 4. Subsequent analysis of SAM II data showed that this type of profile was a fairly common occurrence during winter in both the northern and southern polar regions. Examples of such enhancements in extinction on a daily isopleth plot are presented in figures 5 and 6.

Many hundreds of polar stratospheric clouds were observed during the Antarctic winter (June-October) of 1979. Statistical studies relating the observation of PSC's to low temperatures revealed a high correlation between cloud occurrence and temperatures below 220 K. A week-by-week analysis of the number of clouds as a function of the minimum temperature recorded in the temperature profile is shown in figure 7. Figure 8 shows the same information for the entire winter of 1979 for both hemispheres.

ORIGINAL PAGE IS
OF POOR QUALITY

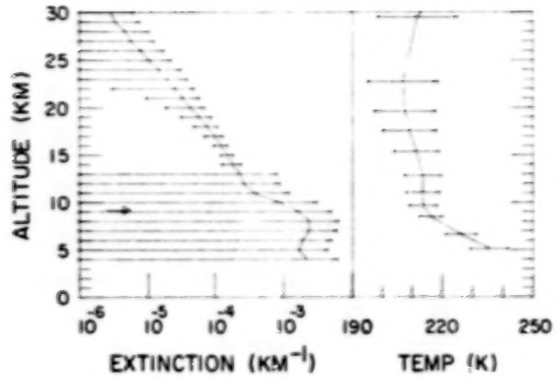

(a) January 1979, 67.1°N latitude.

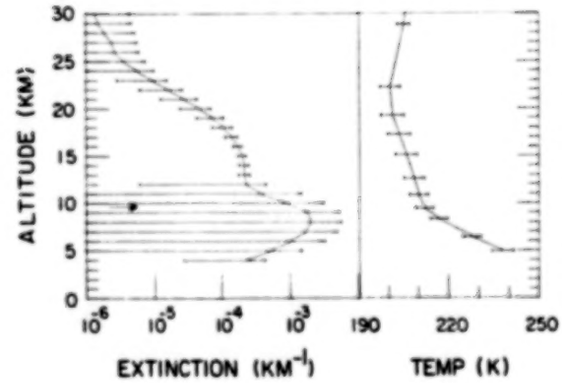

(b) June 1979, 65.2°S latitude.

Figure 2.- Average extinction profile and average temperature profile for Northern Hemisphere measurements, made in January 1979, and Southern Hemisphere measurements, made in June 1979. The error bars give one standard deviation from the mean. The mean tropopause is indicated by the arrow.

ORIGINAL PAGE IS
OF POOR QUALITY

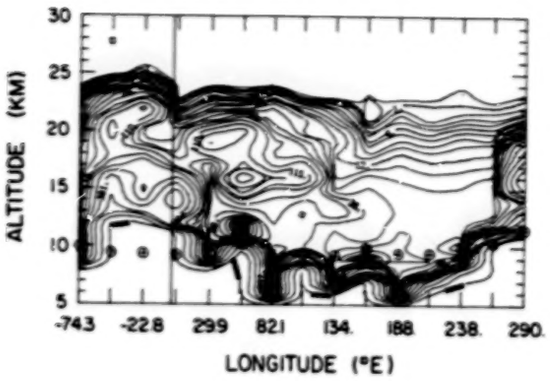

(a) Extinction.

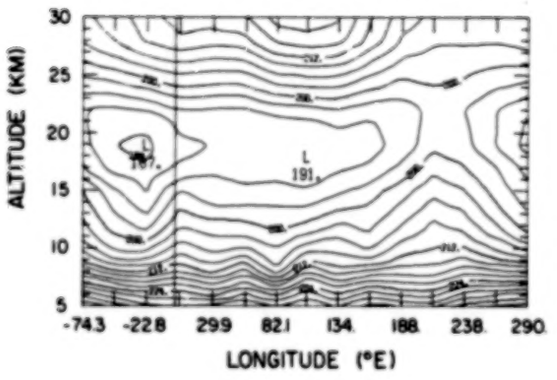

(b) Temperature. Isotherms (K) are separated by 3 K.

Figure 3.- Average extinction and temperature isopleths in 10^{-5} km^{-1} as a function of altitude and longitude for 25 July 1979 at 68°S. The solid vertical line shows Greenwich longitude.

ORIGINAL PAGE IS
OF POOR QUALITY

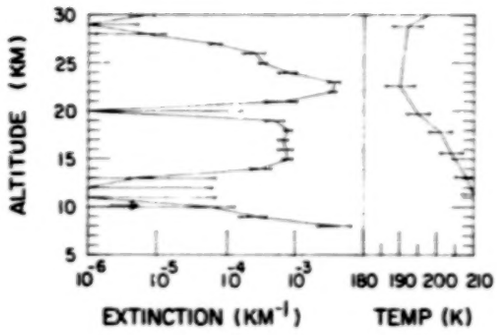

(a) 19 January 1979, 43°E, 67.8°N.

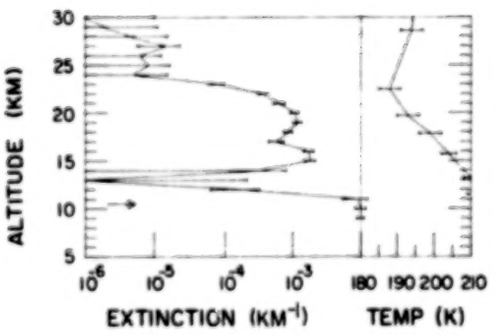

(b) 23 January 1979, 27°W, 68.7°N.

Figure 4.- Extinction and temperature profiles obtained in January 1979.

ORIGINAL PAGE IS
OF POOR QUALITY

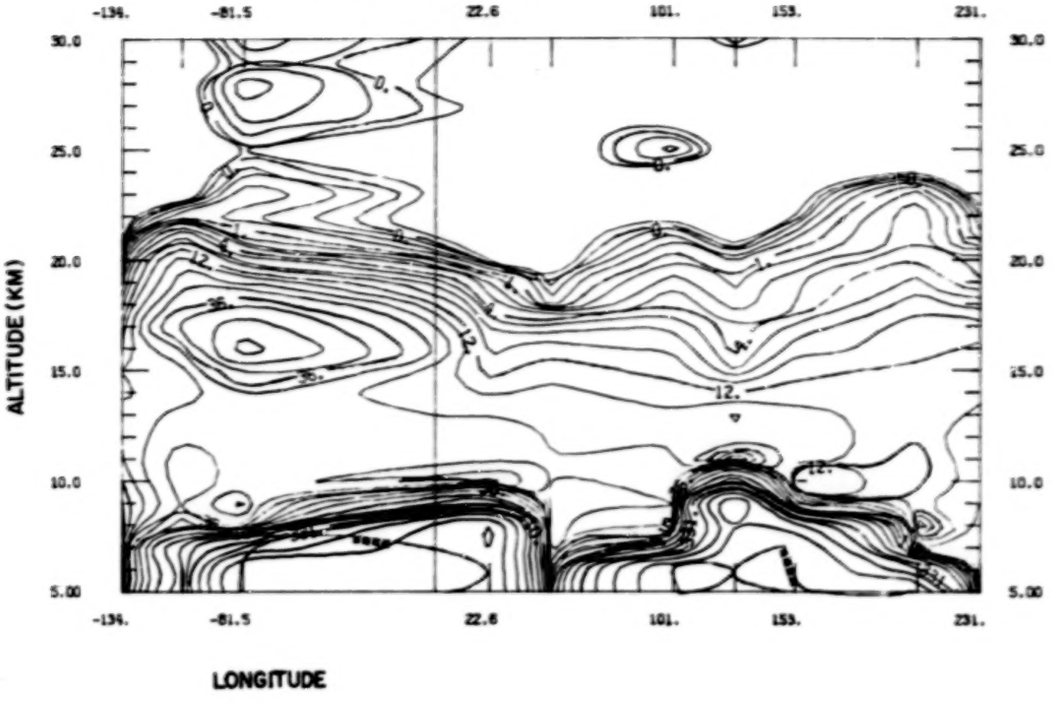

(a) Extinction.

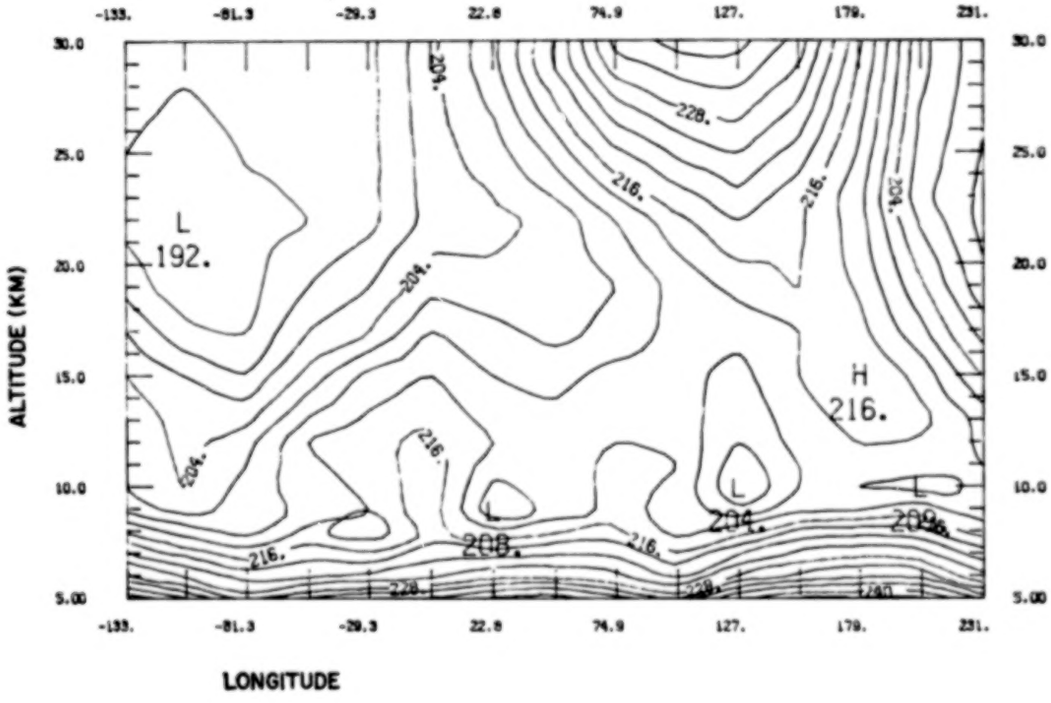

(b) Temperature.

Figure 5.- Extinction and temperature isopleths for Northern Hemisphere, 13 January 1979. Note low temperature at location of polar stratospheric cloud (enhanced extinction at -81° longitude).

ORIGINAL PAGE IS
OF POOR QUALITY

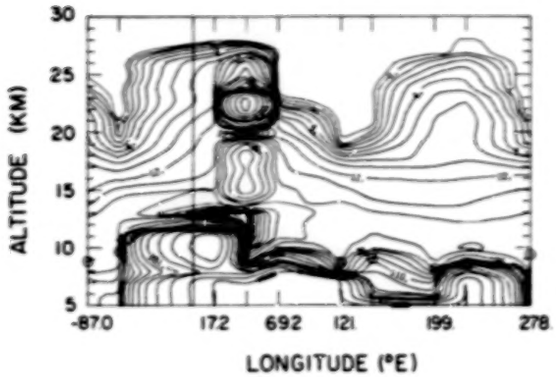

(a) Extinction.

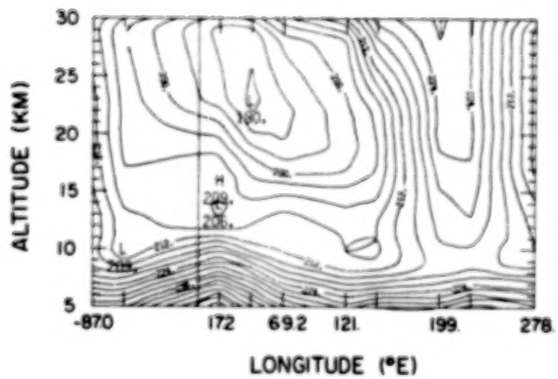

(b) Temperature.

Figure 6.- Extinction and temperature isopleths for 19 January 1979 at 67.8°N. The solid vertical line shows the Greenwich longitude. Note the cold temperature at the location of the cloud (43.2°E).

ORIGINAL PAGE IS
OF POOR QUALITY

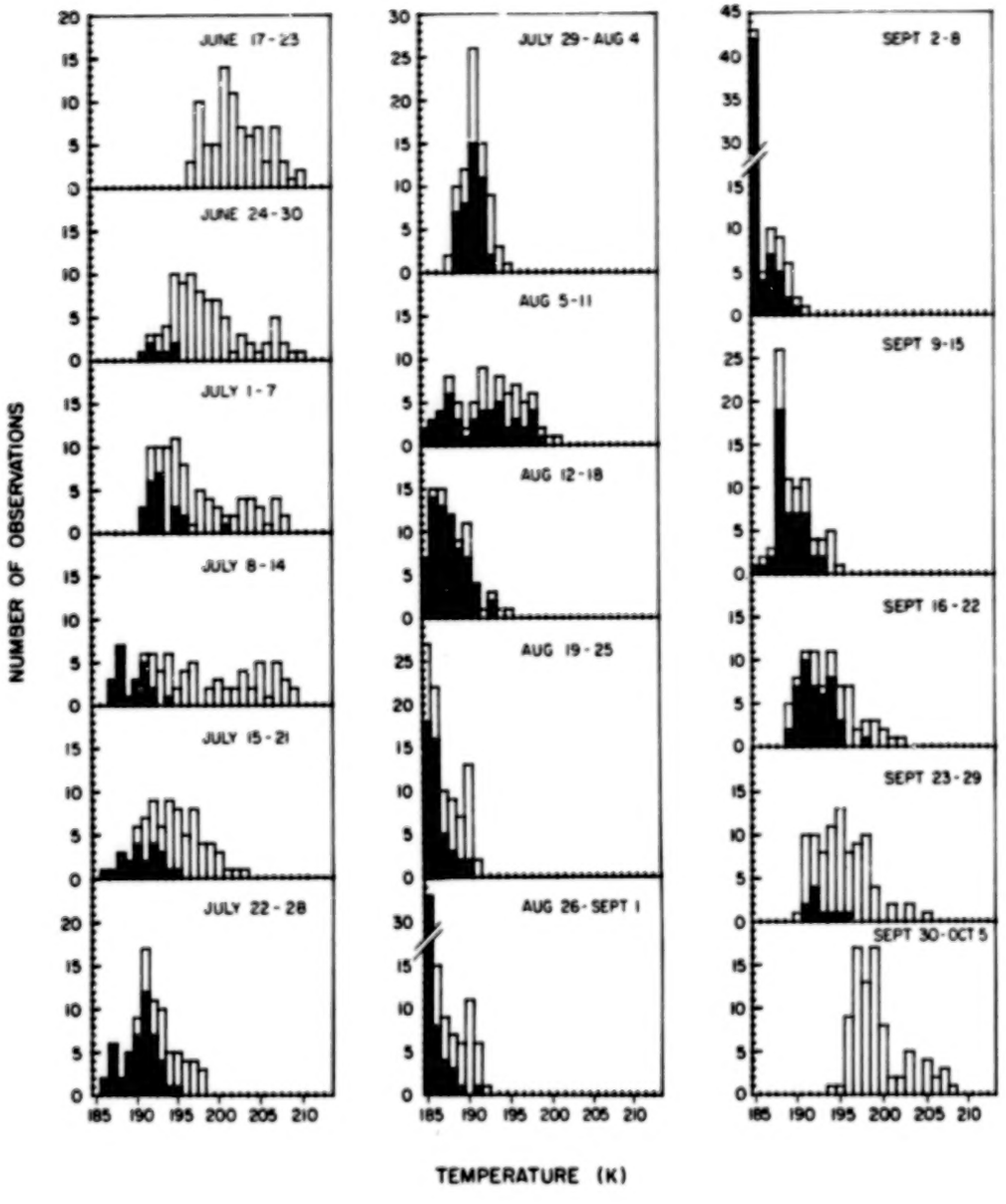

Figure 7.- Number of cloudless events (open areas) and cloud observations (shaded areas) as a function of minimum stratospheric temperature for 16 weeks during the Antarctic winter. Note the changes of scale for the weeks of 26 August to 1 September and 2-8 September. All events for temperatures less than 185 K are included in the 185-K bin (McCormick et al., 1982).

ORIGINAL PAGE IS
OF POOR QUALITY

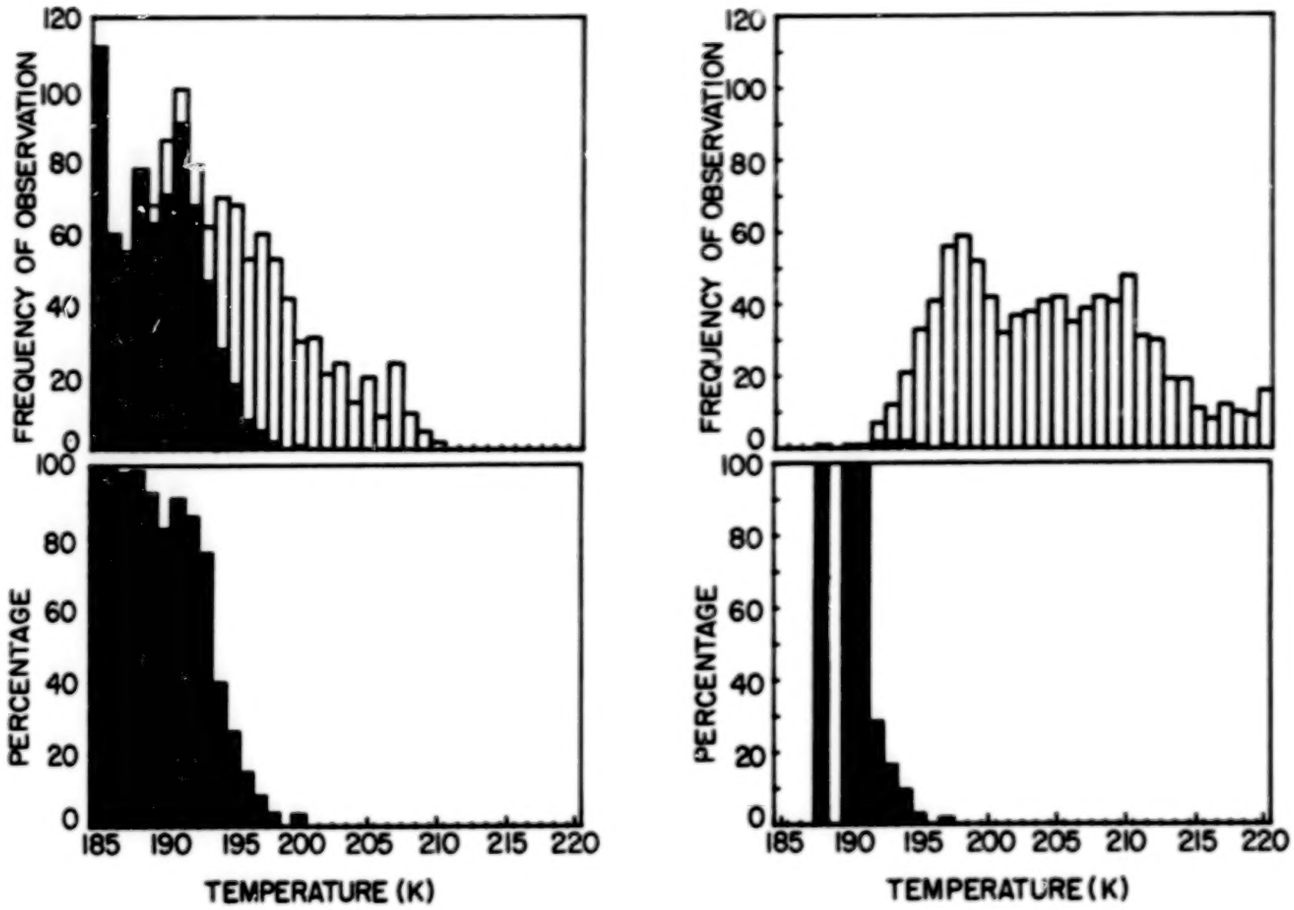

(a) Southern Hemisphere, 16 June to 5 October 1979.

(b) Northern Hemisphere, 25 November 1978 to 16 February 1979.

Figure 8.- Histogram showing the total number of profiles having a given minimum temperature for winter in Northern and Southern Hemispheres. The shaded events represent cloud observations. The frequency of cloud observations as a percentage of the total events with the same minimum temperature is also shown. All events for temperatures less than 185 K are included in the 185-K bin.

It is interesting to consider a plot of average weekly extinction as a function of altitude over a 1-year period. Figures 9 and 10 show the aerosol extinction and temperature isopleths for the Northern and Southern Hemispheres, respectively, for a 12-month period (McCormick et al., 1981). The corresponding latitude of measurement is also shown. Note that the winter period shows a large increase in extinction (particularly in the Southern Hemisphere), and that after the winter there is a very definite "cleansing" of the stratosphere as extinction values fall to low levels.

The SAM II data can also be used to calculate the stratospheric optical depth during the period from 1979 to the present for both the northern and southern polar regions. As would be expected, the optical depth is enhanced during local winters and shows a distinct decrease to minimum values after the winter season. During the Antarctic winter of 1979, for example, the stratospheric weekly averaged optical depth increased by as much as an order of magnitude and was more than double the background for a period of 13 weeks. Similar enhancements have been found in subsequent winters. Of particular interest is the way volcanic activity affects the background optical depth, showing up as a near-secular increase during the past several years. This is due to global volcanic activity, primarily the eruptions of Mount St. Helens and El Chichon.

Statistical analysis of PSC occurrences during the years 1980-1983 is being carried out and results cited are preliminary. Nevertheless, it might be noted that in the Northern Hemisphere there is a fairly large variability in the number of clouds from winter to winter. Volcanic activity is one of the possible underlying causes of this variability. Also, the percentage of cloud occurrences as a function of temperature appears to vary from winter to winter (as illustrated in fig. 11). This may be related to a general trend in the amount of water vapor present in the stratosphere or simply to the "coldness" of the particular winter.

Preliminary data show that the inferred water vapor concentration in the Northern Hemisphere when PSC events were sighted was at least 7 ppmv, and on several occasions it was more than 20 ppmv. Such high values of water vapor concentration might be related to errors in reported temperatures. Nevertheless, the inferred water vapor concentration after correction for temperature errors cannot be brought down to the levels of water vapor concentration reported in the literature (Steele et al., 1983). These results may be due to localized variations in temperature which are masked by the interpolated temperature analysis, or they may be caused by the presence of localized regions of high water vapor content. Another possibility is that some of the clouds are changing state when observed, so that an equilibrium with water vapor has not been achieved.

It was found that the altitudes of the peak extinctions of cloud events have a bimodal statistical distribution. Northern Hemisphere data reveal a major mode at 20 km and a minor one at 15 km. Southern Hemisphere data show many more clouds at 15 km than at 20 km, with the lower clouds found late in the winter when the coldest air mass is at lower altitudes.

The peak extinction values of the clouds can vary considerably. Although maximum reported extinctions are 10^{-2} km^{-1}, the extinction actually exceeds these values on several occasions. Such cases are not reported because the transmission signal is so small that the inversion calculation is terminated when the extinction exceeds 10^{-2} km^{-1}. There are also other cases in which a meaningful extinction

ORIGINAL PAGE IS
OF POOR QUALITY

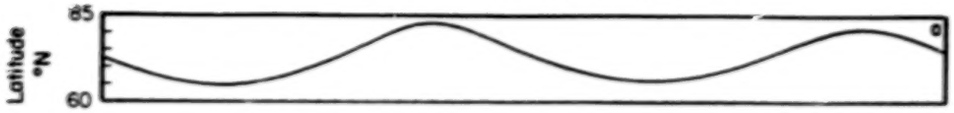

(a) Latitude.

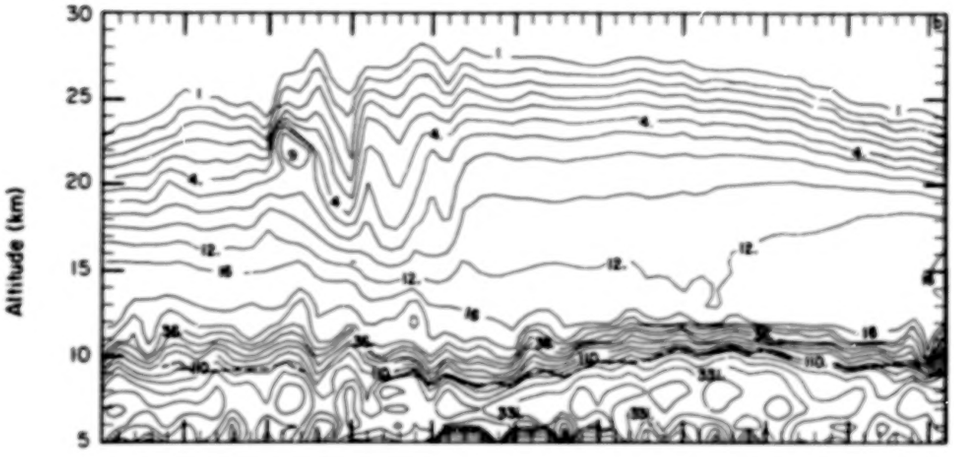

(b) Aerosol extinction at 1 μm in units of 10^{-5}/km. The interval between adjacent isopleths is approximately a multiple of 1.32. Darker dashed line around 10 km indicates the tropopause height.

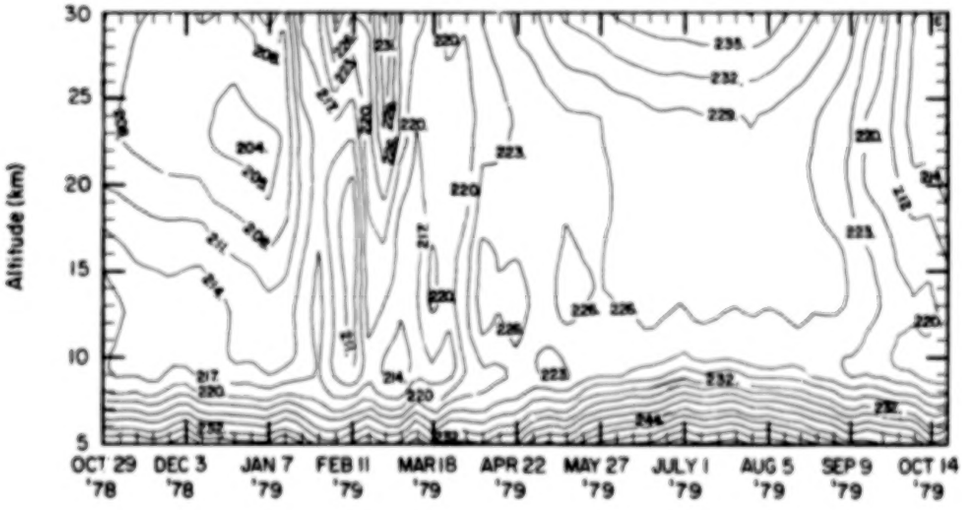

(c) Temperature field (K) at the location of the aerosol measurement. The isotherms are separated by 3 K.

Figure 9.- Northern Hemisphere weekly averaged values. The date marked on the horizontal axis is the first day of the week to which the average value corresponds.

ORIGINAL PAGE IS
OF POOR QUALITY

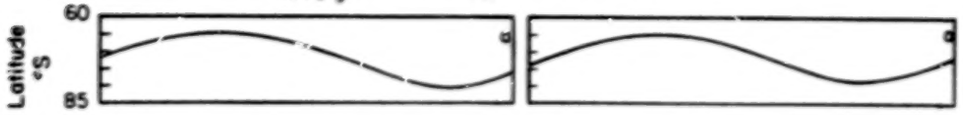

(a) Latitude.

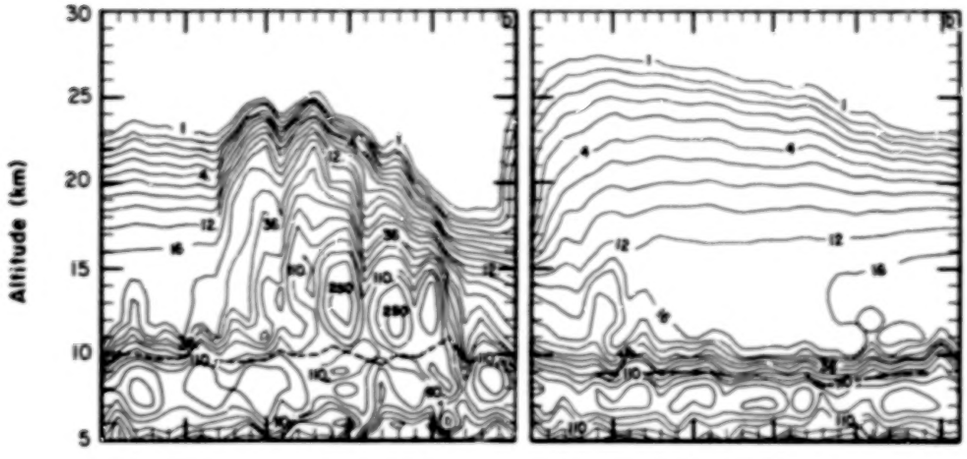

(b) Aerosol extinction at 1 μm in units of 10^{-5} km. The interval between adjacent isopleths is approximately a multiple of 1.32. Darker dashed line around 10 km indicates the tropopause height.

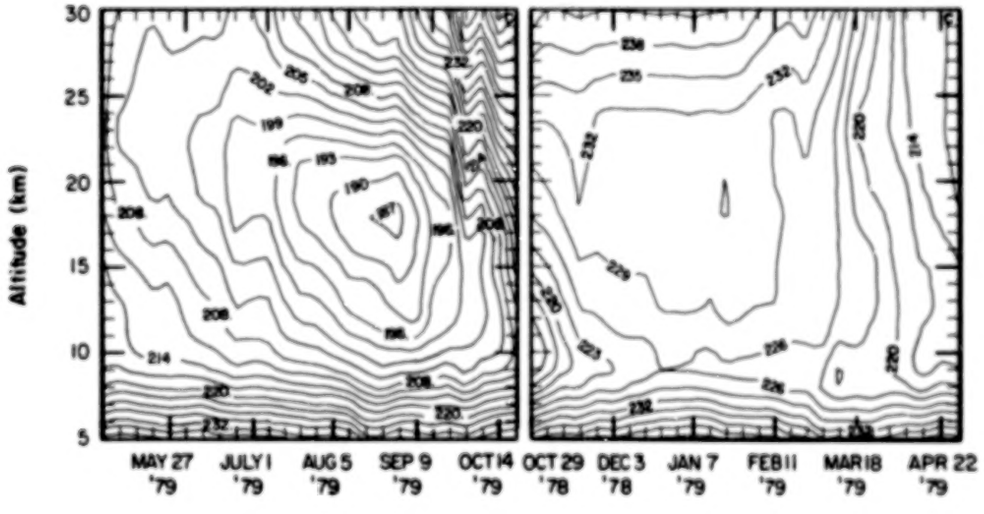

(c) Temperature field (K) at the location of the aerosol measurement. The isotherms are separated by 3 K.

Figure 10.- Southern Hemisphere weekly averaged values. The date marked on the horizontal axis is the first day of the week to which the average value corresponds. This figure covers the same time interval as figure 9 but was divided into two halves which were interchanged so that the same seasons in the two figures are aligned.

ORIGINAL PAGE IS
OF POOR QUALITY

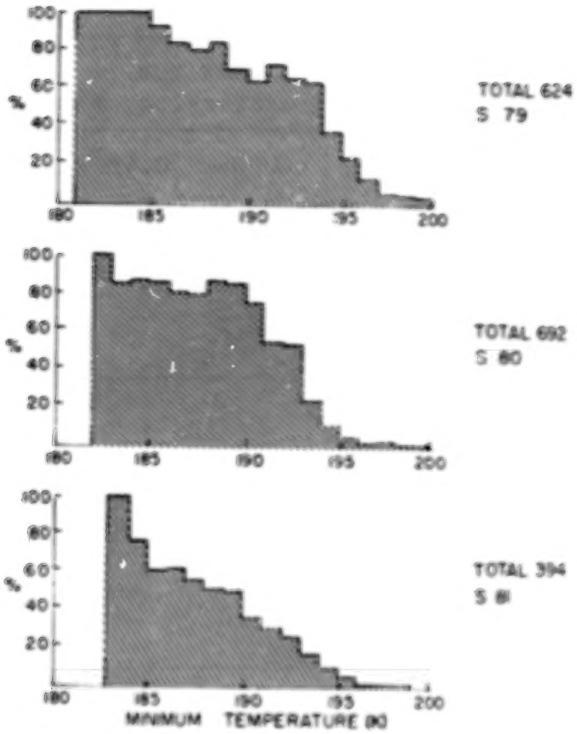

Figure 11.- Percentage of cloud occurrences as a function of minimum temperature in the Southern Hemisphere during the winters of 1979, 1980, and 1981.

profile cannot be obtained and the associated event is considered missed. In general, it was found that in the southern polar regions, a large number of the clouds extended all the way down to the tropopause and the cloud extinction consequently exceeded 10^{-2} km^{-1}. Because of these factors, it is possible to give only a rough estimate of the percentage of cloud events that exceed 10^{-2} km^{-1} in extinction. For example, in the northern winter of 1978-1979, one event out of 12 was not inverted due to very high extinction. It is not unreasonable to assume that up to 30 percent of cloud events have extinctions exceeding 10^{-2} km^{-1}.

4.3 SAGE Observations of Polar Stratospheric Clouds

The SAGE satellite sensor operated from February 1979 to November 1981. The instrument operation is similar to that of SAM II, but geographic coverage is quite different. Because of the orbital inclination of the satellite (55°), the geographic coverage of SAGE ranges from approximately 72°N latitude to 72°S latitude, reaching the peak latitudes in local summer. These maximum latitudes depend on the satellite-Sun viewing angle and vary with season. Consequently there are very few SAGE measurements near polar latitudes during the local winter. Nevertheless, two distinct PSC events have been tentatively identified in the SAGE data set. These occurred on 15 and 16 September 1979 at 60°S. The SAGE experiment retrieves aerosol extinction profiles at two wavelengths, 1.0 and 0.45 μm. The details of the experiment are described in McCormick et al. (1979), and information on the retrieval technique is given in Chu and McCormick (1979).

TABLE 1. LOCATION AND EXTINCTION OF TWO SAGE PSC EVENTS

Aerosol layer	Date	Latitude	Longitude	Maximum extinction, β		Altitude (km)	β(0.45)/ β(1.0)
				1.0 μm	0.45 μm		
PSC's	9/15/79	60.8°S	60.4°W	6.6	19.8	19.0	3.0
	9/16/79	60.2°S	62.1°W	19.2	46.1	19.0	2.4
				Extinction at 19.0 km			
Background	9/15/79	60.3°S	38.8°W	1.7	7.6	19.0	4.5
	9/16/79	60.3°S	14.8°W	1.0	4.9	19.0	4.9

Table 1 lists the locations and extinctions of the two SAGE PSC events. The ratio of the extinction at the two wavelengths is lower for the PSC events than for nearby non-PSC events. This ratio could be utilized in aerosol modeling studies to yield some information on the relative size distribution for these cloud events compared to that for background or nearby SAGE observations. The lower extinction ratio for the PSC clouds suggests the presence of larger size particles. This evaluation needs to be quantified by modeling various aerosol size distributions and performing Mie calculations for expected extinction values at wavelengths of 1.0 and 0.45 μm.

4.4 The Occurrence and Distribution of Polar Stratospheric Clouds as Determined From Nimbus 7 LIMS Data

The Limb Infrared Monitor of the Stratosphere (LIMS) experiment on Nimbus 7 was an infrared limb-viewing instrument for determining profiles of temperature, ozone, water vapor, nitric acid, and NO_2 in the stratosphere and lower mesosphere. The experiment operated from 24 October 1978 to 25 May 1979 and coverage extended from 84°N to 64°S both day and night. The Northern Hemisphere winter of 1978-1979 was monitored very well. Retrieved profiles and maps of LIMS parameters are registered with pressure, and the heights are determined by building hydrostatically from the 50- or 100-mb level using 50- or 100-mb height fields from National Meteorological Center (NMC) 65 × 65 gridded analysis products. Similar height fields are being developed using the Free University of Berlin Institute for Meteorology 50-mb analysis as a base level. These two map analyses are currently being compared.

LIMS data provide several pieces of information for the study of polar stratospheric clouds. These include (1) excellent spatial distribution information for PSC's in the Northern Hemisphere, (2) frequency and duration of specific PSC events, (3) stratospheric temperature distributions for PSC/temperature studies, and (4) concurrent water vapor fields at latitudes and longitudes adjacent to PSC's. Each of these will be discussed in turn.

ORIGINAL PAGE IS
OF POOR QUALITY

PSC's affect the measured radiances from LIMS in that they appear as an added emitter in the ozone, water vapor, and nitric acid channels. In our case this is an unwanted emitter because it contaminates the retrieved species profiles. McCormick et al. (1982) recorded a PSC event observed by SAM II near 20 km on 5 January 1979 at 65.7°N and 2°E. The associated minimum temperature was 194 K at 22 km and the temperature at maximum extinction was 196 K. Figure 12, which presents the 30-mb LIMS temperature field, shows a broad minimum of 196 K from 60°N to the North Pole

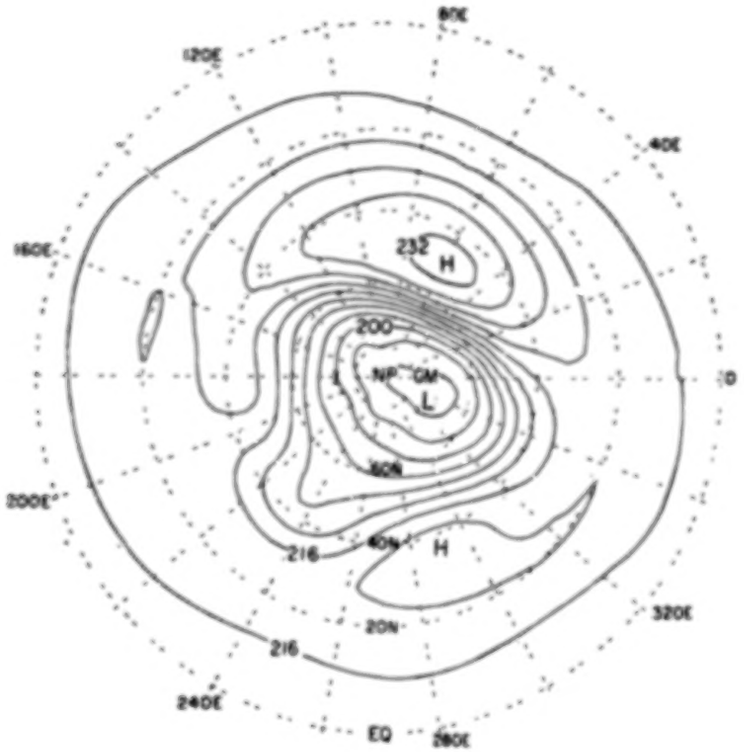

Figure 12.- Northern Hemisphere LIMS temperature field for 5 January 1979 at 30 mb. (Contour interval = 4 K.)

and from 315°E to 60°E. The 30-mb height field derived using LIMS temperature data and a National Meteorological Center (NMC) height analysis of 100 mb for tie-on purposes are shown in figure 13. The minimum height contour near the pole is 22 km (geopotential height), which is close to the altitude of the maximum extinction observed by SAM II from the PSC. Significant troughs occur at 135°E, 280°E, and 0°E.

A discussion of samples of retrieved LIMS profile results follows. A temperature profile for 5 January at 68°N, 16°E has a minimum near 20 mb of about 192 K. The associated ozone has an "anomalous" increase at 30 to 40 mb (about 20 km) and the derived water vapor also exhibits an apparent increase at about those same pressures. For optically thick PSC events, it is possible for the temperature retrieval to be biased warm by up to 1 to 2 K at about the altitude of maximum PSC emission. However, when this increased temperature is applied to a retrieval of ozone from radiances for that same scan, the effect is to reduce the magnitude of

ORIGINAL PAGE IS
OF POOR QUALITY

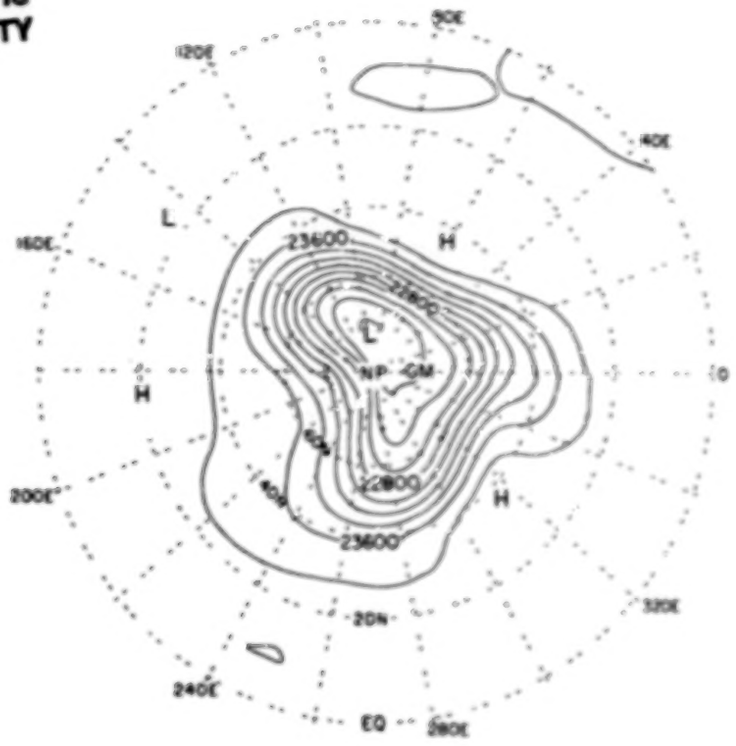

Figure 13.- Northern Hemisphere geopotential height field as derived from LIMS data on 5 January 1979 at 30 mb. (Contour interval = 200 gpm.)

the anomalously large O_3 feature, not to accentuate it. This does not affect our ability to find significant PSC features in ozone, but it may affect our ability to quantify their magnitude.

On 11 January SAM II recorded a PSC at 66.5°N, 257°E with the altitude of maximum extinction near 18 km. The LIMS ozone for 11 January at 68°N, 262°E is shown in figure 14, and a sharp apparent increase in ozone is evident. This coincided with an extensive region of temperatures below 192 K which extended over the pole. An altitude/longitude ozone cross section for the latitude zone 64°N-84°N shows a large "bullseye" centered at 280°E and 50 mb. This sensitivity of the ozone retrieval to changes in radiance ascribed to PSC's led to the development of a criterion for screening PSC's from the data. The algorithm assumed that a change in $(\Delta O_3)/O_3$ greater than +0.5 for the range from 7 to 70 mb was due to a stratospheric cloud. The vertical change in ozone (ΔO_3) was calculated by subtracting ozone between two adjacent points in altitude; thus $\Delta O_3 = O_3/z_1 - O_3/z_2$, where $z_2 > z_1$. The vertical distance between these two points is approximately 1.5 km. The ΔO_3 is then divided by the ozone value at z_2 in the ratio test for a PSC.

The search for PSC's was limited to latitudes north of 40°N. In practice, the algorithm was applied in two steps. If the calculated ratio was greater than 2.0, those data points were flagged as "bad" in the archived data tapes. A second pass through each ozone scan was then made on the remaining "good" profiles or partial profiles, using the 0.5 value as the threshold. If that value was exceeded for any adjacent pair of points, a PSC flag was set for the point at the higher altitude of those two points in the archived data tapes. Thus, any large PSC signatures

ORIGINAL PAGE IS
OF POOR QUALITY

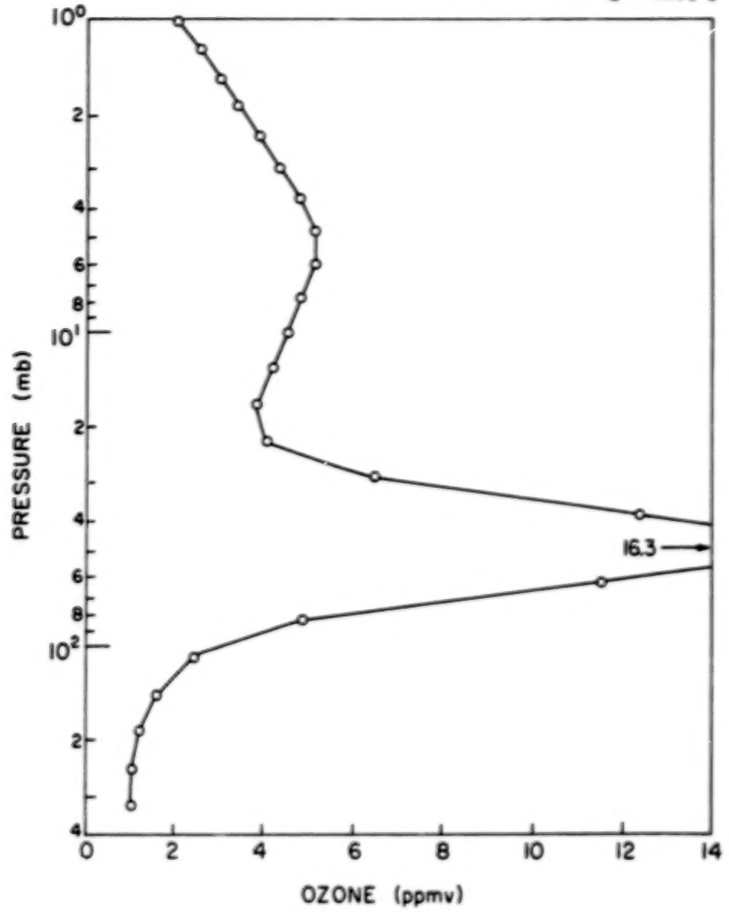

Figure 14.- Retrieved LIMS ozone profile for 11 January 1979 at 68°N, 258°E. Evidence of perturbation due to PSC begins at 22 mb and is a maximum at 49 mb.

(i.e., ratios greater than 2.0) were not tagged with a PSC flag. Nevertheless, these anomalous events were labeled as "bad" profiles and were not included in the development of fields of temperature or species.

By using the ratio criterion of greater than 0.5 but less than 2.0, the following occurrences of PSC's for 5 and 11 January (listed in table 2) were found. Note that there are more events indicated from the LIMS data set than from the SAM II observations, and that the LIMS sightings are concentrated in the 68°N to 80°N latitude range. This is to be expected because the LIMS coverage and sampling are greater than those of SAM II, which operates in the occultation mode. Of course, LIMS may be sampling the same overall PSC several times on a given day, so we could assume that LIMS is experiencing several sightings of the same feature. This can be checked by looking at the latitude and longitude of each sighting. The indicated pressure in table 2 is the level just above that at which the cloud is first sighted as one proceeds along the scan toward the ground. One problem that arises in a LIMS retrieval of a radiance profile that contains PSC emissions is that the extra emission is assumed to have been from a homogeneous distribution of the emitter in the tangent shell. Generally this is not the case for a PSC event, and therefore the indicated latitude and longitude of the extra emitter can be slightly in error. A similar problem could exist for a SAM II retrieval of PSC extinction.

There were no significantly sharp PSC signatures registered by LIMS from days 354 to 360, days 6 and 7, and day 15 (over the period from days 354 to 18).

TABLE 2. PSC SIGHTINGS BY LIMS AND SAM II

Sensor	Latitude (°N)	Longitude (°E)	Initial pressure of sighting (mb)
		5 January 1979	
LIMS	72	22	24
LIMS	76	25	27
SAM II	65.7	2	--
		11 January 1979	
LIMS	68	258	22
	68	271	23
	72	281	17
	72	274	23
	76	302	18
	76	276	21
	76	280	18
	76	254	29
	80	265	21
	80	237	29
	80	317	25
	80	292	24
SAM II	66.5	257	--

Even though the foregoing simple PSC algorithm can be applied to screen from the data those parts of scans that are obviously affected by PSC's, some cloud-contaminated data will still remain. In an attempt to eliminate all cloud effects, an alternate approach was taken in this report. Because the areas of contamination stand out as centers of high apparent O_3 mixing ratio on a Northern Hemisphere map of the lower stratosphere, we have mapped the data ignoring the PSC flags. The mapping was performed using a sequential optimal estimate approach (Kalman filter) for each 4 degrees of latitude.

ORIGINAL PAGE IS
OF POOR QUALITY

Initially we can compare the locations of PSC sightings in table 2 with the 30-mb temperature fields in figures 12 and 15. The correlation with regions of cold temperature is very good. Ozone maps at 30 mb have been plotted from the Fourier coefficients obtained with the Kalman filter technique. Figure 16 shows the ozone map at 30 mb for 5 January, and the effect of PSC features shows up clearly at 0°E, 70°N. The individual scans that were contributing to the apparent ozone increase were investigated, and a subjective maximum value of 5.0 ppmv was imposed to delete those profile segments from the data set from 280°E to 0°E and 50°N to 80°N and from 0°E to 60°E and 65°N to 80°N. Figure 17 shows the result of mapping the 30-mb field from the new set of Fourier coefficients. Removal of the cloud features is good, although some effects of the cloud may remain. One could argue for the removal of all scans from the area of suspected contamination, no matter what mixing ratios were present. Such tactics result in regions devoid of data and can give O_3 fields that are slightly unrealistic because of interpolation across longitudes that are far apart.

In considering the day-to-day variability of the apparent enhancements in ozone at 30 mb from 25 December 1978 to 16 January 1979, one can find that the occurrence of the PSC's is probably less transient than would be supposed from the data in table 1 of McCormick et al. (1982). For the period from 25 December to 15 January, only 25 December and 6 and 7 January seemed to be free of these features, although the strength of the features varied considerably. The location of PSC emission moved from 76°N and 80°N at 0°E on 27 December to 72°N and 270°E on 14 January. At 30 mb, features were most pronounced and extensive on 2-4 and 8-12 January during that 21-day period.

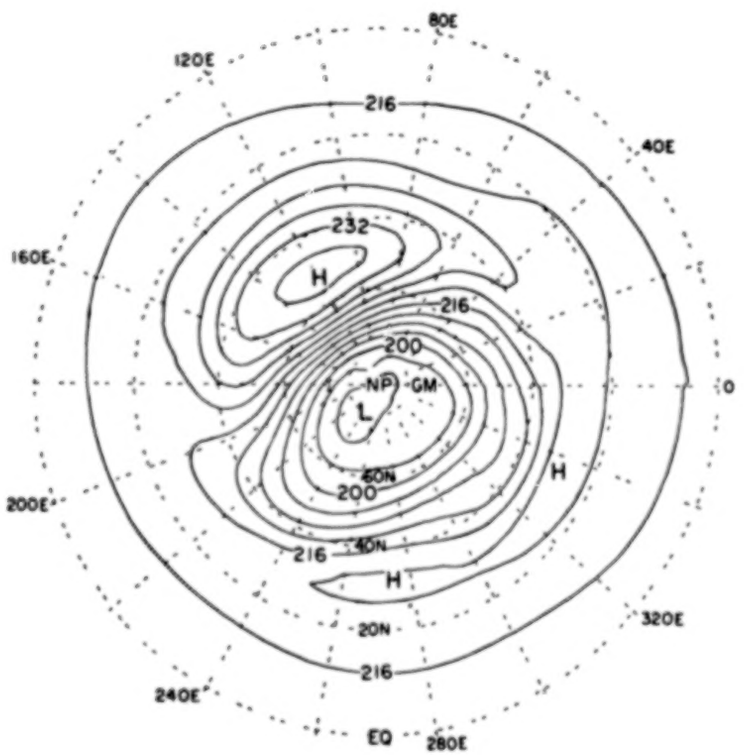

Figure 15.- Northern Hemisphere LIMS temperature field for 11 January at 30 mb. (Contour interval = 4 K.)

ORIGINAL PAGE IS
OF POOR QUALITY

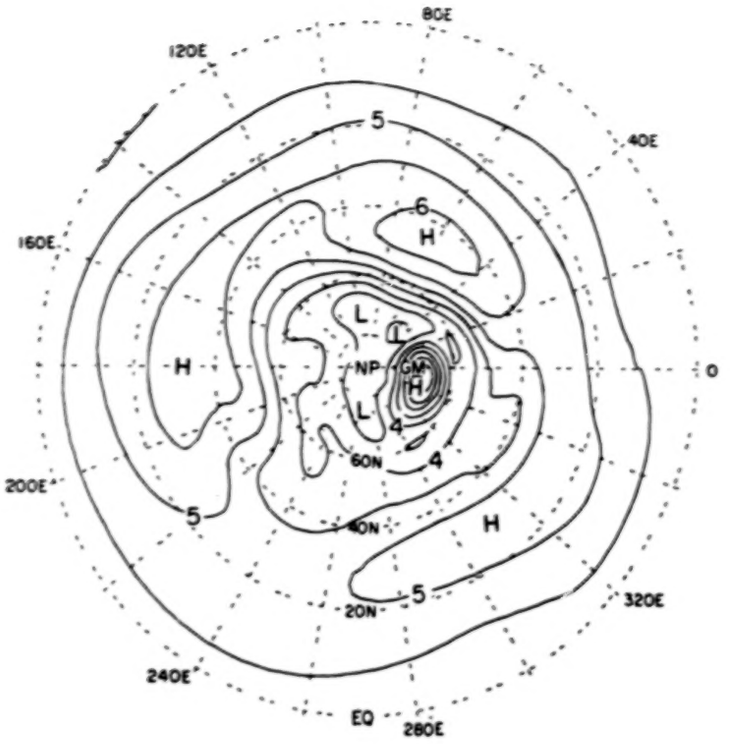

Figure 16.- Northern Hemisphere LIMS ozone field for 5 January at 30 mb. (Contour interval = 0.5 ppmv.).

Figure 17.- Northern Hemisphere LIMS ozone field for 5 January at 30 mb after subjective removal of significant PSC signal. (Contour interval = 0.5 ppmv.)

TABLE 3. LIMS AND SAM II SIGHTINGS OF PSC's AT 30 mb

Latitude (°N)	Longitude (°E)	Observations
	19 January	
64	42	LIMS PSC flag
68	40	LIMS PSC flag
68	43	SAM II (McCormick et al., 1982)
	23 January	
48	292	LIMS PSC flag
56	78	LIMS PSC flag
68	333	SAM II (McCormick et al., 1982)

Table 3 compares other PSC events noted at 30 mb by LIMS for 19 and 23 January with the events in figure 4 of McCormick et al. (1982). The 19 January LIMS PSC events compare very well with SAM II observations, whereas the 23 January events do not, at least at 30 mb. A closer look at the two flagged profiles for 23 January indicates that these scans occur in regions of very strong horizontal temperature gradients and that the retrieved temperatures at 30 mb were above 200 K. Problems in inverting these two profiles began at altitudes above 30 mb, and the PSC flags occurred at 8 mb and 10 mb for those two scans. These ozone anomalies were the result of faulty temperature retrievals, not PSC's. However, substantially high apparent O_3 values at 30 mb did occur at 64°N, 11°E and 64°N, 345°E, and both locations compared well with the sighting by SAM II and the occurrence of a broad temperature minimum (<196 K) stretching from 60°N to 75°N and 300°E to 80°E. Lowest temperatures (<192 K) occurred at 62°N, 320°E and 75°N, 30°E. Thus, the relationship between PSC's and cold temperatures is still supported.

Water vapor mixing ratios are estimated for 6 and 7 January, when pronounced PSC's were not noted in the ozone or water vapor data. At 30 mb and at 64°N and 68°N the zonal mean mixing ratio was 4.5 ppmv with a wavenumber 1 amplitude of 0.75 ppmv. The significance of this wavenumber 1 feature will require further investigation. The water vapor uncertainty at 30 mb has been estimated at ±24 percent.

At 100 mb and at 68°N the zonal mean water vapor was 5.6 ±0.4 ppmv on day 6 and 5.9 ±0.8 ppmv on day 7. However, the estimated uncertainty of LIMS water vapor at 100 mb is about 40 percent. At the same latitudes for May, when temperatures are warmer in the lower stratosphere, the derived water vapor mixing ratio was only about 4.9 ppmv at 100 mb. Such small but important seasonal differences in water vapor at 100 mb are currently under study, particularly to determine whether such trends in the data can be believed.

With regard to saturation with respect to ice, the LIMS data for 18 January at 72°N, 22°E, where SAM II observed large extinction values, were evaluated. LIMS temperature minima approached 186-188 K at 30 mb in the region of the cloud. Such temperatures at 30 mb would lead to saturation if the water vapor mixing ratio were in the range of 5.5 to 7.8 ppmv. Observed mixing ratios approached the lower value of 5.5. Thus, PSC theory and observation seem to be in close agreement.

5. THE ROLE OF POLAR STRATOSPHERIC CLOUDS IN ATMOSPHERIC PROCESSES

5.1. Effect of Polar Stratospheric Clouds on the Global Radiation Balance

Aerosols influence the regional and global radiation balance by interacting with solar and thermal radiation. The resulting changes in atmospheric heating rates lead directly to temperature changes, which in turn can affect atmospheric circulation. Naturally, the modification in heating rate needs to be above a certain threshold value, which can be defined in terms of the natural variability of the atmosphere, before such modifications are considered to be significant.

Because PSC's occur in the winter polar stratosphere, their interaction with thermal radiation represents their key potential impact on the radiation balance. Such an interaction can lead to either a net cooling or a net warming of the layers of the atmosphere in which the PSC's reside, depending upon the relative magnitudes of warming (induced by the absorption upwelling thermal radiation) and cooling (caused by radiation to atmospheric layers above and below). This competition between warming and cooling is affected by the temperature contrast between the clouds and the effective radiating levels beneath them and upon such cloud microphysical properties as size and composition. When the temperature contrast is small, net cooling dominates, and when it is large, the reverse is true. The microphysical properties of the clouds determine both the magnitude of the cloud's infrared opacity and its spectral dependence. The latter is important because absorption at long wavelengths acts to cause a net cooling, whereas absorption at short wavelengths acts to cause a net warming.

In addition to influencing the radiation budget by interacting directly with thermal radiation, as described above, PSC's can also affect the radiation budget in an indirect way. If their continued formation during the polar winter results in a depletion of stratospheric water vapor, this altered amount of water vapor can by itself cause a modification of stratospheric heating rates, again almost entirely at thermal wavelengths.

Table 4 illustrates the dependence of the change in the net heating rates on some key meteorological and microphysical parameters, namely the temperature structure ΔT, the mean particle radius $\bar{r}$, the optical depth τ at a wavelength of 1 μm, and the water vapor mixing ratio α. Calculated values are based on a typical SAM II observation of a PSC event during September in the Antarctic region. At this time the cloud had an optical depth of about 5×10^{-2} at a wavelength of 1 μm, a value representative of Antarctic PSC's in general. The ground temperature was set equal to 196 K and the cloud temperature was 183 K, with a prominent inversion close to the surface, in accord with profiles obtained at the South Pole.

TABLE 4. EFFECT OF PSC PARAMETERS ON THE HEATING RATES IN POLAR WINTER STRATOSPHERE[a]

Case number	τ	$\bar{r}$, μm	α, ppm	Temperature profile[b]	Heating rate at cloud center (K day^{-1})
1	0	-	3	Standard	-0.298
2	0	-	1.5		-0.267
3	0	-	6		-0.346
4	0	-	4.4		-0.321
5	0	-	Saturation[c]		-0.252
6	10^{-2}	0.056			-1.330
7	"	0.18			-0.318
8	"	0.56			-0.264
9	"	1.00			-0.264
10	"	3.20			-0.309
11	"	10.00			-0.382
12	0	-	3		-0.296
13	10^{-2}	0.056			-1.370
14	10^{-1}	"			-1.960
15	10^{-2}	1.00			-0.310
16	10^{-1}	"			-0.411
17	10^{-2}	10.00			-0.428
18	10^{-1}	"			-1.360
19	0	-		No inversion	-0.242
20	10^{-2}	0.056			-0.323
21	"	1.00			-0.242
22	"	10.00			-0.262

[a]Based on calculations by Pollack and McKay (1984).
[b]The assumed temperature profile is based on data obtained at the South Pole over the last 20 years and compiled by A. Hogan. This profile has a prominent inversion close to the surface.
[c]The water vapor profile follows a saturation vapor pressure curve throughout the PSC.

This table shows that for many situations, the model-evaluated changes in heating rates due to the PSC's are nontrivial. (Compare, for example, case 4 (no PSC effects) with case 5 (just H_2O) and case 6 (H_2O and particle effects).) However, for particle sizes on the order of 1 μm (perhaps the most likely size), the direct effects of PSC's are substantially reduced by the 12- and 45-μm absorption bands, which produce comparable changes with opposite sign. (Compare cases 5 and 9.) Significantly larger direct effects characterize both much smaller and much larger particles. (Compare case 5 with cases 6 and 11.) The presence of a large temperature inversion near the surface results in greater direct effects because there is a smaller temperature contrast and hence cooling can more easily dominate. (Compare cases 5-11 with cases 19-22.) Finally, in a number of situations, the indirect effects of the cloud (i.e., its alteration of the water vapor abundance in the cloud region) are more important than its direct effects. (Compare case 4 with case 5 (indirect effects) and case 5 with cases 6-11 (direct effects).)

In order to determine which, if any, of the calculated changes in heating rates are climatically significant on a regional scale, one needs to compare the implied change in temperature with the natural variability of stratospheric temperature in the winter polar region. General circulation model (GCM) simulations, described below, indicate that the natural variability in temperature is about 1 K. Since the radiative time constant for the winter polar stratosphere is about 100 days, the threshold value for climatological significance is about 0.01 K day^{-1}. Many of the cases in table 4 are above this threshold. Thus, if PSC's cause a significant depletion of water vapor in the winter polar region and/or if they occur frequently enough with certain particle sizes or large enough optical depths ($>10^{-1}$), they could impact the radiation budget of the winter polar stratosphere in a nontrivial way.

Because PSC's occur infrequently in the north polar region, they are not likely to cause a significant depletion of water vapor there or to affect the regional radiation balance. But PSC's in the Antarctic do occur often enough (~40% of the time in the winter) for their effects on the regional radiation budget to remain an open question. However, no significant modifications of the global radiation budget are expected.

5.2 A Three-Dimensional Model Sensitivity Study of the Impact of Polar Stratospheric Clouds on Radiation Balance and Climate Feedbacks

The order of magnitude of the potential effects of PSC's on the planetary radiation balance was investigated by means of an extreme experiment with the three-dimensional global climate model (Model II) described by Hansen et al. (1983). The experiment involved adding ice aerosols to layer 8 of this 9-layer model, where layer 8 is at approximately the 100-mb level with a thickness of about 70 mb.

The experiment was an exaggeration in the sense that the visible optical thickness of the aerosol layer was taken as 0.3; this appears to exceed typical measured values by a factor of 3 to 10, although measurements during the polar night, when temperatures may be lowest, are not available. The experiment also assumed the particles to be large (mean radius ~25 μm), so that the optical thickness would be similar in the visible and infrared regions. Full Mie scattering/ absorption calculations were performed, including the spectral dependence of ice optical constants. PSC's were assumed to exist 40 percent of the time for the region 63°S-90°S during the 4-month period from May to August. PSC's were assigned at

ORIGINAL PAGE IS
OF POOR QUALITY

a given gridbox based on the temperature in level 8, using the observed probability distribution of McCormick et al. (1981).

In the first (noninteractive) version of the experiment, the cloud assignment was based on the temperatures in the control run. In the second (interactive) experiment, the cloud assignment was based on the temperatures computed in the experiment run (i.e., the cooling or heating due to the PSC's was allowed to affect the existence of the PSC's).

The temperature changes caused in the model by adding the ice aerosols are shown in figure 18 for each of the four months of the run, integrated over the polar cap region 63°S-90°S. A cooling of approximately 2°C occurs in the layer with aerosols in the noninteractive version of the experiment. This cooling causes the PSC occurrence to increase to 64 percent in the interactive version, a strong positive feedback effect. Figure 18 also indicates a tendency for cooling to occur in the model in layers below the PSC aerosol layer.

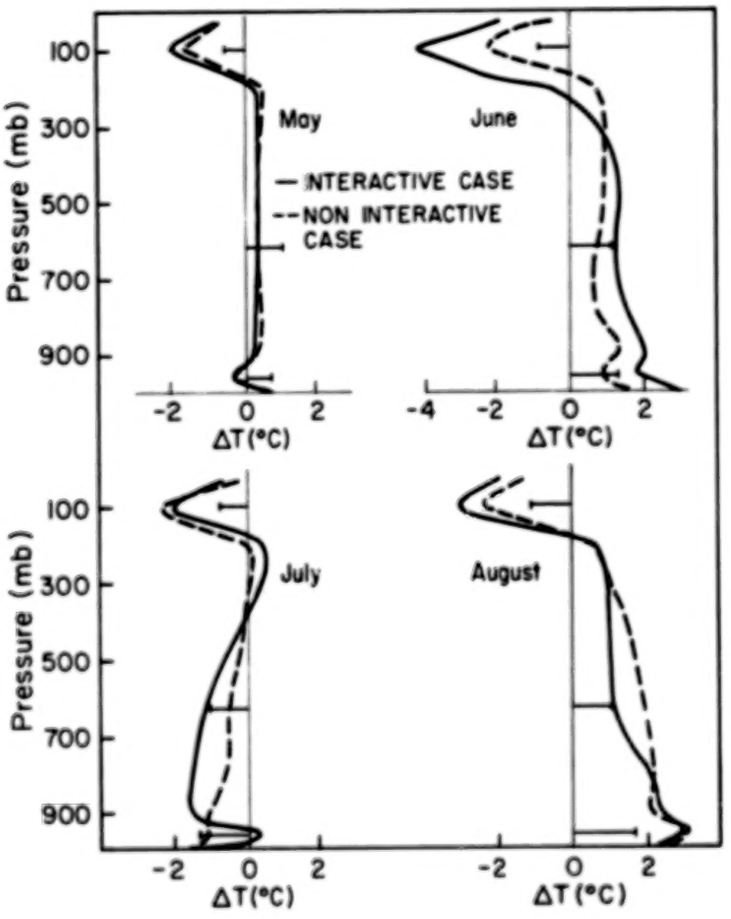

Figure 18.- Temperature change over Antarctica as a result of adding cirrus ice aerosols at the 100-mb level, as simulated with the GISS 3-D GCM (Hansen et al., 1983). The interannual variability (standard deviation) of the temperature in the 5-year control run of the model is indicated by horizontal bars.

ORIGINAL PAGE IS
OF POOR QUALITY

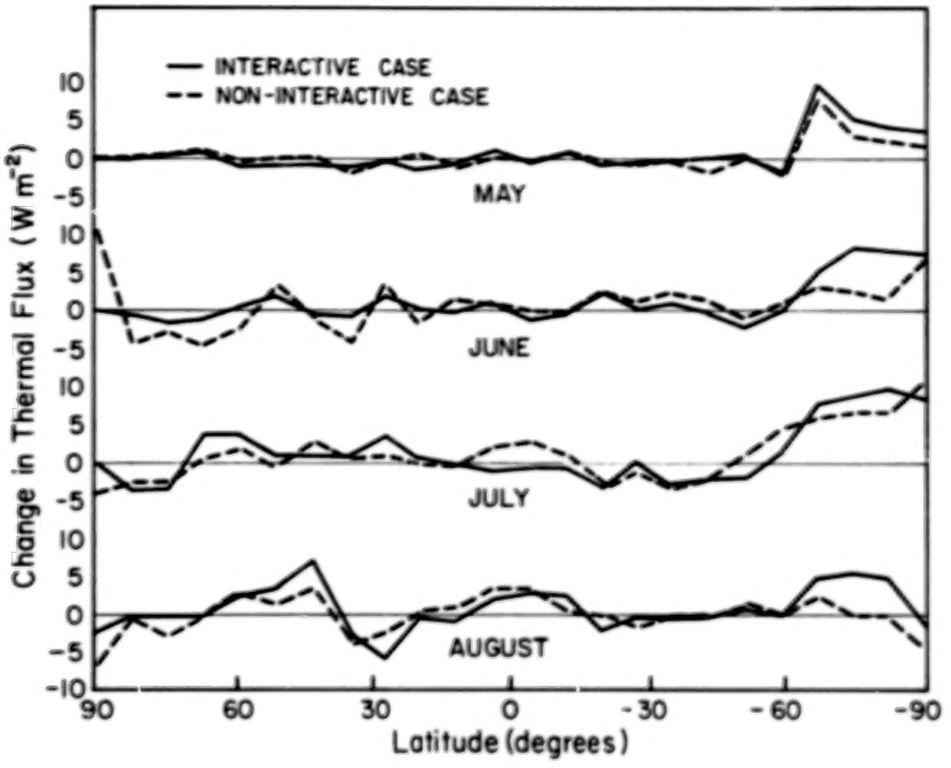

Figure 19.- Reduction in thermal flux to space due to addition of cirrus clouds over Antarctica at 100 mb level, as simulated with the GISS 3-D GCM. The interannual variability (standard deviation) of the thermal flux in the 5-year control run of the model (with fixed ocean surface temperature) is indicated by vertical bars.

The changes in the radiation balance at the top of the atmosphere are shown in figure 19 for both versions of the experiment. For the latitudes at which aerosols were added, the thermal flux to space is reduced on the order of 5 W m^{-2}. Climate models yield an equilibrium change in surface temperature of about 1°C per W m^{-2}. The implied surface warming effect would be reduced by the fact that PSC's occur seasonally, and the regional effect would be reduced by exchange of air with other latitudes. However, for the assumed PSC optical thickness of 0.3, there is a clear impact on the radiation balance.

PSC phenomena may provide a valuable opportunity to study climate feedback processes. Cloud-climate interactions are one of the major uncertainties in our present understanding of the global climate system. The foregoing results suggest that in the winter, the PSC's may exhibit a strong positive radiative feedback effect in which the introduction of PSC's causes stratospheric cooling and thus increases the amount of PSC's. Of course, there are other possible feedbacks, such as the reduction of stratospheric water vapor by the formation and fallout of ice particles. However, this feedback was excluded in the foregoing experiment by arbitrarily keeping the water vapor abundance fixed. Such feedback processes may be investigated with more realistic modeling and comparison with the full range of available data, particularly the seasonal changes of PSC's. Although some useful studies of feedback processes could be made with existing data, it is important to

obtain more precise information on the physical characteristics of the PSC's (for example, particle size, optical depth, and full spatial extents) as input for the studies.

5.3 Polar Meteorology

The observational data presented at the workshop indicate that stratospheric clouds are observed frequently over the Southern Hemisphere in winter, but there are relatively infrequent sightings over the Northern Hemisphere. This increase in frequency of observation is apparently due to the large areas of the southern stratosphere in which temperatures of -80°C or colder occur in winter and to the relatively long life of the southern polar vortex, which yields 6 or 8 more weeks of cold tropopause temperatures in the Southern Hemisphere.

Comparisons of the extrapolated air temperature with cloud observations indicate that frequent and dense cloud observations coincide with air temperatures of approximately -80°C (193 K) or lower. Analysis of available meteorological sounding data indicates that such temperatures are common over Antarctica during austral winter, and stratospheric clouds may extend well beyond the latitude limits from which they can be observed by satellite instruments.

There is a scarcity of meteorological data (especially temperature soundings) between 50°S latitude and the Antarctic coast. The densest series of such observations was made during the IGY of 1957-1959. An important and unbroken series of soundings has continued at the South Pole and on the periphery of Antarctica since that time. Data from the network of IGY stations have been analyzed and presented in map folio series by Weyant (1966). The locations of the stations are shown in figure 20, which also shows the axes from which mean cross sections of tropopause temperature have been extracted. These cross sections are shown in figures 21 and 22. The cross section along a line from Puerto Montt through the South Pole to New Amsterdam Island (fig. 21) shows a symmetric variation of tropopause temperature with latitude. A similar cross section along the date line from Raoul Island through the South Pole and along the Greenwich meridian to Capetown (fig. 22) shows slightly warmer tropopause temperatures at equal latitude on the date line side. This is in agreement with seasonal isobaric analyses also given by Weyant, and indicates a flow into the Antarctic near the tropopause, over Victoria Land. Stanford's (1977) analysis of "stratospheric cyst" from historical surface observations shows a very high frequency of cloud observations by the British-Swedish-Norwegian party at Maudheim, on the Antarctic coast just west of this line. Mother-of-pearl cloud observations are also common at McMurdo station, which is also along this line.

McMurdo is at the edge of astronomical twilight in winter, allowing observation of clouds over Victoria Land. It is possible that stratospheric clouds are frequent over the interior of Antarctica but are not observed because temperatures below -80°C accompany continuous darkness.

ORIGINAL PAGE IS
OF POOR QUALITY

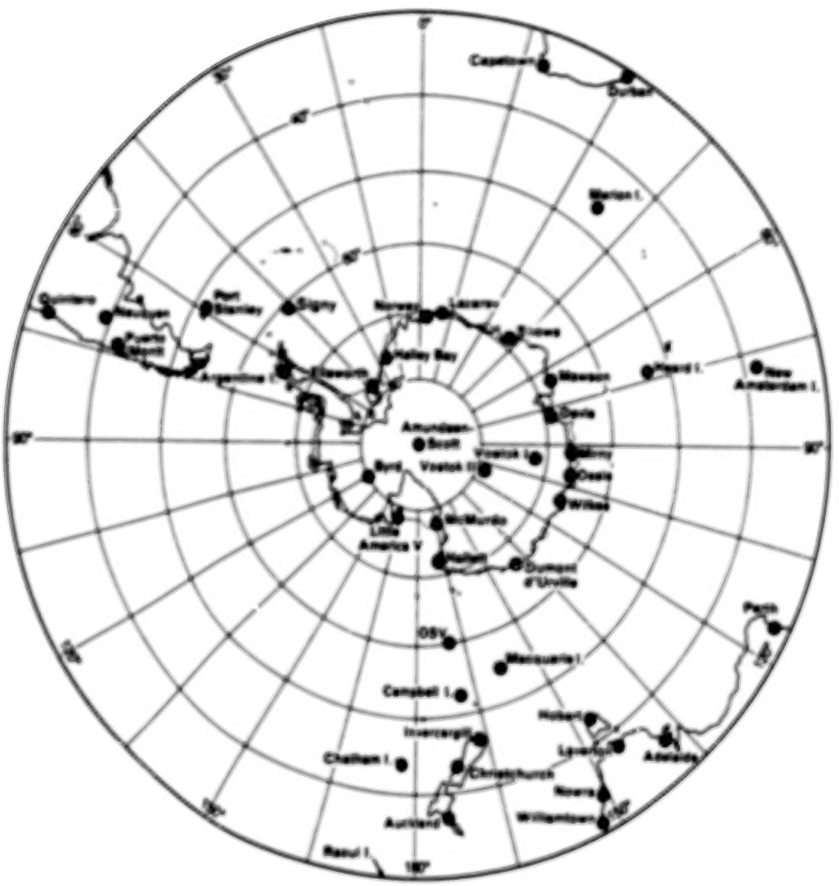

[1] Environmental Data Service, Environmental Science Services Administration, Formerly Office of Climatology, United States Weather Bureau
[2] Polar Research Group, Environmental Science Services Administration

Figure 20.- Antarctic IGY stations (Weyant, 1966). The dark lines are the axes from which mean cross sections of tropopause temperatures have been taken.

ORIGINAL PAGE IS
OF POOR QUALITY

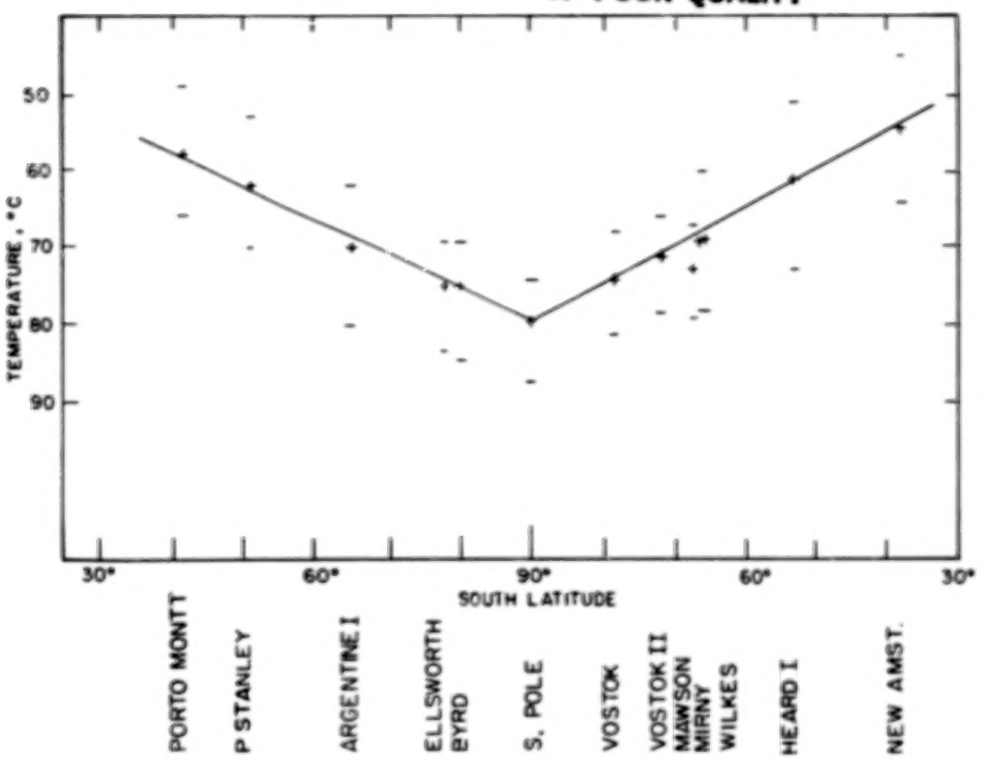

Figure 21.- Tropopause temperature as a function of latitude in cross section from Puerto Montt to New Amsterdam Island (August mean).

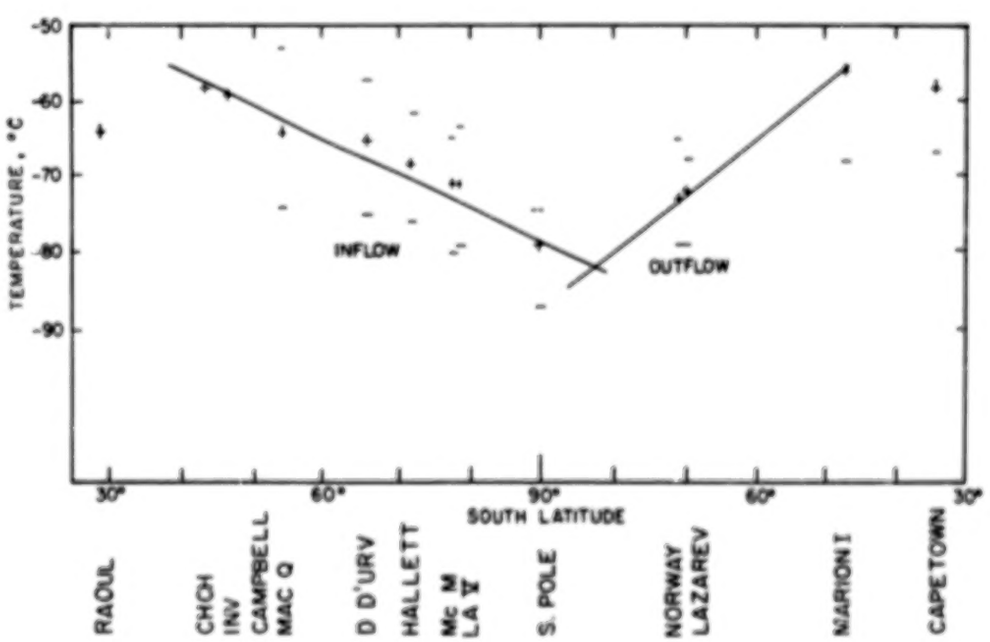

Figure 22.- Tropopause temperature as a function of latitude in cross section from Raoul Island to the South Pole then along the Greenwich meridian to Capetown.

ORIGINAL PAGE IS
OF POOR QUALITY

J. A. Samson (1983) has recently analyzed the radiosonde data from the South Pole and calculated the mean and extreme temperatures and frequency of observed wind direction at several levels from the surface (2865 m at the South Pole) to the 30-mb level. The mean and extreme temperatures as well as wind sectors from which one-half the winds arrive at the South Pole station are shown in figure 23 for several

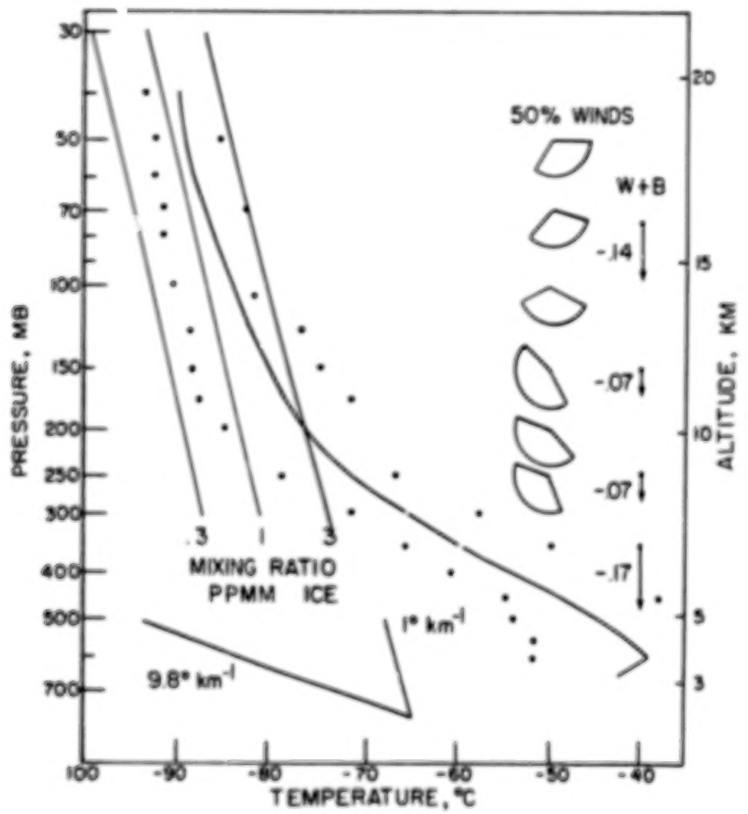

Figure 23.- Mean and extremes in temperature profile at South Pole station (1961-1977). Also given are 50 percent wind sectors at various levels.

levels above 300 mb. The mean temperature structure over the pole is characterized by a strong temperature inversion just above the surface and a near adiabatic lapse rate above 500 mb. There is no sharp temperature inversion to delineate the tropopause. Lower tropospheric winds are generally from the direction of the Weddell Sea (i.e., along about 60°W longitude); winds above 100 mb are from the date line direction, and near calm prevails between 300 and 100 mb. This structure is in agreement with Danielsen's (1982) analysis, which shows advection inward at 50 mb, and subsident outflow all around Antarctica in the lower stratosphere.

The data contain an artifact which biases the mean air temperature toward warmer-than-actual values and causes more frequent reporting of the warmer wind direction. Figure 24 shows the number of balloon ascents reaching a given minimum temperature for August launches during 1961-1976. About 80 percent reached the -80°C level. A review of all August soundings from 1974 to 1982 shows that this is not a random sampling of upper-level temperatures, but is affected by the quality of the balloon batches received at the South Pole station. As an example, many ascents

ORIGINAL PAGE IS
OF POOR QUALITY

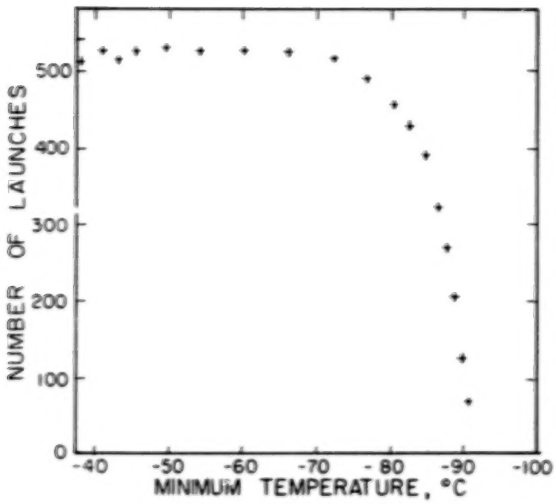

Figure 24.- The number of balloon sounding events which reach a given minimum temperature is plotted for August launches during the years 1961-1976.

reached -90°C in 1974, whereas no balloon reached -80°C in 1978, even though in some launches two 1200-g balloons were pre-warmed and warm aged (S. Barnard, private communication). An apparently very good lot of balloons was in station in 1981. These usually penetrated the coldest layer and showed warming above the 30-mb level.

Three soundings, obtained on 3, 20, and 24 August 1981, are shown in figures 25 through 27 to illustrate various temperature structures present over the interior of Antarctica. The sounding of 3 August (fig. 25) shows a relatively strong wind at the surface, about 20°C of inversion near the surface, and weak winds along the date line at most of the levels above the surface. A cooler surface and stronger inversion were present on 20 August (fig. 26) with slightly stronger winds and cooling to the 50-mb level. Figure 27, for 24 August, illustrates a fairly frequent pattern, with a wind from grid north at the surface, winds from the Weddell Sea in the troposphere, near calm in the lower stratosphere, and slightly stronger winds in the warming layers above 30 mb.

The circumpolar vortex in the Southern Hemisphere is associated with a long, cold period in the upper troposphere and lower stratosphere. August in the Southern Hemisphere is astronomically equivalent to February in the Northern Hemisphere, but the August temperatures shown from the South Pole are much colder than those observed in February at stations in the Canadian Arctic, which report the coldest Northern Hemisphere temperatures. The circumpolar vortex apparently inhibits upper level mixing and exchange in the Southern Hemisphere, whereas such exchange is common in late winter in the Northern Hemisphere.

The lower stratosphere begins to warm over Antarctica during late September and early October, and temperatures below -75°C are seldom observed after mid-October. However, on some occasions the jet stream may penetrate the interior of Antarctica, bringing lower stratospheric cooling concurrent with the demise of the polar vortex. An extreme event of this kind occurred in early November 1982, when temperatures of -85°C were measured over the South Pole, as shown in the time cross section in figure 28.

ORIGINAL PAGE IS
OF POOR QUALITY

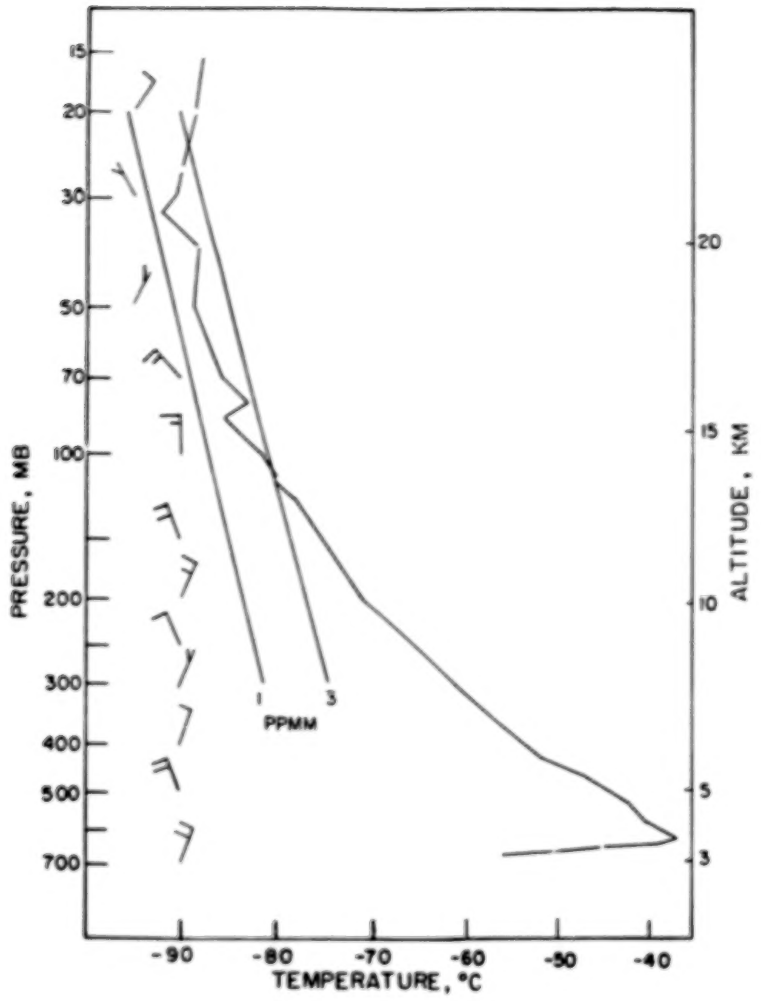

Figure 25.- Temperature sounding at 2300 GMT for 3 August 1981 from South Pole. Also shown are pertinent wind data.

ORIGINAL PAGE IS
OF POOR QUALITY

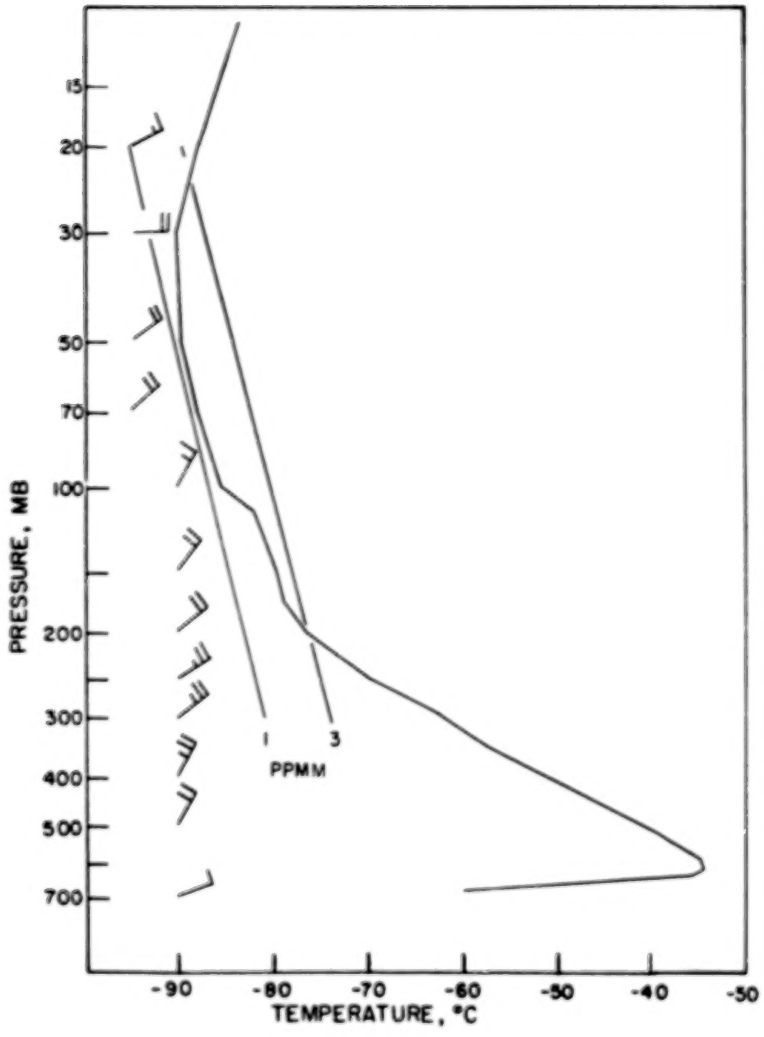

Figure 26.- Temperature sounding at 2300 GMT for 20 August 1981 from South Pole. Also shown are pertinent wind data.

ORIGINAL PAGE IS
OF POOR QUALITY

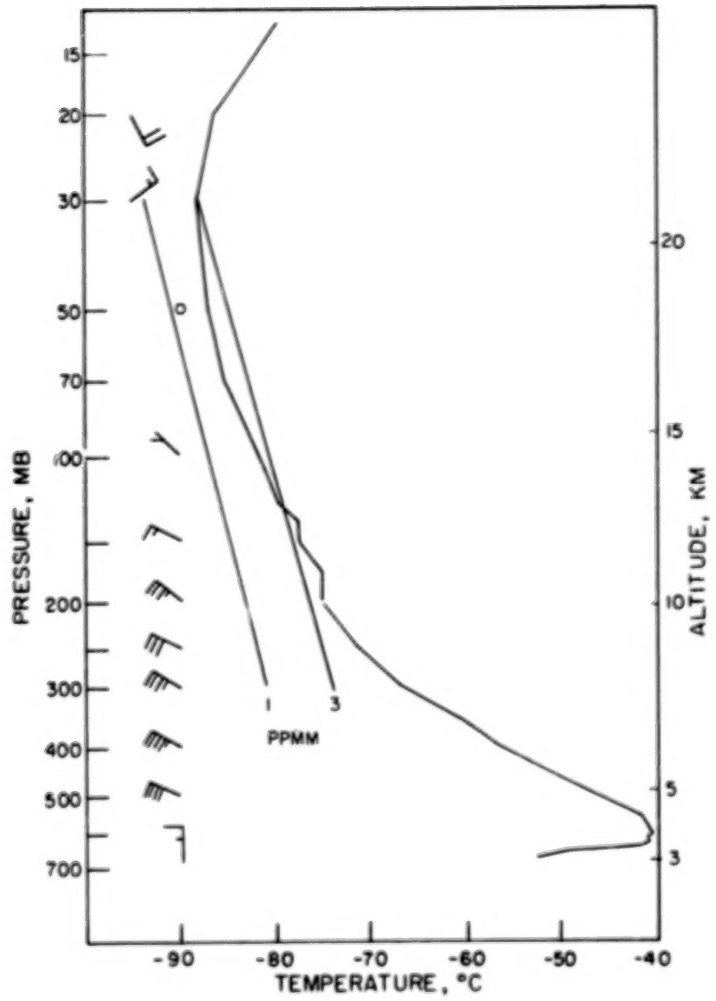

Figure 27.- Temperature sounding at 2300 GMT for 24 August 1981 from South Pole. Also shown are pertinent wind data.

ORIGINAL PAGE IS
OF POOR QUALITY

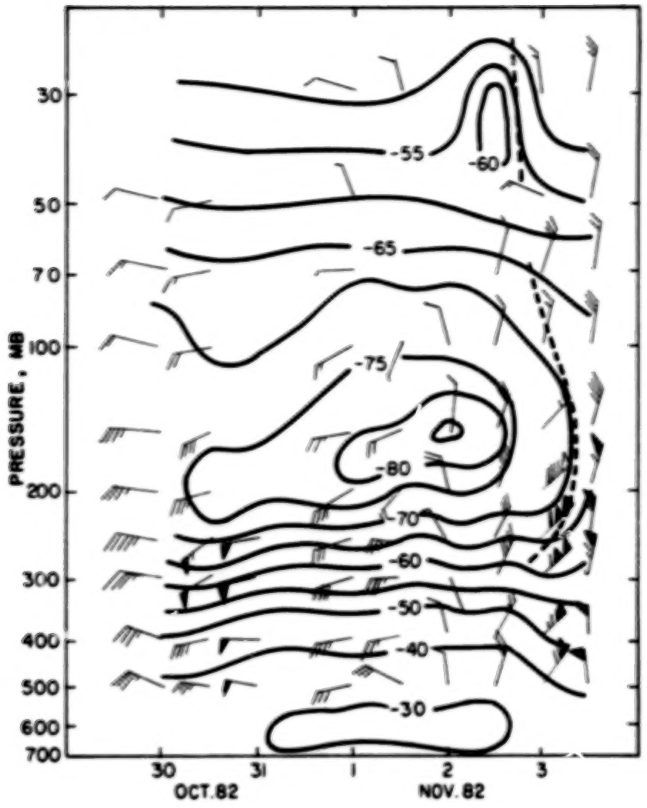

Figure 28.- Temperature-height-time cross section at Amundsen Scott Station, Antarctica, October-November, 1982. Wind data are also shown.

5.4 Potential Surface Effects of Polar Stratospheric Clouds

We consider possible surface effects of PSC's in the context of Antarctic radiation climate research. The Geophysical Monitoring for Climate Change (GMCC) division of NOAA's Environmental Research Laboratory has been making long-term, continuous measurements of particle light scattering, condensation nuclei, solar radiation, and several trace gases, including O_3 and CO_2, at the NSF South Pole station. In addition, outside investigators have measured the chemistry of aerosols over a period of several years and studies of ice crystal formation processes have been conducted. (See, e.g., Harris and Bodhaine, 1983; Mendonca, 1978.) Studies of the radiation balance and heat budget were conducted at various intervals in the past to understand the climatic role of heat and moisture transport into the inner parts of Antarctica. Figures 29 through 33 illustrate some of the South Pole measurements.

ORIGINAL PAGE IS
OF POOR QUALITY

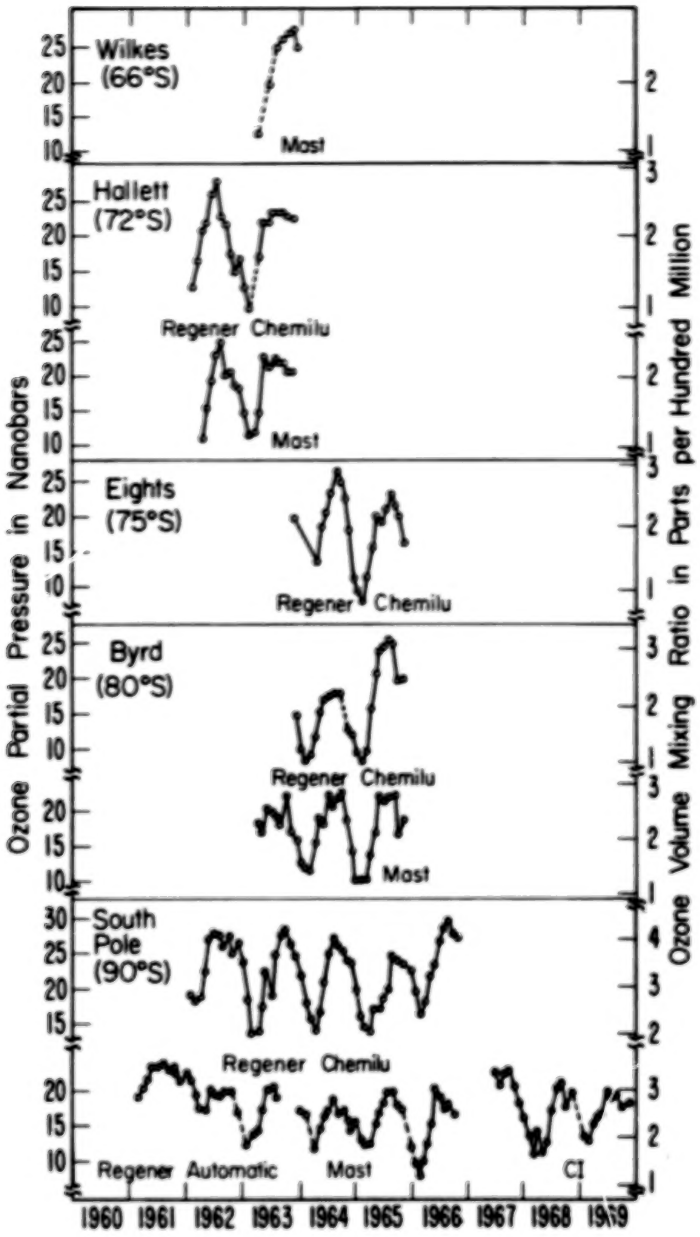

Figure 29.- GMCC data for various Antarctic stations showing monthly average surface ozone partial pressure and ozone volume mixing ratio for intervals spanning 1960-1969. (From Mendonca, 1978.)

ORIGINAL PAGE IS
OF POOR QUALITY

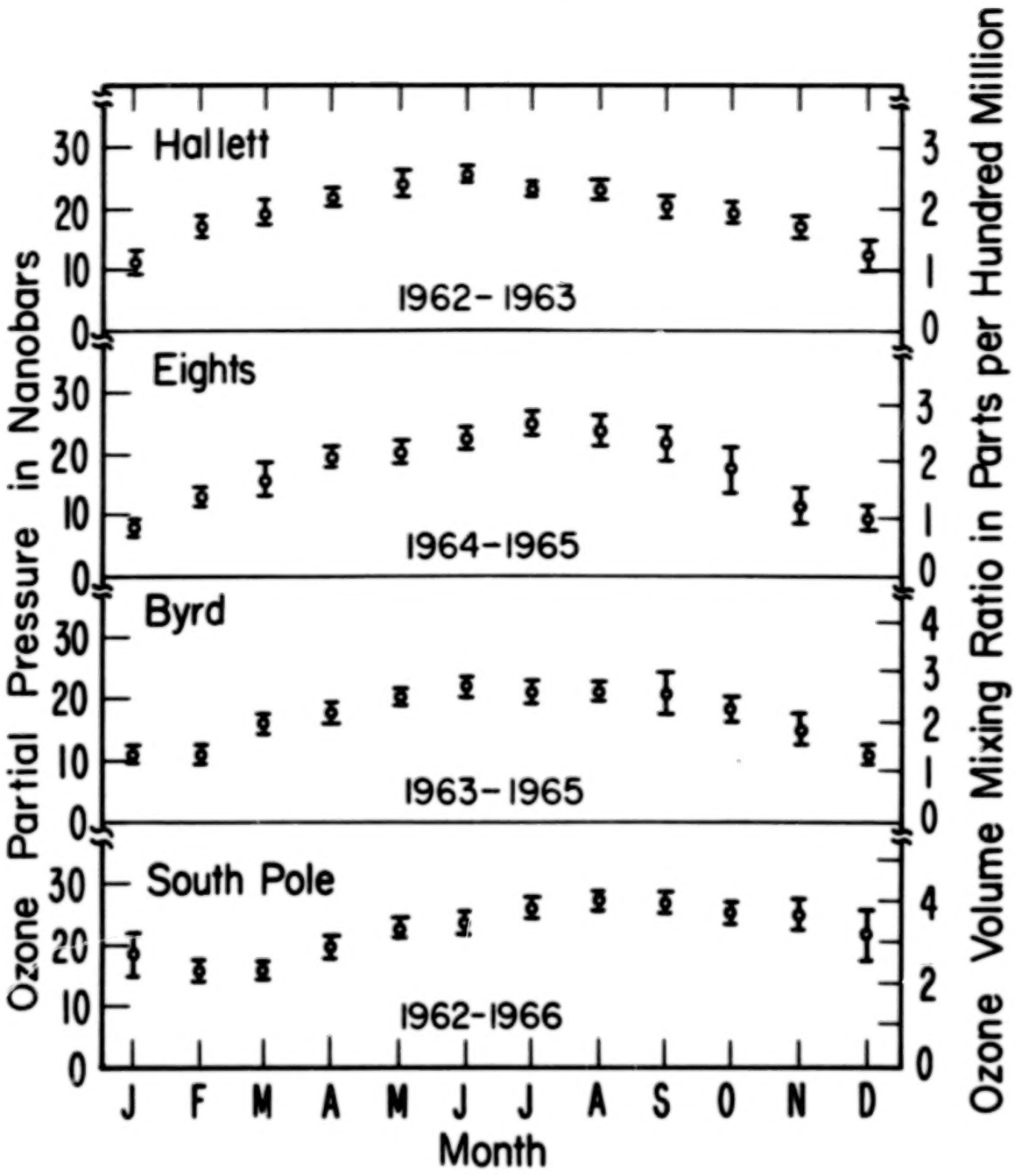

Figure 30.- GMCC data for various Antarctic stations showing annual cycles of surface ozone partial pressure and ozone volume mixing ratio. (From Mendonca, 1978.)

ORIGINAL PAGE IS
OF POOR QUALITY

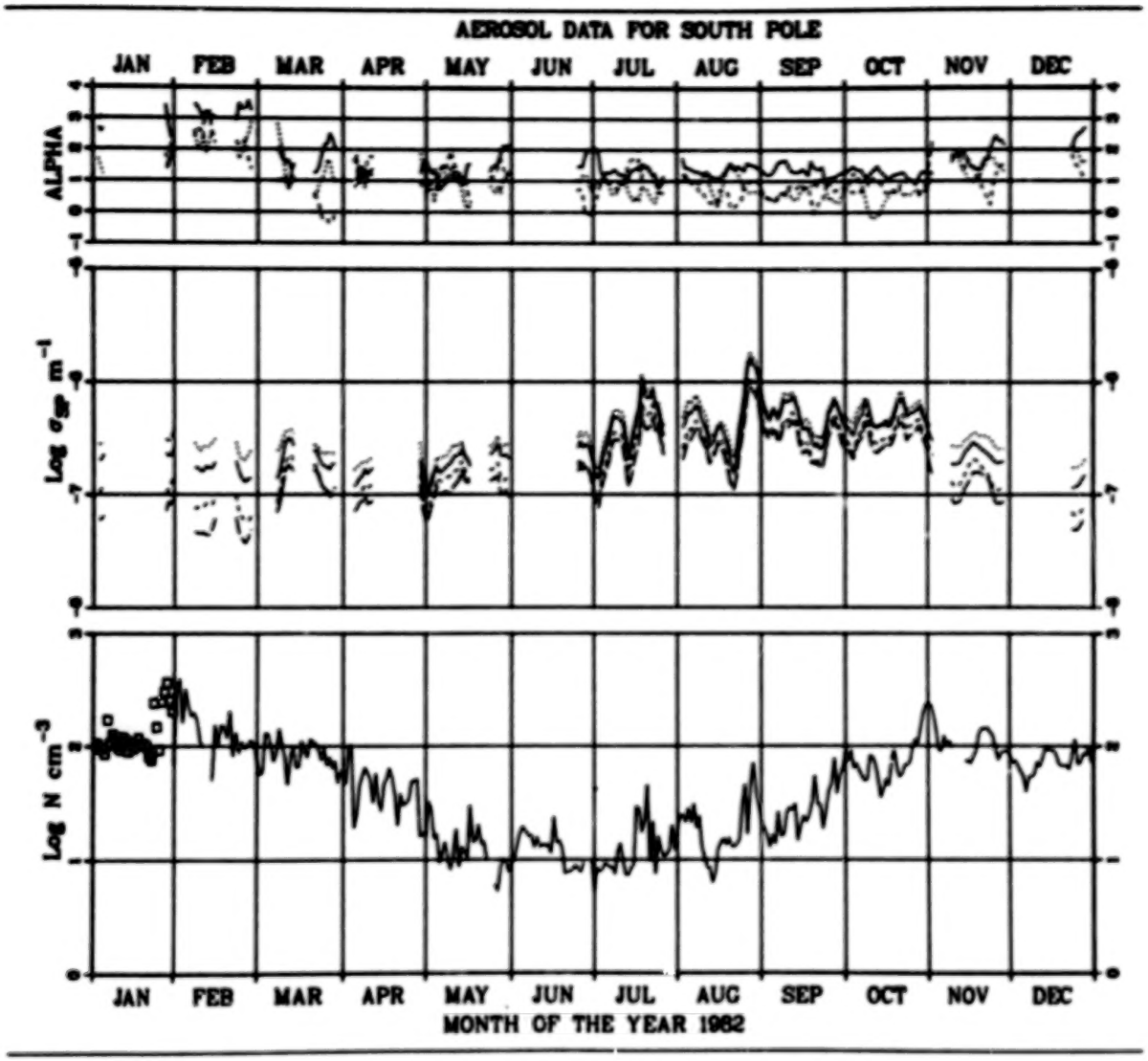

Figure 31.- Daily geometric means of light-scattering and CN data at South Pole. CN concentration (bottom) is shown as a solid line. Light-scattering data (middle) are shown for 450 nm (•••••), 550 nm (_____), 700 nm (----), and 850 nm (- - -). Angstrom exponents (top) were calculated from 450- and 550-nm (•••), 550- and 700-nm (_____), and 700- and 850-nm (---) light-scattering data. (From Harris and Bodhaine, 1983.)

ORIGINAL PAGE IS
OF POOR QUALITY

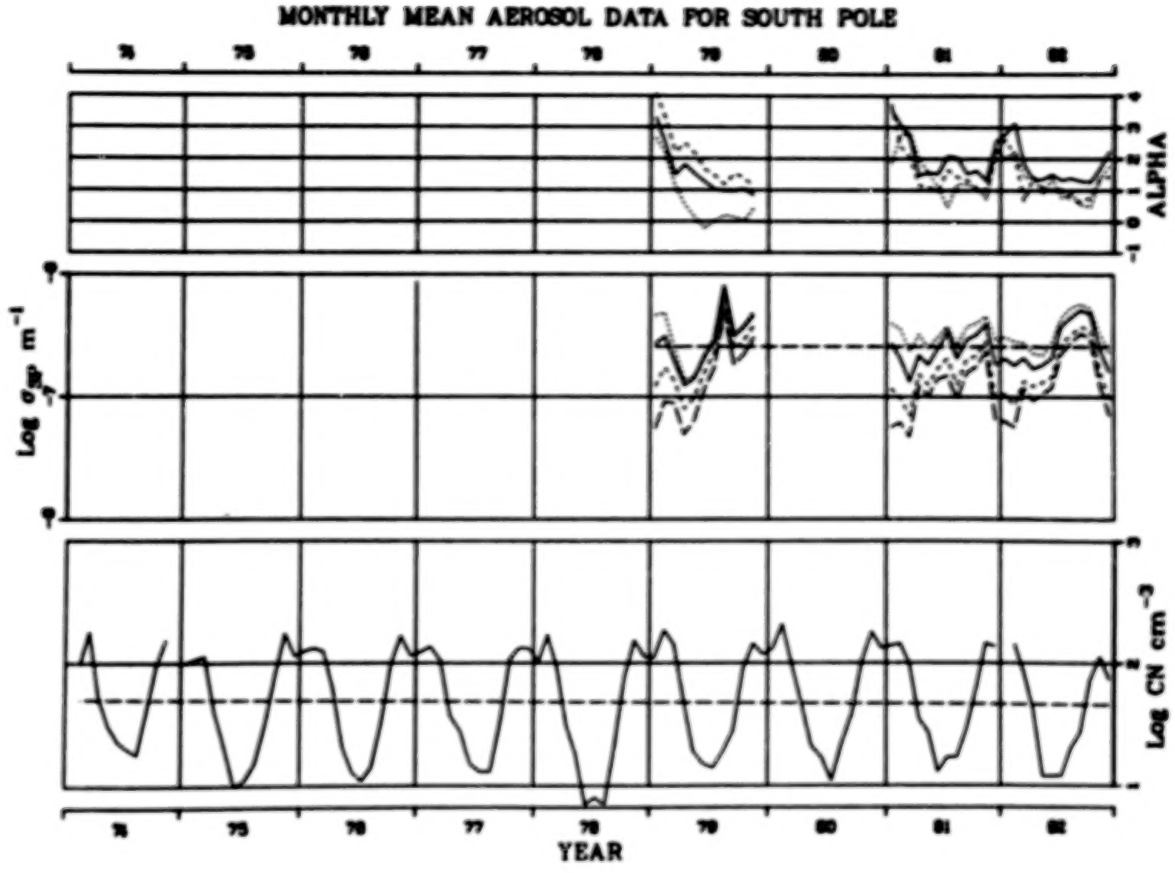

Figure 32.- Monthly geometric means of light-scattering and CN data at South Pole from 1974 to 1982. CN concentration (bottom) is shown as a solid line. Light-scattering data (middle) are shown for 450 nm (••••), 550 nm (——), 700 nm (----), and 850 nm (- - -). Angstrom exponents (top) were calculated from 450- and 550-nm (•••), 550- and 700-nm (——), and 700- and 850-nm (----) light-scattering data. (From Harris and Bodhaine, 1983.)

ORIGINAL PAGE IS
OF POOR QUALITY

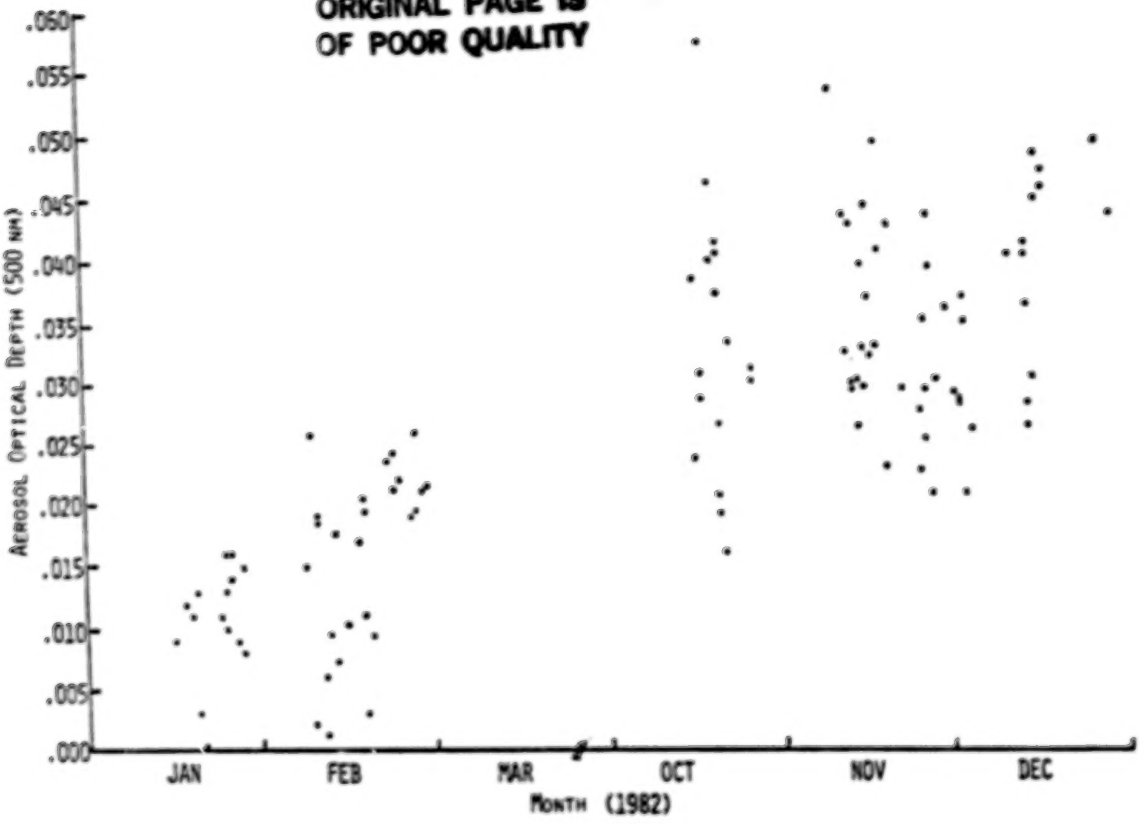

Figure 33.- Unpublished GMCC South Pole aerosol optical depths data for 1982 (for 500-nm channel). The increase during the fall of 1982 is presumed to be from the eruption of El Chichon.

The observation of aerosol properties at the South Pole station has led some investigators to conclude that a certain component of the aerosol is of stratospheric origin. It is believed that the polar aerosols influence the formation processes of ice crystals, which in turn are thought to play a significant role in polar infrared cooling processes, although this still must be verified by observation.

The quantity of material transported from the stratosphere to the surface can potentially be augmented dramatically by volcanic injections of crystal particulates and sulfuric acid, as was observed by the recent Arctic Gas and Aerosol Sampling Project (AGASP). However, the true rate at which the exchange process occurs between stratosphere and surface is not known. It is quite possible that a link can be established between the presence of PSC's and the cleansing of the stratosphere. If so, this would aid greatly in interpreting the many interesting and unexplained features of the South Pole measurements, as well as in developing a quantitative understanding of the physical processes controlling the Antarctic radiation balance.

There is an interest among several scientists in the U.S. in embarking on a stepwise program to study the heat budget of the Antarctic. Such a study would entail surface measurements of radiation fluxes, clouds, and heat fluxes as well as satellite measurements of the radiation balance. The study is aimed at the eventual monitoring of the Antarctic heat budget as an indicator of climatic variability which could be included in the set of climatic indicators now in existence.

PSC's, if found to be extensive over the polar regions, could conceivably influence the radiation balance, and therefore it is important to know whether and to what extent they are present interior to Antarctica during the polar winter.

5.5 The Potential Role of Polar Stratospheric Clouds in Atmospheric Dynamical Processes

Whether polar stratospheric clouds have a significant role in influencing atmospheric dynamical processes depends largely on the magnitude and duration of the enhancement of the cooling rates caused by the clouds. McCormick et al. (1982) report infrequent occurrence of PSC events during the Northern Hemisphere winter. In contrast, PSC events are extremely prevalent during the Southern Hemisphere winter.

The presence of a PSC is strongly corrrelated with temperature. McCormick et al. (1982) indicate that a PSC was observed in 45 percent of the instances in which the temperature was less than 193 K. With this correlation in mind, the fundamental difference in the frequency of PSC occurrence between the Northern and Southern Hemisphere winters is understandable. Minimum temperatures in the Southern Hemisphere winter polar vortex tend to be much colder than those in Northern Hemisphere winter. In addition, the areal extent of the minimum temperature regions in the Southern Hemisphere is significantly greater than in the Northern Hemisphere.

The differences in the circulation and thermal structure of the winter polar vortex arise largely because of the different tropospheric forcing in the two hemispheres. In the Northern Hemisphere, large-amplitude planetary-scale waves induced by orography and land-ocean thermal contrast propagate upward into the winter stratosphere. These waves distort the polar vortex and transport momentum and heat poleward in high latitudes, which partially compensates for radiative cooling. In contrast, substantially smaller amplitude waves penetrate the Southern Hemisphere winter stratosphere because of the lesser tropospheric forcing. The vortex tends to be more symmetric and colder than the Northern Hemisphere winter polar vortex.

Because of the long radiative time constant (about 100 days) at high latitudes in the lower winter stratosphere, a relatively small enhancement of the cooling rate by the presence of PSC's could produce a significant temperature change and a more vigorous Lagrangian mean circulation. The incremental cooling rates expected to result from the PSC's seem unlikely to produce a large effect when one considers the persistence and limited region of occurrence of PSC's as suggested by the McCormick et al. (1982) data. These calculated cooling rates and the conclusions predicated on them must be viewed with some caution, however. As noted earlier, there could be large uncertainties due to the lack of knowledge of parameters (e.g., opacity) which characterize the cloud.

Ramanathan et al. (1983) demonstrated important radiative-dynamical coupling and the sensitivity of dynamics to radiative cooling. They presented results from two GCM simulations. The two simulations differed only in their treatment of radiative processes. In their control case, cooling rates in the polar region were 0.2-0.3°C day^{-1} less than for the other case. The control case exhibits a marked improvement in the simulated zonal mean winds and temperatures. In a subsequent analysis of these simulations by Grose (unpublished results, 1983), the differences

in the mean circulation and the structure of the waves in the stratosphere are examined. Although these experiments are not directly an assessment of the effect of PSC's on dynamical processes, they do provide some perspective on radiative-dynamical coupling and the sensitivity of dynamics to radiative cooling rates.

A separate question, not yet addressed, is whether PSC's can significantly influence short-duration transient phenomena, such as stratospheric warming. Based upon our present understanding of warmings, the disparity between the radiative time constant (about 100 days) and the characteristic time over which warmings develop (a few weeks), coupled with the estimates of the enhanced cooling from PSC's, suggest a negligible role.

An intriguing possibility, however, is whether PSC's could have a role in "preconditioning" the stratosphere. It has been suggested that stratospheric warmings may develop only when the stratosphere has been preconditioned by a mechanism which may act to focus wave energy into the polar cap. This theory is somewhat speculative and it is uncertain whether PSC-enhanced cooling might be a factor.

5.6 Effect of Polar Stratospheric Clouds on Stratospheric Water Vapor Distribution and Budget

It is highly probable that polar stratospheric clouds in the Southern Hemisphere affect the water vapor distribution in the stratosphere by dehydrating air descending in the polar cyclonic vortex, thus contributing to the dryness of the middle and perhaps even the lower stratosphere. However, based on current measurements and chemical and physical reasoning, it is highly improbable that PSC's have a significant effect on the total water vapor budget of the stratosphere.

Dehydration of descending air is possible only when radiative cooling exceeds adiabatic warming by compression and when the cooling is maintained until the temperature decreases below the dew point or frost point. In the upper stratosphere (30 to 50 km), radiative heating in the sunlit summer polar region couples with radiative cooling in the dark winter polar region to produce an interhemispheric circulation. Air rising and diverging from the summer pole generates a warm anti-cyclonic flow with cross-equatorial drift. As it converges towards the winter pole it generates a cold cyclonic vortex and descends.

According to Louis' (1974) diagnostic analyses, descending motions dominate the winter hemisphere between 30 and 50 km with the maximum descent at 50 km ($\bar{w}$ = -6 mm sec^{-1}) between 60°S and the pole. The vertical velocities $\bar{w}$ decrease in magnitude to -1 mm sec^{-1} at 30 km despite horizontal convergence, because of the large increase (15/1) in air density from 50 to 30 km. Below 30 km the area of descending motion reduces, but descending speeds less than or equal to 1 mm sec^{-1} extend down to the Antarctic continent.

In late June and July, when PSC's appear to form between 20 and 25 km, the minimum temperatures of about 180 K are in this same height range. If the air is descending at 1 mm sec^{-1}, it must cool 0.63 K day^{-1} to attain this minimum. Again, according to Louis (1974), this is a reasonable rate for 20 to 25 km during the winter darkness. Since the air is descending from the upper stratosphere it is reasonable to assume water vapor concentrations of about 6 ppmv, with 3 ppmv attributable to methane oxidation. Under these assumptions, the descending air

in the polar vortex would reach saturation with respect to ice at 18.5 mb or 23.6 km and saturation with respect to liquid water at 23 mb or 22.4 km. Both height limits are within the observed range of PSC's; therefore, if saturation with respect to liquid water is required for the ice phase to form, this imposes no improbable constraint.

After the ice particles have formed, the air must continue to cool at 0.65 to 0.7 K day^{-1} to overcome adiabatic compressive heating, and the particles must grow to develop a finite terminal velocity relative to the air in order to dehydrate the descending air. If the removal process is efficient, about 4 ppmv of water vapor can be removed between 23 and 19 km (20 to 45 mb), but the amounts decrease with decreasing heights due to warmer temperatures. Dehydration will cease near 12 km (150 mb) at which point 6 ppmv represents saturation with respect to ice (196 K). As the ice falls to lower elevations it will evaporate as a consequence of the warmer temperatures and the small size of the ice particles.

Estimates of the size and number of particles per unit volume vary. If there is 1 particle cm^{-3} and 4 ppmv of water vapor available for deposition, a spherical particle would have a radius of 3.23 μm and a terminal velocity of -2.35 mm sec^{-1} at 23 km, which decreases in magnitude to -1.95 mm sec^{-1} at 16 km. When added to a descending air velocity of -0.6 or -1.0 mm sec^{-1} the particle will descend between 8 and 9 km $month^{-1}$. Figure 2 of McCormick et al. (1981), which depicts the descending trend of weekly averaged extinction values, indicates that this descent is much too fast.

The cloud formation process may activate all available nuclei, so 5 to 6 particles cm^{-3} is considered probable. Increasing the number reduces the radius to about 2 μm and changes the terminal velocities to -1.17 mm sec^{-1} at 23 km and -0.84 mm sec^{-1} at 16 km. Under these conditions the particles descend 4 to 5 km $month^{-1}$, which is in good agreement with figure 2 of McCormick et al. (1981). The maximum averaged extinction reaches about 12 km in some 70 days. Below 12 km the extinctions decrease before merging with tropospheric values, an observation consistent with an evaporation threshold.

The extinction values contoured in figure 2 of McCormick et al. (1981) have a lower limit of 10^{-5} km^{-1}. As the winter season advances, this limiting contour descends from 24 to 25 km to 18 km in about 80 days. A descent of 2.3 to 2.7 km $month^{-1}$ corresponds to $\bar{w}$ = -0.89 or -1.04 mm sec^{-1}, which is in close agreement with the assumed value of -1 mm sec^{-1}. If all nuclei in the descending air have been activated and subsequently removed by particle growth and sedimentation, we would expect the descending air to be quite clean, as the observations suggest. Also, the potential temperature θ of this clean dehydrated air, which could contain approximately 2 ppmv of water vapor, has decreased from greater than 500 K to about 425 K, a potential temperature close to that of the water vapor minimum measured by Kley et al. (1979) at lower latitudes.

We know that radioactive rhodium 102, produced by a rocket-borne bomb detonated in the mesosphere during the 1958 Hardtack series, descended first at high latitudes before it spread to subtropical and tropical latitudes (Telegadas and List, 1964). Also, the descent occurred during the winter season in both the Northern and Southern Hemisphere. Therefore, on the basis of both direct and indirect evidence, we suggest that the PSC's in the Southern Hemisphere, where the mean temperatures are much colder than they are in the Northern Hemisphere, can affect the water vapor distribution in the lower middle (θ = 400-500 K) stratosphere.

However, it is quantitatively improbable that PSC's significantly affect the stratospheric water budget. The stratospheric water budget is very sensitive to the lower boundary used in the computations. By tradition the tropopause is defined as the upper limit of the troposphere. Above the tropopause, water vapor concentration decreases rapidly by one to two orders of magnitude to about 4 ppmv in a transition layer of finite depth. Because water content and density in the transition layer are large, the mass of H_2O in the transition layer is 5 to 10 times the mass in the stratosphere above this layer.

We assumed that the transition layer was always a mixture of tropospheric and stratospheric air; consequently, we based our computations on values obtained above this layer. Consistent with this assumption, Danielsen and Mohnen (1977) used the strontium 90 aircraft and deposition observations of 1959-1960 and 1962-1963 to estimate the mass of air transported from the lower stratosphere to the troposphere. For the Northern Hemisphere this mass outflow is 3.8×10^{20} g yr^{-1}, with an estimated uncertainty of ±20 percent. If we take 6×10^{20} g yr^{-1} as a reasonable global value and 5 ppmv (3.1 ppmm) as a representative mixing ratio, the mass outflow of H_2O is 1.9×10^{15} g yr^{-1}. This value is approximately 200 times the mass removed from the air descending in the Antarctic polar low. An upper limit for the latter is only 4×10^{13} g yr^{-1} because it is restricted to a small polar area during one season. Douglass and Stanford (1982) concluded that the annual sink of the PSC's was approximately 2 percent of the total stratospheric H_2O burden by assuming that the ice particles precipitated into the troposphere. Here we are not comparing a precipitation sink to a burden; instead we are comparing a rate of dehydration in one part of the stratosphere (it represents a source to another part) to a rate of removal from the stratosphere. Nevertheless, the conclusions are similar. The PSC's do not process a sufficient amount of water to affect the stratospheric water vapor budget significantly.

5.7 Possible Effects of Polar Stratospheric Clouds on Trace Gases in the Upper Stratosphere

As indicated above, the diabatically driven circulation in the upper stratosphere is unique because it is interhemispheric. Louis' (1974) computations show a maximum meridional velocity at approximately 45 km from the summer to the winter hemisphere, with a reduced return flow at approximately 25 km. Also, it was mentioned in the previous discussion that this circulation is consistent with the movement of rhodium 102 from the mesospheric rocket bomb test. Rhodium 102 entered the upper stratosphere at the winter pole in both the Northern and the Southern Hemisphere and then spread toward the equator and downward into the lower stratosphere.

In the Southern Hemisphere where the winter temperatures are sufficiently cold to produce ice particle clouds, aerosols and water-soluble trace gases will probably experience an enhanced vertical transport velocity and net vertical displacement if they are incorporated into the ice particles. Although the ice particles probably evaporate at close to 12 km, the air in which they evaporate will probably continue to descend and enter the troposphere between 40°S and 65°S latitude.

We remind the reader that this process represents the only rapid vertical transfer process from the upper stratosphere and lower mesosphere to the troposphere and the Earth's surface. The transfer is thought to be restricted to the Southern Hemisphere because of the axial symmetry of the Antarctic continent. Unlike the

Northern Hemisphere, where there is strong topographic and thermal forcing for wavenumber 1, the flow in the Southern Hemisphere tends to remain zonal. The vortex becomes more intense and the core temperatures extremely cold.

5.8 The Importance of Accurate Water and Temperature Measurements

A critical question with regard to both the determination of PSC's from remote measurements and the microphysics of PSC particle development is the accuracy of the ambient temperature measurements used in the analysis. In the Arctic regions the occurrences of very cold temperatures (<195 K) appear to be localized and possibly difficult to define with a conventional rawindsonde network. Satellite temperature retrievals for the lower stratosphere offer better coverage, but there is still some question about the accuracy of the satellite temperatures where large horizontal and/or vertical gradients occur. Comparisons of conventional analyses of temperatures (NMC and Berlin) with satellite-derived temperature fields are under way and differences are being noted. The PSC questions should provide additional incentives for understanding any differences between the several temperature analyses.

In the case of LIMS and SAMS satellite measurements of water vapor, temperatures are required in the retrievals. Therefore, any biases in temperature can potentially affect the subsequent retrieved water vapor profiles, and this effect should be carefully assessed. Presently, the LIMS water vapor values are on the order of 4.5 to 5.5 or 6.0 ppmv with little variability.

In terms of temperature accuracy, we desire values on the order of 2 K from both the retrieval and the microphysics point of view. Because saturation mixing ratios for water and ice vary exponentially with temperature, one must know temperatures to better than 2 degrees. The water vapor fields determined from LIMS seem to be fairly uniform spatially and have a long residence time; therefore, in order to evaluate the water vapor budget from the water vapor data, high accuracy in the water vapor data will be required.

5.9 Measurements of Stratospheric Water Vapor

It is the general consensus of the workshop members that PSC's consist of water ice. Once a PSC has formed, phase equilibrium between gaseous and solid water (ice) should exist. Therefore, the atmospheric temperature must be a variable closely related to PSC's, and indeed it is. From a knowledge of the temperatures at which PSC's are observed, it is possible to deduce the water mixing ratio. The range of mixing ratios thus obtained extends from about 2 to 22 ppmv. Although most values are in the few ppmv range, these is a substantial data base for the larger mixing ratios as well.

The generally accepted theory of stratospheric water vapor is that of Brewer (1949). The essentials of this theory are now summarized. The source of stratospheric water is upward diffusion of air through the tropical tropopause, where it is freeze dried at the tropopause temperature of roughly -80°C. To counteract upward-directed diffusion of water at extratropical latitudes, Brewer postulated a one-cell flow (in each hemisphere) with subsiding motion through the extratropical tropopause. If -80°C is the representative tropical temperature at 100 mb (16 km), then the stratospheric water vapor mixing ratio would be 5.5 ppmv.

It is known that in addition to this physical source of stratospheric water vapor, there are chemical sources from oxidation of CH_4 and H_2. If these are fully oxidized, the increase from CH_4 and H_2 oxidation is $\Delta H_2O = 2 \times 1.65 + 0.5 = 4$ ppmv, which if added to the physical source indicates a total of 9.5 ppmv. This figure should be the upper limit of the observable water mixing ratio in the stratosphere.

Spurred by water measurements in the tropical stratosphere made by Kley et al. (1979), Newell and Gould-Stewart (1981) proposed that a temperature of -82.4° rather than -80°C would be more representative of the equivalent cold trap temperature. They identified the tropopause over Micronesia during the Northern Hemispheric winter as the most likely injection region. At 100 mb, -82.4°C corresponds to only 3.5 ppmv of water vapor, which was the mixing ratio observed by Kley et al. (1979) over Brazil at 60 mb. This pressure level seems to show an omnipresent minimum of tropical water mixing ratio (Kley et al., 1982), with values around 3 ppmv. The altitude of the minimum was termed the hygropause. Danielsen (1982) and Kley et al. (1982) discussed injection of water into the stratosphere by giant thunderstorms. There seems to be the possibility that most, if not all, of the exchange of air to the stratosphere is confined to the hot towers of cumulus convection. This concept is not new but has lacked evidence so far. Water and temperature measurements from the NASA 1980 Panama Experiment definitely point in that direction. The new water measurements at the hygropause point to mixing ratios of approximately 3 ppmv rather than 5.5 ppmv. Measurements of water vapor in the lower stratosphere at mid-latitudes are generally consistent with thunderstorm injection over the tropics. Values around 4 ppmv are most likely representative. If injection is combined with the chemical source, the upper limit of stratospheric water vapor will then be 8 ppmv.

A significant number of reports in the literature show measured water mixing ratios that are too high to be explained by the Brewer (1949) theory (Thacker et al., 1981; Gibbins et al., 1982). Most of these have been measured in the middle to upper stratosphere. Some mesospheric water mixing ratios also showed large values. However, those are now being revised downward (Bevilacqua et al., 1983) to mixing ratios less than or equal to 10 ppmv.

It must be pointed out that in the absence of other sources (i.e., extra-terrestrial ones), large mixing ratios of "total" water (total water = $H_2O + 2CH_4 + H_2$) must be present at one time or another at the tropospheric-stratospheric boundary. However, no reliable data with such large values are known. We therefore conclude that if the large water mixing ratios inferred from some of the PSC observations and temperature data prove to be real, the injection must have occurred over an area of the globe that has not been sampled well for stratospheric water vapor. This basically leaves the polar regions. However, it must be pointed out that of the few available polar measurements (spot and satellite), none has indicated mixing ratios above 8-9 ppmv. Data from LIMS (Remsberg, private communication) for the polar region are below these values in the stratosphere and do not exceed them in the mesosphere.

5.10 Stratospheric Condensation Nuclei

Condensation nuclei (CN; $r \sim 0.01$ μm) are the precursors of the stratospheric aerosol layer and thus are important as sites for the development of PSC particles. CN are generally detected by causing them to grow to radii greater than 0.1 μm and counting them optically. This results in an integral measurement of all aerosol particles with radii greater than about 0.01 μm and typically yields a value of

5-10 cm^{-3} at the 20-km level (Rosen and Hofmann, 1977). Following volcanic injections to the stratosphere, large concentrations (~500 cm^{-3}) of CN are observed, but they coagulate to preeruption concentrations within 1-2 months (Hofmann and Rosen, 1982a). The main composition of those particles with radii greater than 0.15 μm is a sulfuric acid-water solution (~75% H_2SO_4 by weight). Some of the particles may contain a nonvolatile core of radius less than 0.15 μm, although the mass is probably dominated by a sulfuric-acid component (Rosen and Hofmann, 1981; Hofmann and Rosen, 1982a). The size distribution is typically log normal with a mode radius of about 0.08 μm and a geometric standard deviation of about 1.6.

Transient increases of CN at high altitude have been observed. These CN "events", depicted in figure 34, are apparent annual increases in the concentration of CN at 25-35 km (Rosen and Hofmann, 1981, 1983; Hofmann and Rosen, 1982b, 1983). Enhanced layers of particles are observed at midlatitude on certain occasions during the January-March period when polar air is somewhat directly transported over the United States as a high pressure system over the Aleutians attempts to replace the winter polar low. These transient CN increases are important in this study because they represent a polar stratospheric particle formation process which can be observed at midlatitude under proper conditions. These events appear to be associated with stratospheric warmings that occur at this time; thus actual PSC's never accompany these events because of the elevated temperature.

From volatility and size studies, these condensation nuclei have been determined to be small ($r \sim 0.015$ μm) sulfuric acid-water droplets similar in composition to the main stratospheric aerosol layer. They are thus invisible to conventional backscatter or extinction measurements. The new droplets are thought to have been thermally nucleated (by cooling during transport from arctic regions associated with stratospheric warmings to midlatitude regions of normal temperature) from H_2SO_4 vapor present in the polar region. The vapor is derived either through transport from lower latitudes, where sulfurous gas from volcanic eruptions is probably the ultimate source, or through evaporation of the pre-existing sulfuric-acid aerosol, which has been transported to polar regions and exposed to the relatively high temperature associated with stratospheric warmings at 30 km (commonly -5°C to -20°C). CN concentrations as high as 10^3 cm^{-3} ($r > 0.01$ μm) have been observed in these events. During the course of the year, the event layer is diffused uniformly throughout the Northern Hemisphere, and because of diffusion and coagulation, the concentration is reduced to approximately 10 cm^{-3}. Vertical diffusion (sedimentation is unimportant for these particles) eventually spreads these particles into the 20-25 km range, where they could be important as sites for PSC formation, especially during volcanically quiescent times when an insufficient concentration (~0.5 cm^{-3}) of the larger ($r > 0.15$ μm) aerosol is present at the 20-km level.

Figure 35 shows the time variation of the CN mixing ratio at 20 km and at the peak of the event layer (25-35 km) during the period of SAM II PSC measurements. Although the events appear to have become more intense because of increased volcanic activity and associated aerosol and/or H_2SO_4 vapor injection, the 20-km CN level shows mainly a small gradual increase (except for the 1982 episode of CN nucleation at 20 km due to the eruption of El Chichon, which rapidly coagulated away). Thus, if the existing aerosol distribution at approximately 20 km is the ultimate source of PSC's, this source has not changed drastically with the recent elevated level of volcanic activity. This is in general agreement with the time variation of the SAM II PSC sighting frequency over the same period.

ORIGINAL PAGE IS
OF POOR QUALITY

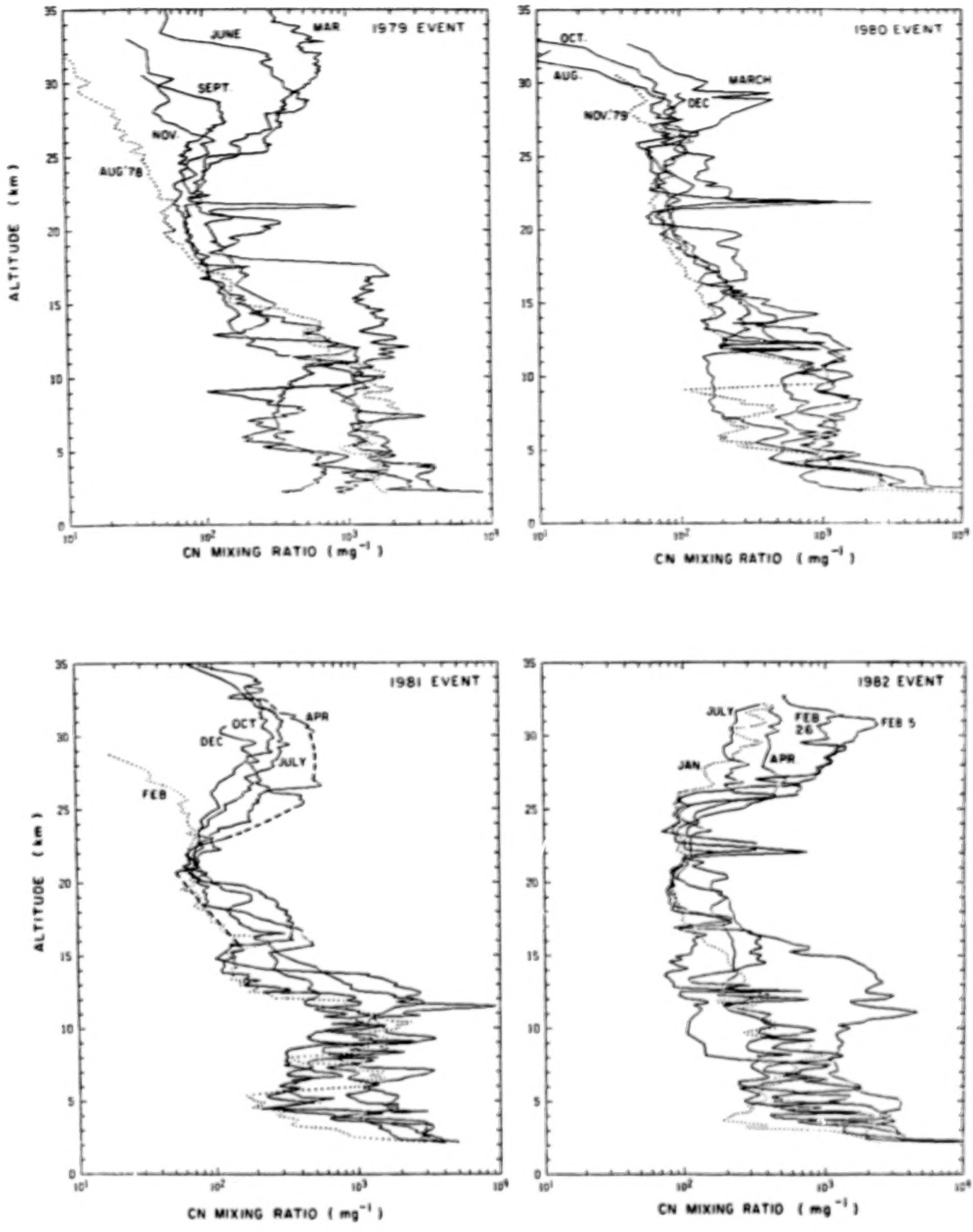

Figure 34.- Mixing ratio (particles per mg air) profiles of condensation nuclei ($r > 0.01$ μm) measured by balloon-borne detectors at Laramie, Wyoming (41°N) over a 4-year period. The enhancements observed in the 22-35 km region are particles associated with CN events. The dotted profiles are pre-event profiles.

ORIGINAL PAGE IS
OF POOR QUALITY

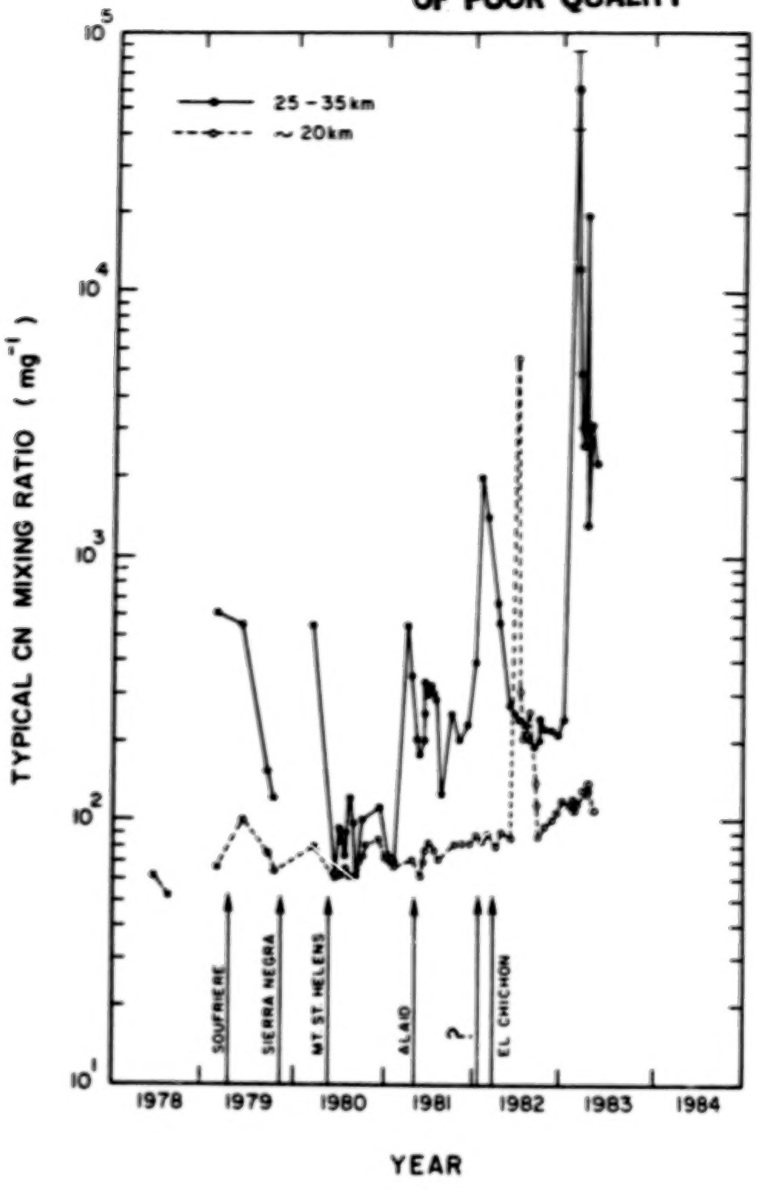

Figure 35.- Typical CN mixing ratio (particles per mg air) versus time for the 25-35 km CN event layer and the relatively stable 20-km PSC region measured by balloon-borne detectors at Laramie, Wyoming (41°N). Concentrations (cm^{-3}) of particles may be established by dividing the mixing ratio by approximately 10 and 50 at 20 and 25-35 km, respectively.

5.11 Growth of Water Droplets and Ice Particles Within Polar Stratospheric Clouds

It is believed that the particles comprising the PSC's are ice particles. Observations of ice crystals in clouds in the temperature range from about 192 to 196 K in equatorial regions would suggest that the crystal forms in the PSC's are columnar and trigonal plate-like shapes.

The following scenario suggests a mechanism for particle formation within the PSC's. The air cools prior to PSC formation, and sulfuric-acid CCN's begin to pick

up water. The sulfuric-acid nuclei serve only to depress the freezing point of the water droplets below that for homogeneous nucleation of pure drops. The largest "haze" particles or "solution drops" form on the largest nuclei, and successively smaller haze particles form on successively smaller nuclei. As the temperatures become increasingly lower, the drops freeze (through homogeneous nucleation), thereby producing ice crystals. These crystals then grow rapidly and at the same time they begin to drive down the relative humidity.

Estimating the size distribution of the ice crystals formed by this process requires treatment of the growth of ice particles in a fairly realistic way. The only information available to estimate their growth comes from data acquired in the Marshall Islands at temperatures from 192 to 196 K. From this data, the following assumptions seem to be justified. First, crystal growth should be calculated assuming that the particles grow with a columnar shape, with axial ratios of about 3 to 1. The bulk density for their growth is about 0.3 g cm^{-3}, but the density may actually decrease with particle diameter. Enhanced growth of the particles through ventilation needs to be considered. Depletion of the water vapor by the ice particle growth also needs to be considered, along with an increase in the available vapor due to the continued cooling of the air in which the particles are growing.

The above discussion points out that deficiencies exist in our knowledge of the microphysics of PSC's. A need exists to sample the clouds and measure the size distributions and particle properties to infer the microphysical processes operative in these clouds and their importance to the radiation properties and dynamics of the stratosphere. It is necessary to provide some means of direct collection of the particles (e.g., ice crystal replicator) to provide the data required to address the basic microphysical questions.

5.12 Gaseous Constituents in the Polar Region

There are only limited observations of gaseous constituents at high latitudes (>60°). These are reviewed in The Stratosphere 1981: Theory and Measurements (WMO Global Ozone Research and Monitoring Project, 1981). With regard to polar stratospheric clouds, the most important constituent is water vapor, which is discussed in a separate section. Other constituents which are expected in polar regions include O_3, HO_x (OH, HO_2, H_2O_2), NO_y (NO_2, N_2O_2, HNO_3), Cl_x (HCl, ClO, $ClONO_2$), and SO_x (SO_2, H_2SO_4, OCS). Some of the gases may contribute to PSC formation by initiating nucleation or affecting water vapor equilibrium pressures (e.g., H_2SO_4, HNO_3, HCl). Others may be affected by PSC's through sequestering in ice or chemical transformation on particle surfaces (e.g., N_2O_5, H_2O_2, $ClONO_2$).

Knowledge of polar-air composition should expand rapidly in the next few years with the advent of regular satellite surveillance at high latitudes. Systems currently (or recently) operating (LIMS, SBUV, SME) and those planned (SAGE II, UARS) will greatly increase the polar data base. Yet within PSC's, data acquisition may be limited by optical and infrared interference caused by the cloud particles. Accordingly, simultaneous in situ observations of gas and particle composition may eventually be required to answer basic questions.

Some gaseous constituents may also be used as tracers of atmospheric motions, stratosphere-troposphere exchange at high latitudes, and dynamical anomalies associated with the breakdown of the polar winter vortex and stratospheric warmings. For example, tracking of ozone and fluorocarbons may provide useful data on such meteorological phenomena. The budget of the polar winter stratosphere may also be

illuminated in this way. Gases and particles trapped in the stable winter vortex may be dispersed to lower latitudes or into the troposphere in spring. The magnitudes of these relative sinks could be determined. In situ measurements could also be used to complement satellite observations and provide ground truth.

(a) Sulfur

We are concerned with sulfur for two reasons. First, pre-existing ambient sulfate aerosols may act as water vapor condensation nuclei in PSC formation, and second, sulfur vapor (H_2SO_4) in combination with water vapor may nucleate to form additional cloud particles. The first effect, activation of sulfate aerosols into ice crystals, is discussed in another section. The role of H_2SO_4 in homogeneous heteromolecular nucleation of ice particles is probably secondary. Background sources of H_2SO_4, primarily oxidation of OCS, would be suppressed at reduced light levels in the winter polar environment. Moreover, the sink (condensation on particle surfaces) could be enhanced. H_2SO_4 evaporation from existing aerosols would be inhibited by extremely low temperatures. Finally, the rate of cooling of polar air which triggers PSC's may be considerably slower than the rate of cooling in orographically induced clouds. A slow rate of cooling implies less homogeneous nucleation relative to condensation on pre-existing particles.

Measurements of OCS and SO_2 in the polar atmosphere could provide valuable information on the following questions. First, is there a source of condensed sulfur from gas phase sulfate formation under polar winter conditions? Second, would observation of SO_2 concentrations place limits on the concentrations of OH, which drives many of the other chemical cycles? Third, can SO_2 and OCS be used as tracers of polar stratospheric motions and possible mesosphere-stratosphere exchange?

(b) Nitrogen

Fixed-nitrogen compounds include NO, NO_2, N_2O_5, and HNO_3. Of these, HNO_3 may contribute to aerosol nucleation at very low temperatures (in combination with H_2O, H_2SO_4, and HCl) and may affect the water vapor equilibrium pressure and freezing point of the cloud particles (if a sufficient amount is absorbed into or condenses on the particles). The behavior of the nitrogen gases at high latitudes is of general scientific interest. The Noxon "cliff," for example, illustrates the rapid redistribution of NO_y compounds under varying conditions of solar illumination and atmospheric dynamics. Studies of the nitrogen compounds, including concentrations and vertical gradients in the vicinity of the tropopause, can provide information on stratosphere-troposphere exchange, the NO_y budget of the stratosphere, the importance of the auroral source of NO_y, and the origin of nitrate in polar ice cores. Also, polar conditions may be favorable for detecting species such as N_2O_5 and $ClONO_2$, which may be more abundant and thus more accessible to measurement. These species would be useful in validating photochemical and transport models.

(c) Chlorine

Ancillary studies of chlorine compounds in the polar winter stratosphere could provide important information to stratospheric scientists. Insights concerning the atmospheric cycle of chlorine might be gained by such studies. For example, the photochemical balance of $ClO/ClONO_2/HCl$ may place constraints on current chlorine and ozone theories. The source-sink relationship between Cl_x and fluorocarbons might also be clarified.

(d) Ozone

Ozone is one of the most important stratospheric species with regard to photochemistry and climatology. Measurements during PSC missions would provide useful additional data for atmospheric scientists.

5.13 Microphysical Processes and the Formation of Polar Stratospheric Clouds

We shall briefly consider a number of microphysical processes which can affect the formation of polar stratospheric clouds. These are nucleation, coagulation, coalescence, condensation, evaporation, and sedimentation. However, before we begin, it will be helpful to give a brief outline of the pertinent characteristics of the stratospheric aerosol layer.

The stratospheric aerosol is believed to be composed of sulfuric-acid-solution droplets of about 75 percent H_2SO_4 by weight (Rosen, 1971). The particles are probably sustained primarily by volcanic injections of SO_2 into the stratosphere and the diffusion of OCS from the troposphere. These sulfur-bearing gases are photodissociated to form gas phase H_2SO_4. The H_2SO_4 is believed to participate with water in heteromolecular nucleation to form solution droplets. These droplets grow by heteromolecular condensation, sediment gravitationally, undergo vertical diffusion and horizontal advection, and evaporate when they reach a region of high temperature. In the scenario presented below, the stratospheric aerosol particles play a fundamental role in the formation of PSC's.

(a) Nucleation

Nucleation is the basic process of particle formation. Stratospheric aerosols may nucleate on particles that originated in the troposphere, on meteoric debris (heterogeneous nucleation), or on water-sulfuric acid droplets (homogeneous nucleation). Many theorists believe that nucleation on ions or radicals may be important. This type of nucleation is favored because of the enhanced binding energy of radicals and ion clusters compared with that of pure materials. Friend et al. (1980) propose that radical precursors of H_2SO_4 nucleate whenever they collide and form stratospheric aerosols. Experimentally, it is difficult to distinguish the various possible types of nucleation.

(b) Coagulation

Brownian motion causes particles to collide with each other. Collisions usually result in the sticking together of particles, which reduces the particle number and creates larger particles. When coagulation is important, the observed number of particles is usually determined by a balance between the mean residence time of the particles and the rate of loss by coagulation.

The coagulation rate for monodispersed particles whose size is smaller than that of the mean free path of the gas, as is generally the case for particles above the tropopause, yields an "e" folding time (Hamill et al., 1977) of

$$\frac{1}{\tau_c} = \frac{1}{N}\left(\frac{dN}{dt}\right) = 4\left(\frac{3k_B T}{\rho}\right)^{1/2} \quad Nr^{1/2} = 10^{-6}\ Nr^{1/2}$$

where k_B is Boltzmann's constant, T is temperature, ρ is the particle density, N is the number density of particles, and r is a typical particle radius. The coagulation time is much longer than the lifetimes of nacreous or noctilucent clouds. Coagulation is not very important for large stratospheric aerosols (Toon et al., 1979).

(c) Sedimentation

Gravitational sedimentation is not as important a process above the tropopause as might be suspected. The time to fall a typical distance l through an atmosphere whose density varies exponentially with height to reach altitude Z_0 for a particle smaller than the mean free path of air molecules can be expressed by

$$\tau_f = H/V(Z_0)(1 - \exp[-l/H]) \approx 2 \times 10^{-21} \frac{H}{r} N_g(Z_0)(1 - \exp[-l/H])$$

where H is the scale height of the atmosphere $V(Z_0)$ is the fall velocity at Z_0, and $N_g(Z_0)$ is the gas density at Z_0. The expression for $V(Z_0)$ is given by Hamill et al. (1977).

Stratospheric aerosols smaller than 0.1 μm do not fall out of the stratosphere. Particles larger than 0.1 μm at altitudes between 30 and 25 km have fall times that are comparable to their observed residence time. Consequently, such large particles are affected by sedimentation near the top of the layer.

Stanford (1973a) has argued that persistent Antarctic clouds forming at moderately low altitudes with large particle sizes might have a significant sedimentation transport across the tropopause. This, however, is uncertain because the SAM II data usually show a clear region below the PSC's, which would indicate that the particles do not fall through the troposphere. Late in the winter, however, the PSC's tend to merge with tropospheric clouds and significant water transport may occur.

(d) Condensation

Condensation and evaporation occur when molecules enter or leave a volatile aerosol. Both processes occur continually, and whether the particles as a whole expand or shrink depends upon whether the partial pressure of the gas phase molecules exceeds the vapor pressure (condensation) or is less than the vapor pressure (evaporation). This balance is very sensitive to temperature because of the strong dependence of vapor pressure on temperature.

We now consider the growth of stratospheric aerosol particles as the temperature decreases (Steele et al., 1983). We assume a log-normal size distribution described by

$$\frac{dN(r)}{dr} = \frac{N_0}{r\sqrt{2\pi}\,\ln\sigma} \exp\left[-\frac{\ln^2(r/r_g)}{2\ln^2\sigma}\right]$$

with $r_g = 0.0725$ μm, $\sigma = 1.86$, and $N_0 = 10$ particles cm^{-3}. This agrees with global measurements made by Rosen et al. (1975).

ORIGINAL PAGE IS
OF POOR QUALITY

If there is a drop in temperature, the vapor pressure of the droplet will decrease and the droplet will begin to absorb water from the atmosphere. The weight percentage of sulfuric acid in the solution then decreases, and consequently the water vapor pressure increases. Equilibrium is established (vapor pressure = partial pressure) by a change in the composition of the solution droplet (i.e., the droplet grows more dilute).

The effect of a temperature change on a solution droplet is quite different from the effect on a pure substance. For a droplet of pure water, a decrease in temperature will cause a lowering of its vapor pressure which cannot be compensated by a change in composition. Consequently, for equilibrium to be re-established, a droplet of pure water must absorb water from the environment until the environmental water content has been depleted to the point that the partial pressure is once again equal to the vapor pressure. Thus, for pure water, equilibrium is re-established by changing the partial pressure of water in the atmosphere, whereas for solution droplets it is re-established by a change in the vapor pressure of water in the droplet, and the partial pressure remains essentially constant.

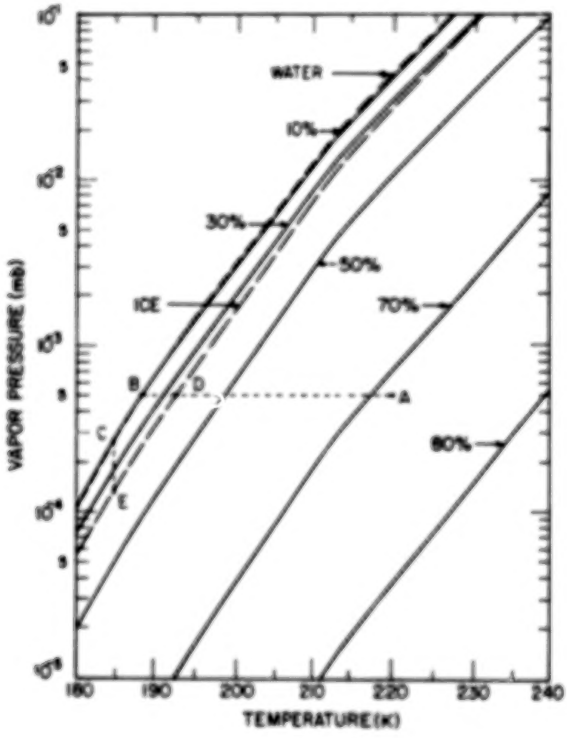

Figure 36.- Vapor pressure of water over sulfuric acid-water solutions as a function of temperature for five different H_2SO_4 weight percentages. The dashed curves represent the vapor pressure of pure ice and the vapor pressure of pure water.

An example of the dilution process is represented in figure 36 by the dotted line marked ADB. In this example, the environmental partial pressure is taken as 5×10^{-4} mb (5 ppmv at 100 mb). The line AB shows that as the temperature drops from 220 K to 189 K, the composition of the droplet changes from approximately 72 percent to approximately 10 percent H_2SO_4 (by weight). This compositional change is equivalent to a mass increase of the droplet by a factor of about 7 and a radius

ORIGINAL PAGE IS
OF POOR QUALITY

increase of just less than 2. During this dilution process, the environmental water content is depleted by the amount of water absorbed into all the droplets. However, this is a very small fraction of the water present in the environment, and so the partial pressure in the atmosphere remains constant until a 10-percent solution is reached.

If the temperature drops even further, the droplet maintains equilibrium by further compositional change, asymptotically approaching the curve for pure water. Now the nature of the growth process changes completely. Further temperature drops cause a decrease in the water vapor pressure (curve BC in fig. 36) which must be compensated by the absorption of relatively large amounts of water from the atmosphere. The only way equilibrium can be re-established is by a lowering of the environmental partial pressure. Naturally, this results in a substantial depletion of the environmental water content as well as significant droplet growth. For example, if the temperature falls to 185 K (point C on fig. 36) the droplets absorb an amount of water corresponding to a decrease in the atmospheric partial pressure from 5×10^{-4} to 2.7×10^{-4} mb.

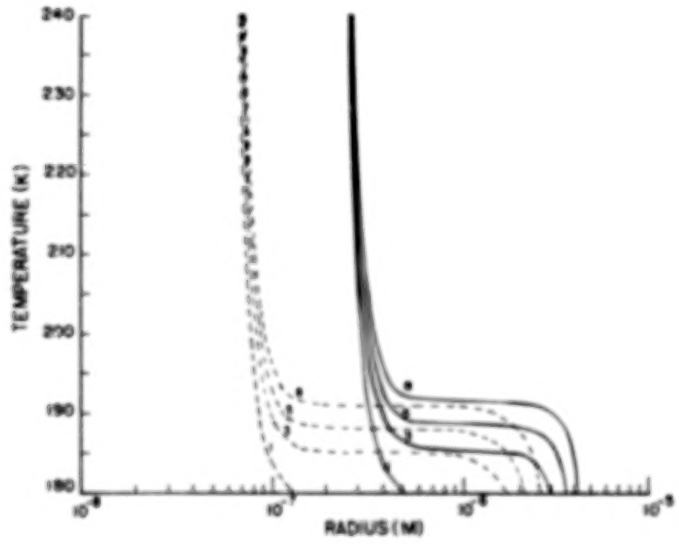

Figure 37.- Droplet radius as a function of temperature for water vapor mixing ratios of 1, 3, 5, and 8 ppmv at 100 mb. The aerosol particles are assumed to remain liquid throughout.

The derived effect of temperature changes on the radius of supercooled droplets is shown in figure 37. The dashed set of curves represents aerosols of initial radius 0.0725 μm at 220 K and 3 ppmv, and the solid curves represent aerosols of initial radius 0.29 μm for the same environmental parameters. The curves are labelled with the assumed partial pressure of water in the atmosphere. Until saturation is reached the particles all grow at the same rate. At saturation, large increases in particle radius occur, and the small ones approach the large ones in size. A further reduction in temperature causes the particles to continue to grow, but at a lesser rate because the atmospheric water content has been substantially depleted.

ORIGINAL PAGE IS
OF POOR QUALITY

The derived size distribution of the aerosols as a function of temperature (calculated for several different H_2O partial pressures) was used in conjunction with a Mie scattering program to calculate the extinction at 1 μm. The refractive index for the aerosols was interpolated from the data of Palmer and Williams (1975) for a temperature of 300 K and adjusted for lower temperatures by the application of the Lorentz-Lorenz correction. The resulting extinction curves as a function of temperature are shown in figure 38 for a total particle number density of 10 particles cm^{-3}.

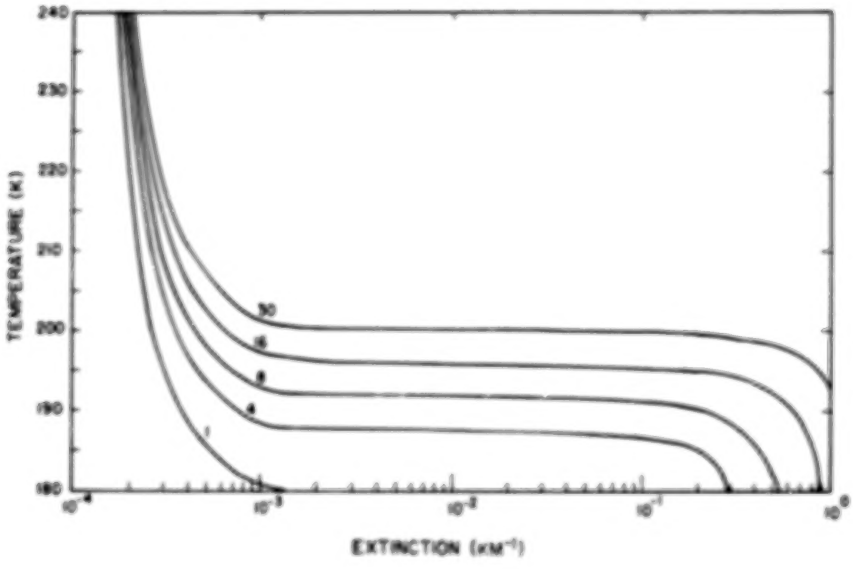

Figure 38.- Extinction at 1 μm as a function of temperature for water vapor mixing ratios of 1, 4, 8, 16, and 30 ppmv at 100 mb. The aerosol particles are assumed to freeze when the H_2O partial pressure is equal to the saturation pressure over ice.

Figure 38 shows the results for droplets which freeze when saturation with respect to ice is achieved (path ADE of fig. 36). The curves are labelled with the initial H_2O partial pressure in units of ppmv at 100 mb. The extinction increases gradually as the temperature falls until the saturation temperature is reached. At saturation, a slight lowering of the temperature causes a large growth of the droplets and a consequent large increase in the derived extinction.

In order to study the effect of temperature on the aerosol and to examine the formation of stratospheric clouds, we have taken the extinction data from a 3-month period during the Arctic winter and a 4-month period during the Antarctic winter. The temperature data used are supplied by the Climate Analysis Center of NOAA at the time and location of SAM II measurements. The Arctic data presented cover the period from 26 November 1978 to 25 February 1979 and latitudes from 65°N to 78°N. The Antarctic data are for the period from 3 June to 7 October 1979 and latitudes from 65°S to 80°S. All 1483 Antarctic data points and 1038 Arctic data points available during this time at the 100-mb pressure level are plotted on a grid of temperature versus extinction, as shown in figure 39. The circles represent Antarctic measurements and the crosses represent Arctic data. Overlaid on figure 39

ORIGINAL PAGE IS
OF POOR QUALITY

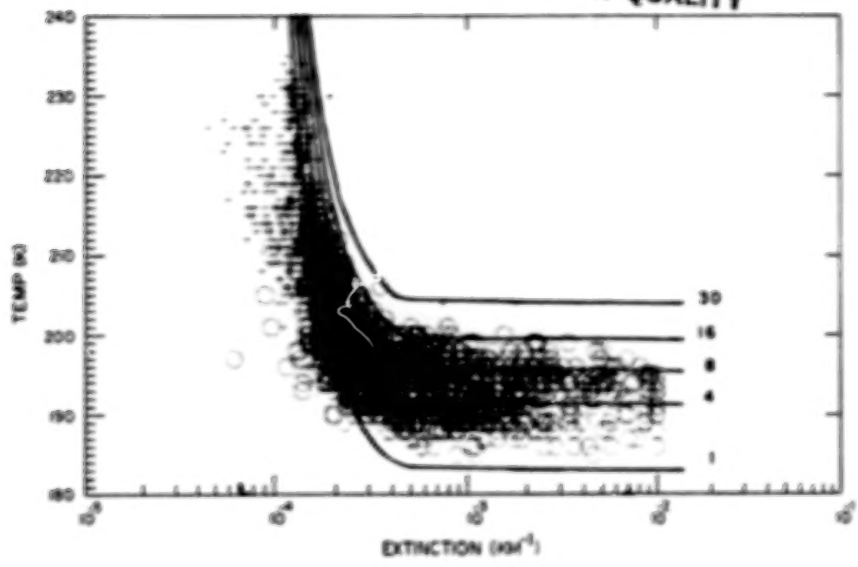

Figure 39.- Theoretical curves (fig. 38) overlaid on SAM II data at 100 mb.
The circles show the Antarctic data taken between 3 June and 7 October 1979.
The crosses show the Arctic data taken between 26 November and 25 February 1979.

are the theoretical curves showing the predicted trend in extinction with repect to temperature for a number density of 6 particles cm^{-3}. Each curve is for a different value of H_2O partial pressure. The curves in figure 39 are for droplets that freeze. It can be seen that the theoretical curves show very good agreement with the SAM II data.

When saturation is reached, small temperature changes cause large increases in extinction. The temperature at which this occurs can be used to evaluate the water vapor mixing ratio, and the spread in the temperatures will give an indication of its variability. Shifting the theoretical curves in figure 39 to the right or left, parallel to the abscissa, is equivalent to changing the total particle number density used in the extinction calculation. By shifting the curves to get a best fit to the SAM II data, we can evaluate the approximate number density of stratospheric aerosols.

Results obtained indicate that the best agreement for the theoretical curves with the SAM II data show an average number density of 6.4 particles cm^{-3} and water vapor content of 7.6 ppmv for supercooled liquid droplets, or a number density of 6.9 particles cm^{-3} and water vapor content of 5 ppmv for frozen particles. If the aerosols are supercooled, the water vapor mixing ratio estimate is somewhat higher than the 3-5 ppmv generally assumed for the stratosphere.

If it is assumed that the particles are frozen, the average water content is 5 ppmv and the number density 6.9 particles cm^{-3}. (See table 5.) This suggests that the formation of clouds does not require an influx of water vapor or a significant increase in number density, but rather that clouds will form whenever low enough temperatures occur for freezing to take place.

TABLE 5. DERIVED WATER VAPOR MIXING RATIO AND TOTAL PARTICLE NUMBER DENSITY FOR ANTARCTIC DATA

[Data from Steele et al., 1983]

Iteration	Region I average water vapor (ppmv)	Region III average water vapor (ppmv)	Average water vapor from I and III combined (ppmv)	Region II average particle number density (no. cm^{-3})
	Supercooled droplets			
1	11.1	7.8	8.3	6.2
5 (convergence)	11.0	7.1	7.6	6.4
	Frozen droplets			
1	5.8	5.1	5.2	6.9
5 (convergence)	5.8	4.9	5.0	6.9

These results lead us to conclude that the average water vapor mixing ratio at 100 mb in the Antarctic region during the winter months is around 5 ppmv, and that clouds are formed by frozen droplets. The standard deviation is about 3.6 ppmv, suggesting quite a large variability in the stratospheric humidity.

The data for the Arctic region (shown by crosses in fig. 39) are predominantly low-extinction data, and contain insufficient high-extinction data from which to derive a water vapor distribution. In order to determine whether the Arctic data are consistent with the results derived for the Antarctic, we have combined the two sets of data to see if the number density and water vapor distributions are affected.

Table 6 shows the results of the combined Arctic and Antarctic data assuming both supercooled and frozen droplets. We conclude that the most plausible explanation for stratospheric cloud formation is the freezing of aerosols. Based on this formation mechanism, the SAM II data indicate a background number density of about 6-7 particles cm^{-3} (for a log-normal distribution) and a water content of 5-6 ppmv. The growth of mixed-phase clouds (containing both ice and supercooled-water droplets) would lead to estimates for the water content and particle number density that are between those presented for the frozen and liquid phases.

TABLE 6. DERIVED WATER VAPOR MIXING RATIO AND TOTAL PARTICLE NUMBER DENSITY FOR COMBINED ARCTIC AND ANTARCTIC DATA

[Data from Steele et al., 1983]

Iteration	Region I average water vapor (ppmv)	Region III average water vapor (ppmv)	Average water vapor from I and III combined (ppmv)	Region II average particle number density (no. cm^{-3})
	Supercooled droplets			
1	11.1	8.5	8.8	5.2
5 (convergence)	11.1	8.0	8.4	5.6
	Frozen droplets			
1	5.8	5.6	5.7	5.9
5 (convergence)	5.8	5.6	5.6	6.0

5.14. Properties of Polar Stratospheric Clouds

We present a compilation of the known properties of polar stratospheric clouds in tabular form. Table 7 lists a number of parameters, the values of these parameters, why they are important, and how they are measured.

5.15. Possible Effects of Polar Stratospheric Clouds on Satellite Remote Sensors

PSC's can conceivably interfere with satellite remote sensors viewing in the nadir direction. Important factors that produce the interference are the altitude of high particle concentrations, particle optical properties related to particle chemical constituency (e.g., strongly or weakly absorbing, ice or water, etc.), and size. Sensors working at UV and visible wavelengths generally will be affected by particle scattering of solar radiation, whereas sensors working at certain solar and terrestrial infrared wavelengths generally will be affected by particle absorption as well as by scattering.

The magnitude of any effects on satellite remote sensors can be reasonably assessed with a knowledge of the topical properties of PSC's and the use of accurate radiative transfer routines now readily available. Because of the low concentrations of particles in PSC's, interference may not be obvious even when comparing satellite observations with direct in situ observations because of the normal variability encountered with such comparisons (i.e., plus or minus a few degrees C for temperature sounders and ±10-20 percent (or greater) for ozone profiles giving

ORIGINAL PAGE IS
OF POOR QUALITY

TABLE 7. PROPERTIES OF PSCS

Parameter	Most likely value	Range of plausible values	Significance	Measurement techniques (R = remote; I = in situ)
Composition	H_2O[a]	Sulfate solutions Various minor impurities	Affects optical constants, vapor pressure relationship	IR spectra of 12-μm ice bands (R), filter sample analysis for trace constituents (I)
Physical state	Ice[b]	Liquid	Affects vapor pressure relationship, optical constants, phase function	Vapor pressure and temperature measurements (I), lidar depolarization (R), scattering phase function (I), replicator samples (I), IR spectra (R)
Particle shape	Almost equidimensional[c]	Plates or hollow columns	Affects scattering phase function, fall velocity, growth rate	Replicator samples (I), scattering phase functions (I)
Mean particle radius	1 μm[d]	0.1 to 10 μm	Strongly affects wavelength dependence of extinction, strongly affects particle fall speed	Size spectrometers, quartz microbalance, total particle counters, impactors with replicators (I), multiwavelength optical observations (R)
Mean particle concentration	Ambient CN ($5-20\ cm^{-3}$ at 20 km)[e]	10^3 to $<1\ cm^{-3}$	Strongly affects particle size	CN counters (I), multiwavelength optical observations (R), size spectrometer
Particle size dispersion	Monodisperse[f]	Multimodal	Affects wavelength dependence of optical properties	Size spectrometers, quartz microbalance, total particle counters, impactors with replicators (I), multiwavelength optical observations (R)
Optical depth[g] and column mass	10^{-2} $6 \times 10^{-7}\ g\ cm^{-2}$	10^{1} to 10^{-3} 10^{-7} to $10^{-3}\ g\ cm^{-2}$	Affects radiation field, ability to remove H_2O from stratosphere	Satellite, lidar, radiometers in conjunction with size distribution (R, I)
Altitude	20 km mean[h] (tropopause to 25 km)	Observed	Affects water vapor removal, ability to sample	Lidar, satellite (R)
Horizontal extent	10 to 10^3 km[i]	Observed	Affects remote observations of area of Earth impacted	Lidar, satellite (R)
Geographic extent	From 70° to pole[i]	Observed	Affects area of Earth impacted	Lidar, satellite (R)
Duration	Hours to months	Observed	Affects ability of cloud to remove water, impact on radiation field	Lidar, satellite (R)

[a]Inferred from close correspondence between measured temperature of formation, H_2O vapor concentration, and vapor pressure of ice. Smaller particles may have substantial sulfate component.
[b]Assumed because of low temperatures. Smaller particles with large sulfate concentrations could remain liquid.
[c]Assumed because of relatively small size.
[d]Obtained from angular dependence of cloud color in nacreous clouds, from temperature dependence of SAM II extinction, and from partitioning all available water over all available condensation nuclei. Nucleation might produce many small particles, or preferential growth might lead to a few large particles. At 20 km, 3 ppm H_2O can form 1 particle cm^{-3} of 4 μm radius or 64 particles cm^{-3} of 1 μm radius; 3 ppm H_2O at 14 km can make 1 particle cm^{-3} of 5 μm radius or 125 particles cm^{-3} of 1 μm radius. $N_{H_2O} \propto N^3$.
[e]Based on the assumption that all stratospheric aerosols grow to become PSC particles; also consistent with SAM II extinction measurements and assumed size. Nucleation could produce a large number of new particles, or preferential growth could produce a few large cloud particles, leaving a large number of ambient aerosols remaining.
[f]Assumed because of coloration of nacreous clouds, chemical similarity of CN, and rapid growth rate.
[g]A lower limit to the optical depth is obtained from SAM II. The column mass can be crudely inferred using the lower limit optical depth and the most likely particle radius and assuming $q_{ext} = 2$ from $M = 4/3\ \pi r^3 / q_{ext}$. If all the H_2O mass in the stratosphere above 300 mbar condenses to form clouds then $\sim 10^{-3}\ g\ cm^{-2}$, whereas the stratospheric aerosol mass is about $10^{-7}\ g\ cm^{-2}$.
[h]Well defined by observations of SAM II.
[i]Partially defined by observations of SAM II and ground-based observers.

data for the lower stratosphere). It would be more practical to identify the presence of PSC's coincident with other satellite remote sensing events to gain insight into the magnitude of possible error effects, and then compare satellite results with results of radiative transfer calculations.

Examples of satellite remote sensors affected by stratospheric aerosols from El Chichon are NOAA's SSTS (Sea Surface Temperature Sounder), NASA's SBUV ozone profiler, and the University of Colorado's SME (Solar Mesosphere Explorer). Of course, aerosol concentrations from El Chichon were much greater than those found in PSC's, but the El Chichon interference was also very obvious and by no means subtly obscured by the intrinsic noise of the observational technique.

We have already seen that solar occultation and limb radiance type sensors can have their radiances perturbed by the presence of PSC's. Fortunately, the PSC's in the Northern Hemisphere winter are fairly localized in space at high latitude and they are normally fairly optically thin. The effect of PSC's on temperature retrievals is believed to be very small, although this needs to be quantified for each sensor. As far as species retrievals are concerned, we have seen effects on O_3, H_2O, and HNO_3 in LIMS data. The easiest way to isolate the effects of PSC's on species retrievals seems to be to create maps and note the occurrence of bull's eye type patterns. This seems to work well in the Northern Hemisphere, where the PSC's are fairly localized and transient. In the Southern Hemisphere, where PSC's are semipermanent features in winter, it may be better to resort to an analysis of profile shapes to isolate any contamination. The correlation of PSC's with regions of cold temperature also seems to be very good.

For limb-viewing sensors such as SAMS, which have broader vertical weighting functions, the effect of a PSC on species radiance profiles will be smeared out more and perhaps will be more difficult to detect. A quantitative appraisal of this uncertainty should be made, if it has not already been done.

For more traditional nadir-viewing sensors that operate in the infrared, it is conceivable that PSC's could be a problem. Sensors that view scattered sunlight, such as SBUV, would also be affected by PSC's at high latitudes, but because most of the PSC's occur during the polar night, this possible problem has not been addressed.

6. PANEL RECOMMENDATIONS

The workshop participants felt that polar stratospheric clouds are an interesting phenomenon deserving further study. The fact that these clouds are found in the stratosphere means that they are a "clean" and relatively simple system which should be amenable to analysis using existing measurement techniques. Unlike studies of tropospheric atmospheric phenomena, which are complicated by many factors, studies of the polar stratospheric clouds have a high probability of success.

The particular recommendations formulated at the workshop are given here.

1. Continue to carry out the analysis of the SAM II data to evaluate polar stratospheric cloud characteristics.

2. Carry out modeling studies of cloud microphysics, the effects of the clouds on radiation balance, and stratospheric chemistry and dynamics.

3. Review nonsatellite data that bear on the physical properties of polar stratospheric clouds. These data, such as observations of nacreous clouds, may provide first-order estimates of key quantities such as particle size.

4. Analyze satellite data (in addition to those from SAM II) which give frequency and other physical characteristics of polar stratospheric clouds; for example, LIMS observations of Northern Hemisphere polar stratospheric clouds and SAGE multispectral data.

5. Obtain measurements of polar stratospheric clouds as required to determine their impact on radiation balance, especially polar stratospheric cloud seasonal variation and spatial extent (horizontal and vertical extent, including the PSC coverage of the polar night area), optical thickness, size distribution, water vapor profiles, infrared radiances from the polar stratospheric clouds, and particle composition and shape.

6. Determine the relationship between polar stratospheric cloud occurrence and meteorological conditions, for example, to establish any relation between PSC formation and quasistationary orographic waves.

7. Determine the effects of polar stratospheric clouds on the water vapor content of the polar stratosphere. This should include determining whether there is a significant latitudinal gradient of water vapor at high latitudes in winter and whether there is vertical transfer of water vapor due to polar stratospheric clouds.

8. Make a special effort to extend radiosonde coverage through the temperature minimum; this requires balloons that can survive temperatures as cold as about -100°C. Accurate knowledge of temperature conditions under which polar stratospheric clouds form is needed.

9. Obtain improved definition of the Antarctic upper air temperature fields. This may serve as a useful proxy for defining the spatial and temporal extent of the polar stratospheric clouds. These fields could be obtained through a combination of analysis of Antarctic radiosonde data and satellite temperature sounding, once the latter is validated by comparison with the radiosonde data and radar tracking.

10. Obtain routine lidar measurements of aerosol vertical profiles from the South Pole. This will provide accurate data in the polar night region, and from the time dependence should provide information on horizontal inhomogeneity. It is desirable to obtain temperature and water vapor profiles simultaneously with the lidar aerosol profiles.

11. Determine water vapor concentration and temperature fields in and around polar stratospheric clouds. It is particularly important to have accuracy in temperatures of at least 3°C.

12. Measure the water vapor budget in a cloud, including both water vapor and condensed water in the cloud as well as water vapor upwind and downwind of the cloud.

13. Observe SO_2 and OCS concentrations and vertical and latitudinal distributions.

14. Identify potential tracers of polar dynamics which may be used to study air motions involved in cloud formation and other high-latitude winter phenomena.

15. Make simultaneous measurements of nitrogen oxides, including NO_2, N_2O_5, and HNO_3, and, at higher altitudes, NO. Absolute concentrations and vertical and latitudinal gradients should be evaluated. Minimum requirements are column abundances.

16. Determine the concentrations and distributions of chlorine species, including source compounds such as fluorocarbons.

17. Obtain ozone measurements within and around polar stratospheric clouds.

18. Measure other potentially important species such as H_2O_2.

7. SYMBOLS AND ACRONYMS

Symbols

g	gravitational constant
H	scale height of atmosphere
k_B	Boltzmann's constant
l	typical distance
M, m	mass
N	number density, particles cm^{-3}
N_0	reference number density, particles cm^{-3}
$N(r)$	number density per unit particle radius, particles cm^{-3}
$N_g(Z_0)$	gas number density at Z_0, molecules cm^{-3}
q_{ext}	extinction efficiency
r	particle radius
r_g	mode radius
$\bar{r}$	mean particle radius
T	temperature
t	time
$V(Z_0)$	fall velocity at Z_0
Z_0	altitude
α	water vapor mixing ratio
θ	potential temperature
$\bar{\omega}$	vertical velocity
ρ	particle density
σ	geometric standard deviation
τ	optical depth at 1 μm
τ_c	characteristic time for coagulation
τ_f	time for particle to fall typical distance l

Acronyms

CCN	cloud condensation nuclei
CN	condensation nuclei
GCM	global circulation model
GMCC	Geophysical Monitoring for Climate Change (NOAA)
LIMS	Limb Infrared Monitor of the Stratosphere
NMC	National Meteorological Center
SBUV	Solar Backscattered Ultraviolet
SME	Solar Mesosphere Experiment
SSTS	Sea Surface Temperature Sounder
UARS	Upper Atmosphere Research Satellite

8. REFERENCES

Bevilacqua, R. M., J. J. Olivero, P. R. Schwartz, C. J. Gibbins, J. M. Bologna, and D. L. Thacker, 1983: An observational study of water vapor in the mid-latitude mesosphere using ground-based microwave techniques. J. Geophys. Res., 88, 8523-8534.

Brewer, A. W., 1949: Evidence for a world circulation provided by the measurements of helium and water vapour distribution in the stratosphere. Quart. J. Roy. Meteorol. Soc., 75, 351-363.

Chu, W. P., and M. P. McCormick, 1979: Inversion of stratospheric aerosol and gaseous constituents from spacecraft solar extinction data in the 0.38-1.0 μm region. Appl. Opt., 18, 1404-1413.

Danielsen, E. F., 1982: A dehydration mechanism for the stratosphere. Geophys. Res. Lett., 9, 605-608.

Danielsen, E. F., and V. Mohnen, 1977: Project Dustorm report: Ozone transport, in situ measurements and meteorological analysis of tropopause folding. J. Geophys. Res., 82, 5867-5877.

Douglass, A. R., and J. L. Stanford, 1982: A model of the antarctic sink for stratospheric water vapor. J. Geophys Res., 87, 5001-5008.

Friend, J. P., R. A. Barnes, and R. M. Vasta, 1980: Nucleation by free radicals from the photodissociation of sulfur dioxide in air. J. Phys. Chem., 84, 2423-2436.

Gibbins, C. J., P. R. Schwartz, D. L. Thacker, and R. M. Bevilacqua, 1982: The variability of mesospheric water vapor. Geophys. Res. Lett., 9, 131-134.

Hamill, P., O. B. Toon, and C. S. Kiang, 1977: Microphysical processes affecting stratospheric aerosol particles. J. Atmos. Sci., 34, 1104-1119.

Hansen, J., G. Russell, D. Rind, P. Stone, A. Lacis, S. Lebedeff, R. Ruedy, and L. Travis, 1983: Efficient three-dimensional global models for climate studies: Models I and II. Mon. Wea. Rev., 111, 609-662.

Harris, Joyce M., and Barry A. Bodhaine, eds., 1983: Geophysical monitoring for climatic change - No. 11, Summary report 1982. National Oceanic and Atmospheric Administration, Environmental Resources Laboratories, Air Resources Laboratories, Dec. 1983.

Hesstvedt, E., 1969: The physics of nacreous and noctilucent clouds. Stratospheric Circulation, W. L. Webb, ed., Academic Press, 209-217.

Hofmann, D. J., and J. M. Rosen, 1982a: Balloon-borne observations of stratospheric aerosol and condensation nuclei during the year following the Mount St. Helens eruption. J. Geophys. Res., 87, 11,039-11,061.

Hofmann, D. J., and J. M. Rosen, 1982b: Stratospheric condensation nuclei variations may relate to solar activity. Nature, 297, 120.

Hofmann, D. J., and J. M. Rosen, 1983: Condensation nuclei events at 30 km and possible influences of solar cosmic rays. Nature, 302, 511.

Kley, E. D., E. J. Stone, W. R. Henderson, J. W. Drummond, W. J. Harrop, A. L. Schmeltekopf, T. L. Thompson, and R. H. Winkler, 1979: In situ measurements of the mixing ratio of water vapor in the stratosphere. J. Atmos. Sci., 36, 2513-2524.

Kley, D., A. L. Schmeltekopf, K. Kelly, R. H. Winkler, T. L. Thompson, and M. McFarland, 1982: Transport of water through the tropical tropopause. Geophys. Res. Lett., 9, 617-620.

Liljequist, G. H., 1956: Halo-phenomena and ice-crystals. Norwegian-British-Swedish Antarctic Expedition, 1949-52: Scientific Results, Vol II, Part 2A, Norsk Polarinstitutt, Oslo.

Louis, J. F., 1974: A two-dimensional transport model of the atmosphere. Ph.D. thesis, Univ. of Colo., Boulder.

McCormick, M. P., Patrick Hamill, T. J. Pepin, W. P. Chu, T. J. Swissler, and L. R. McMaster, 1979: Satellite studies of the stratospheric aerosol. Bull. Amer. Meteor. Soc., 60, 1038-1046.

McCormick, M. P., W. P. Chu, G. W. Grams, Patrick Hamill, B. M. Hennan, L. R. McMaster, T. J. Pepin, P. B. Russell, H. M. Steele, and T. J. Swissler, 1981: High-latitude stratospheric aerosols measured by the SAM II satellite system in 1978 and 1979. Science, 214, 328-331.

McCormick, M. P., H. M. Steele, Patrick Hamill, W. P. Chu, and T. J. Swissler, 1982: Polar stratospheric cloud sightings by SAM II. J. Atmos Sci., 39, 1387-1397.

Mendonca, Bernard G., ed., 1978: Geophysical monitoring for climatic change - No. 7, Summary report 1978. National Oceanic and Atmospheric Administration, Environmental Resources Laboratories, 1978.

Newell, R. E., and S. Gould-Stewart, 1981: A stratospheric fountain? J. Atmos. Sci., 38, 2789-2796.

Palmer, K. R., and D. Williams, 1975: Optical constants of sulfuric acid; applications to the clouds of Venus? Appl. Opt., 14, 208-219.

Pollack, J. B., and C. P. McKay, 1984: On the impact of polar stratospheric clouds on the heating rates of the winter polar stratosphere. J. Atmos. Sci., submitted.

Ramanathan, V., E. J. Pitcher, R. C. Malone, and M. L. Blackmon, 1983: The response of a spectral general circulation model to refinements in radiative processes. J. Atmos. Sci., 40, 605-630.

Rosen, J. M., 1971: The boiling point of stratospheric aerosols. J. Appl. Meteor., 10, 1044-1045.

Rosen, J. M., and D. J. Hofmann, 1977: Balloon-borne measurements of condensation nuclei. J. Appl. Meteorol., 16, 56.

Rosen, J. M., and D. J. Hofmann, 1981: Stratospheric condensation nuclei. Rep. AP-678, Dep. of Phys. and Astron., Univ. of Wyoming, Laramie, Wyoming.

Rosen, J. M., and D. J. Hofmann, 1983: Unusual behavior in the condensation nuclei concentration at 30 km. J. Geophys. Res., 88, 3725.

Rosen, J. M., D. J. Hofmann, and J. Laby, 1975: Stratospheric aerosol measurements II: The worldwide distribution. J. Atmos. Sci., 32, 1457-1462.

Samson, Julie A., 1983: Some Characteristics of the South Polar Atmosphere. Atmospheric Science Research Center, Publication 990, Albany, N.Y.

Stanford, J. L., 1973a: Possible sink for stratospheric water vapor at the winter Antarctic pole. J. Atmos. Sci., 30, 1431-1436.

Stanford, J. L., 1973b: On the physics of stratospheric (nacreous) cloud formation. Tellus, 25, 479-482.

Stanford, J. L., 1977: On the nature of persistent stratospheric clouds in the Antarctic. Tellus, 29, 530-534.

Stanford, J. L., and J. S. Davis, 1974: A century of stratospheric cloud reports: 1870-1972. Bull. Amer. Meteor. Soc., 55, 213-219.

Steele, H. M., Patrick Hamill, M. P. McCormick, and T. J. Swissler, 1983: The formation of polar stratospheric clouds. J. Atmos. Sci., 40, 2055-2067.

Stormer, Carl, 1929: Remarkable clouds at high altitudes. Nature, 123, 260-261.

Telegadas, K., and R. J. List, 1964: Global history of the 1958 nuclear debris. J. Geophys. Res., 60, 4741-4753.

Thacker, D. L., C. J. Gibbins, P. R. Schwartz, and R. M. Bevilacqua, 1981: Ground-based microwave observation of mesospheric H_2O in January, April, July and September 1980. Geophys Res. Lett. 8, 1059-1062.

Toon, O. B., R. P. Turco, P. Hamill, C. S. Kiang, and R. C. Whitten, 1979: A one-dimensional model describing aerosol formation and evolution in the stratosphere. II. Sensitivity studies and comparison with observations. J. Atmos. Sci., 36, 718-736.

Weyant, W. S., 1966: The Antarctic atmosphere: Climatology of the troposphere and lower stratosphere. Folio 4. Antarctic Map Folio Series, Amer. Geographic Society.

WMO Global Ozone Research and Monitoring Project, 1981: The Stratosphere 1981: Theory and Measurements. Rep. no. 11, World Meteorological Organization.

END

DATE

FILMED

NOV 13 1984